Beiträge zur Hydrogeologie / 52 / Seiten 7–102 / Graz 2001

Tracers in the Unsaturated Zone

Markierungsstoffe in der ungesättigten Zone

(W. BERG, B. ČENČUR CURK, J. FANK, F. FEICHTINGER, G. NÜTZMANN, W. PAPESCH, V. RAJNER, D. RANK, S. SCHNEIDER, K.-P. SEILER, K.-H. STEINER, E. STENITZER, W. STICHLER, B. TRČEK, Z. VARGAY, M. VESELIČ, H. ZOJER)

Content

1. Introduction (K.-P. SEILER, M. VESELIČ)

The unsaturated zone stretches from the ground to the groundwater surface:

- It qualitatively and quantitatively regulates the subsurface branch of the water balance.
- It produces different forms of subsurface discharge.
- It determines together with the prevailing climatic conditions weathering of sediments and the design of landscapes.
- Its soil mechanical properties influence the long-term stability of all kinds of constructions.

All these properties depend mainly from the hydraulic functions of the unsaturated zone (suction/water-content-relation or suction/hydraulic-conductivity-relation) and its variations in space and time; they get modified from the chemical, physical and microbial interrelations between seepage and solid phases and thus focus in the flow and transport mechanisms within the seepage zone.

In the past, the unsaturated zone was mostly of isolated and individual interest (soil sciences, soil mechanics and hydrogeology) and processes in it have been considered predominantly from singular scales, rather seldom in scale steps. Therefore, past results mostly prevented the recognition of relations and interchanges in between different compartments. This has changed in the present research. Essential tools to achieve this change into a more integrated view have been interdisciplinary and combined investigations relating to different scales in dedicated investigation areas; in this effort, tracer investigations linked to hydraulic studies and mathematical simulations on seepage in the unsaturated zone have been one outstanding tool. With this combination it was possible

- to control results on flow and transport in the unsaturated zone through independent methods and to achieve by this way a better conceptual model,
- to get better quantitative results on homogeneity and heterogeneity of the unsaturated zone by inter-comparing these results and
- to highlight the origin and transport potential of discharges for solutes and particles within the subsurface.

Discharges in landscapes are classified into quick (direct discharge) and slow discharges (indirect discharge). This classification relates to the observation that after storm events a quick response occurs in rivers and during dry weather conditions slow flow components sustain the discharge over a long period of time thus preventing the drying out of rivers.

Both direct and indirect recharges in rivers relate to reservoirs with small and significant storage capacities, respectively, thus also reflecting quick and slow flow velocities in subsurface systems. Slow discharges relate to the matrix flow of seepage and the groundwater flow in the subsurface with flow velocities of meters per year in the unsaturated zone and of meters per day in groundwater systems in humid areas. Contrary, direct recharge refers to low storage capacities and has mostly been correlated with overland flow that had only sparse contact with solid phases. By using chemical and environmental tracer analysis in river discharges (M. G. SKLASH & R. N. FARVOLDEN, 1979), however, it got evident that the quick discharge has both a component with close and one with no significant contact with solid phases (J. KÖRNER, 1996); the component with close contact with solid phases is attributed to the interflow, which itself is

generated by bypass- or preferential flow (see P. F. GERMANN, 1990, N. DEMUTH & A. HILTPOLD, 1993) that changes from vertical to lateral directions along interfaces with significant changes in hydraulic conductivities (K.-P. SEILER & D. BAKER, 1985).

The direct and indirect discharges are evaluated using hydrograph methods (E. NATERMANN, 1951). Contrary, indirect discharge plus interflow are determined by chemical and environmental tracer methods; the difference of results from both methods leads to the quantification of the overland flow. Actually, both methods got standard exercises and need no further explanation. They refer, however, only to large scale transport processes of water, particles and solutes and do neither relate to the genesis of the discharge components nor to detailed transport processes and interactions in the unsaturated zone. Such a lack of knowledge does not allow defining strategies

- to manipulate flow processes in the unsaturated zone,
- to enhance and protect functions of ecosystems and
- to better contribute to groundwater protection measures.

The more detailed view, however, can be achieved applying tracer methods (chap. 2.) on low and large scales and linking these results with mathematical simulations (chap. 5.).

Contrary to groundwater flow, seepage has usually to cross all bedding planes, along which changes in the hydraulic properties may occur. As a consequence, in the unsaturated zone flow undergoes much more reflections and refractions along such interfaces than in the saturated zone. These interfaces often turn vertical into lateral flow or produce transient or permanent perched groundwater. Such interfaces may be of sedimentary origin and than mostly occur without any relations to the existing morphology of the landscape. Others have been produced during glacial ages by frost/thaw activities or eolic sedimentation or more recently depend from human activities like ploughing, from the existence of a plant root zone and animal activities in it or from subsurface constructions; all the latter mostly follow actual topography and enable to produce a subsurface flow paralleling morphology (interflow).

The role of these interfaces in the unsaturated zone is highlighted if the hydraulic functions and its changes along these interfaces are considered (K.-P. SEILER & D. BAKER, 1985). Some generalized examples of these hydraulic functions according to laboratory experiments (D. BAKER & K.-P. SEILER, 1982) demonstrate

- that the grain size related classification into aquifers, aquitards and aquicludes, being valid for the saturated zone, does generally not apply for the unsaturated zone and
- that even in the unsaturated zone this classification doesn't hold for the whole array of water contents or suctions.

The unsaturated zone is significantly non-homogeneous with respect to flow by nature as well as through biotic and human activities. These can easiest get highlighted using tracers and interpreting tracer breakthrough behaviour on short and long distances.

In consolidated rocks, the unsaturated zone is even more non-homogeneous than in unconsolidated sediments (B. TRČEK et al., 2001); here, the rock material is mostly covered by a weathering and dilatation zone acting simultaneously as a collector for infiltration and as a distributor of infiltration to interflow, fissures and the rock matrix. In these rocks interflow is mostly produced at the interface rock/weathering zone and mostly amounts to a higher percentage of infiltration than in unconsolidated rocks. Discharge and tracer investigations in karst (K.-P. SEILER et al., 1987) and sandstones (G. EINSELE et al., 1968) demonstrate that during storm events about 30–50 % of the infiltration reappears rather quickly in springs and rivers as preferential flow; obser-

vations on fissure flow, however, proves that their influence on preferential flow seems not to be too pronounced because of a lack of quick vertical exfiltration out of the weathering and dilatation zone into wide fissures or because fissure flow is interconnecting with a quite efficient matrix porosity sucking most of the fissure water and transferring it into a slow seepage-flow component. This incorporation of fissure flow into matrix pores within the unsaturated zone may get so pronounced that it significantly influences environmental isotope based determination of mean residence times of subsurface waters (K.-P. SEILER et al., 1996). Such observations are known from most of the consolidated rocks contributing for drinking water supply (sandstones, reef carbonates and chalk). The mechanism of these dual or multi porosity systems is best investigated by means of tracer experiments.

2. Role of Tracers in the Unsaturated Zone

(K.-P. SEILER, H. ZOJER)

According to the climatic conditions, matrix flow in the unsaturated zone ranges from few meters to less than few millimetres a year. In humid areas it is predominantly directed vertically down and in semi-arid to arid climates also vertically up if groundwater table is not to far from the land surface. Beside matrix flow there exists during infiltration events also bypass- or preferential flow in the unsaturated zone (D.E. HILL & J.-Y. PARLANGE, 1972, K. BEVEN & P. F. GERMANN, 1982, D. R. NIELSEN et al., 1986, R. J. GLASS et al., 1989, K.-J. S. KUNG, 1990a, 1990b, R. S. BAKER & D. HILLEL, 1991, T. S. STEENHUIS & J.-Y. PARLANGE, 1991, D. CHAPMAN, 1992), which interacts with matrix flow by mass and ion exchange, retardation processes or turns into lateral flow (chap. 4.3.) producing perched groundwater or interflow.

In unconsolidated sediments matrix flow is the dominant factor (> 70 %), in consolidated rocks, however, bypass-flow mostly gets pronounced and amounts to 40–60 % of infiltration.

Classical hydraulic methods to calculate seepage flow are based on the hydraulic functions

$$k(u) = f(\Psi), \tag{2.1}$$

$$\Psi \cdot = f(\Theta), \tag{2.2}$$

where

$k(u)$ = hydraulic conductivity at an unsaturated state of the media,
Ψ = matrix suction,
Θ = water content.

Equation (2.1) and (2.2) are rather difficult to determine by field or laboratory exercises. Therefore Y. MUALEM (1976) and M. Th. VAN GENUCHTEN (1980) developed empirical relations to determine these hydraulic functions using basic parameters of soils and sediments. To solve these equations measurements of suction and water content under undisturbed conditions in the field are needed.

In most conceptual models to simulate seepage, it is supposed that fluxes are homogeneous within small compartments and mostly vertical; both these boundary conditions can hardly be controlled by means of statistical evaluations of suction and water content measurements and therefore often remain theoretical. To reduce this

uncertainty tracer methods (artificial as well as environmental tracers) are applied to support and improve hydraulic evaluations. Both methods, however, only develop optimal results in combination with numerical simulations and with an appropriate conceptual model, which may be deduced also from tracer experiments.

2.1. Tracer Properties

To measure water fluxes in the unsaturated zone, it is requested that tracers

- are applied in small quantities to avoid gravity convection,
- do not interact with the solid inorganic and organic phases,
- are neither taken up by plants nor disintegrated by microbial activities in the soil zone,
- do not undergo significant accumulations or losses through fractionation as a consequence of evaporation,
- do not change significantly ion balance in soil solutions and
- are detectable in very small concentrations because seepage abstraction for analytical purposes is restricted in quantity within short time intervals.

Most of the above mentioned requirements are best fulfilled by the use of isotope fluxes from hydrogen (^{2}H, ^{3}H) and oxygen (^{18}O) labelling both the water molecule. However, since mass differences, especially for hydrogen, are greatest, fractionation processes may alter significantly the respective isotope concentration or – ratio. Therefore it is recommended that these tracers are predominantly applied during the cold season, when evaporation is low and infiltration is highest; this specially is guaranteed during snow melt times when infiltration moves quickly away from the evaporation interface soil/atmosphere. During this season, however, long freezing periods should be avoided because they locally stop flow processes close to the surface and may provide shrinking cracks, which increase the potential evaporation surface and bypass-flow during melting periods. Therefore best seasons to use these isotope tracers are the beginning (F. EULENSTEIN & H. DRECHSLER, 1992) or the end of the winter season in the moderate climate.

The application of natural ^{18}O and ^{2}H is highly recommended for studies of water migration through the unsaturated zone considering and utilizing the various isotopic effects based on temperature and fractionation. Tracer experiments in Leibnitzer Feld, a flat Quaternary basin, have been carried out with water from high Alpine region representing very low stable isotope concentration (H. ZOJER, 1993). The test was repeated with local water and high isotope content. The results obtained from these experiments show a clear evidence for the understanding of water transport phenomena in the soil zone neglecting hydrochemical and biochemical reactions.

Fluorescent dyes that are favourably applied in groundwater do not well apply in the unsaturated zone enriched with humic substances. Humic substances absorb significantly fluorescent dyes, thus producing retarded tracer propagation and simultaneously reducing the measurable recovery. Since in the unsaturated zone particle favoured transport through DOC also plays an important role (see P. M. JARDIN et al., 1990, K.-P. SEILER & C. HELLMEIER, 2000) during infiltration events, fluorescent dyes are transported through DOC; this transport mechanism plays a significant role at infiltration during storm events and is mostly related to bypass- or preferential flow (K.-P. SEILER & C. HELLMEIER, 2000). Since retarded and DOC favoured flow may interact, dye tracers results from the unsaturated zone are often difficult to interpret.

Also few is known about the microbial disintegration and disintegration speed of dye tracers in the soil zone.

Fluorescent dye may favourably apply in the unsaturated if the humic cover is removed and soil and sediment are not too abandoned in silt and clay.

Analogue to groundwater, fluoresceine proved to be a better tracer in the unsaturated zone than eosin and both these tracers apply better than rhodamine and sulforhodamine.

Often halogenides are used to trace the unsaturated zone and in between these mostly bromide is used because it has mostly a very low natural and human related background. There are, however, observations that ion exclusion of the anionic halogenides leads to a quicker flow than isotope tracers and that plant take up bromide by their roots and accumulate it in tissues (K.-J. S. KUNG, 1990); these effects significantly influence the halogenide balance. On the one hand bromide can occasionally remain in the effective root zone and will be retarded there for a reasonable time due to boundary conditions demanded by the soil, the season of cultivation and by plant characteristics. On the other hand sodium bromide has been tested as an excellent conservative tracer in Quaternary gravels and can be used for calibration of transport models in the unsaturated zone (J. FANK & T. HARUM, 1994).

Other anionic tracers like nitrate and sulphate or the isotopically labelled nitrate (R. RUSSOW et al., 1995) have also been applied. They proved, however, as non-conservative or non-ideal due to plant uptake, chemical precipitation and microbial disintegration.

Since weathering under atmospheric conditions produces from silicates mostly clay minerals or releases clay incorporated e.g. in carbonates, most soils are clay rich and consequently significantly negatively charged; this mostly prevents the application of anionic tracers.

2.2. Application of Tracers

Tracers should be applied according to their detection limit, according to the prevailing water content, according to the fact that suction cups do not cover a wide range of stream bundles and according to the non-homogeneous structure and texture of the unsaturated zone.

Tracer experiments in the Scheyern test side (chap. 4.3.) have been performed with deuterium exceeding in the maximum of the breaktrough curve about five orders of magnitude (+2000 ‰) the mean annual deuterium concentrations (–60 ‰). Considering bypass-flow, which was detectable with these high concentrations (Fig. 2.1) it can be demonstrated that the recognition of it was no more possible at concentrations exceeding "only" three to four orders of magnitude the mean annual δ^2H. This is due to the very small quantities of event related bypass-fluxes (as an average 17 % of infiltration) as compared to the existing water content (25–30 %), which corresponds to a contribution of less than 0.5 % of the pre-existing water content; therefore, because of the small sector of the flow field sampled in the unsaturated zone and because of the detection limit of deuterium, the mixing range must be spread to an extend that small quantities of e.g. bypass-fluxes are still recognizable. Using fluorescent dyes, much smaller quantities could be applied but they only partly penetrate through the soil with its abundant organic matter.

Tracers should not remain longer than a few hours at the ground surface to avoid fractionation or enrichment through evaporation (stable isotopes, respectively chemical

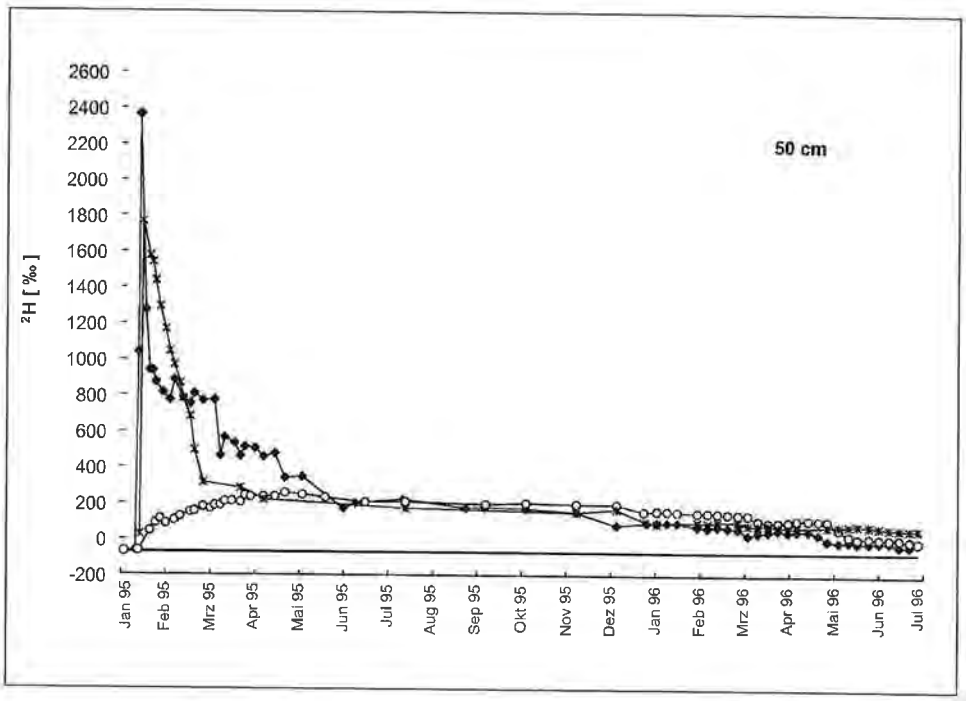

Fig. 2.1: Results of a tracer experiment performed in the unsaturated zone and sampled by three individual cups at 50 cm depth.
Ergebnisse eines Markierungsversuchs in der ungesättigten Zone, die Beprobung erfolgte in 50 cm Tiefe mittels dreier Saugkerzen.

tracers) or photolytic disintegration (fluorescent dyes). Therefore it is recommended to trace during continuous sprinkling or to trace a melting snow cover above an unfrozen soil.

2.3. Sampling in the Unsaturated Zone

In general water samples from the unsaturated zone may be collected directly by gravity lysimeters, by special devices like suction cups and plates and by extracting water from sediments by replacement, heating or dilution techniques. Suction cups and plates mostly are permanently installed in the unsaturated zone. The suction efficiency of these cups is restricted to between a few and about 800 hPa depending on soil tension. In dryer materials typical for sediments and soils close to the land's surface, for instance during the vegetation period or in dry lands, the water has to be extracted either by replacement, dilution or by heating of the core material.

Suction cups should consist of inert materials like ceramics or sinter materials. The pore sizes of it are to be adapted to the main pore sizes of the sediment. As an example, suction cups with 20 µm pore size are well adapted to most sediments in the vadose zone. Before the implantation of the cups they should become conditioned with water similar to that encountered in the unsaturated zone. This is especially true for the chemical analyses. The under pressure employed should not differ too much from the prevailing one, in order to avoid degassing of the water causing disturbance of gas rela-

ted components like carbonates. Since flow and water content in the unsaturated zone are mostly low, sampling of water will always cover a longer time interval.

Since the unsaturated zone is rather inhomogeneous as compared to the spherical space influenced by the suction cup, it is emphasized to have samples collected by more than one cup at the same level. Figure 2.1 demonstrates differences in the results of a tracer experiment, in which samples were collected with three cups at the same depth, at a mutual distance of about 0.5 m.

Determination of the quantity of pore water by the (chemical or isotopic) dilution analysis aims in the first instance at saturating the sediment to some extent to make water easier extractable. This dilution should be combined with a homogenization of the two waters. In the second step homogenized water is extracted by centrifugation or with suction cups. For the dilution analysis extreme compositions of waters are used like distilled water for chemical analysis or Antarctic Water for stable isotopic analysis. The water content of the sample (Q_s) and its natural isotopic or chemical composition (C_s), the added quantity of water (Q_a) and its isotopic or chemical composition (C_a) and the resulting composition of mixed waters (C_m) can easily be determined. From the mass balance

$$C_s Q_s + C_a Q_a = C_m (Q_s + Q_a) \tag{2.3}$$

follows:

$$C_s = \frac{C_m (Q_s + Q_a) - C_a Q_a}{(Q_s)} . \tag{2.4}$$

In this way the isotopic or chemical composition of the water from the unsaturated zone (C_s) is determined from the mixing equation.

The distillation of waters from sediments (see L. ARAGUAS-ARAGUAS et al., 1995, N. L. INGRAHAM & C. SHACHEL, 1992) must be performed in closed systems and till the point of complete dryness of the sediment. Only under these conditions isotope fractionation does not play any more any role and an uneven distribution of isotope concentration in the pore water has no more influence on the analytic result.

In some special cases also replacing methods (N. L. INGRAHAM & C. SHACHEL, 1992) have been used in applying a wetting liquid that replaces water in the sediment pores. The transition between the two liquids does not go off with a sharp front; the mixing area between both has to be considered in the evaluation of analytic results.

3. Flow Systems (J. FANK, K.-P. SEILER, W. BERG)

3.1. Unsaturated Flow and Water Table

DARCY's law and the concepts of hydraulic head and hydraulic conductivity have been developed with respect to a saturated porous medium, that is one in which all the voids are filled with water. It is clear that some soils and sediments, especially those near the ground surface, are seldom saturated. Their voids are usually only partially filled with water, the remainder of the pore space being taken up by air with a sharp interface to water.

The flow of water under such conditions is termed flow in unsaturated or partially saturated media. For saturated flow the moisture content is equal to the porosity, for unsaturated flow moisture content is lower than porosity.

The simplest hydrologic configuration of saturated and unsaturated conditions is that of an unsaturated zone close to the surface and a saturated zone at depth. We commonly think of the water table as being the boundary between the two, yet we are aware that a saturated capillary fringe often exists above the water table. The water table is best defined as the surface on which the fluid pressure (p) in the pores of a porous medium is exactly atmospheric. If p is measured in gage pressure, then on the water table $p = 0$. This implies that the tension head (ψ) equals 0, and since $h = \psi + z$, the hydraulic head at any point on the water table must be equal to the elevation z of the water table at that point.

If $\psi = 0$ at the water table, it follows that $\psi < 0$ in the unsaturated zone. This reflects the fact that water in the unsaturated zone is held in the soil pores under surface tension and capillary forces.

Regardless of the sign of ψ, the hydraulic head h is still equal to the algebraic sum of ψ and z. However, above the water table, where $\psi < 0$, piezometers are no longer a suitable instrument for the measurement of h. Instead, h must be obtained indirectly from measurements of ψ determined with tensiometers.

The hydraulic conductivity of an unsaturated soil increases with increasing moisture content. If we write DARCY's law for unsaturated flow in the x-direction in an isotropic media as

$$v_x = -K(\psi)\frac{\delta h}{\delta x}, \tag{3.1}$$

we see that the existence of the $K(\psi)$ relationship implies that, given a constant hydraulic gradient, the specific discharge v increases with increasing moisture content respectively decreasing ψ. In actual fact, it would be impossible to hold the hydraulic gradient constant while increasing the moisture content. Since $h = \psi + z$ and $\theta = f(\psi)$, the hydraulic head is also affected by the moisture content. In other words, a hydraulic head gradient infers a pressure head gradient (except in pure gravity flow), and this in turn infers a moisture content gradient.

In the saturated zone we have the two fundamental hydraulic parameters saturated hydraulic conductivity and effective porosity; in the unsaturated zone these become the functional relationship $K(\psi)$ and $\theta(\psi)$. The DARCY approach to unsaturated flow is the one used almost universally by soil physicists, but it is, at root, an approximate method. Unsaturated flow is actually a special case of multiphase flow through porous media, with two phases, air and water, coexisting in the pore channels with a sharp interface. The single phase approach to unsaturated flow leads to techniques of analyses that are accurate enough for almost all practical purposes.

It is worthwile at this point to summarize the properties of the unsaturated zone – or, as it is sometimes called, the zone of aeration or the vadose zone (R. A. FREEZE & J. A. CHERRY, 1979):

1) It occurs above the water table and above the capillary fringe.
2) The soil pores are only partially filled with water; the moisture content ist less than the porosity.
3) The fluid pressure is less than atmospheric; the pressure head is less than zero.
4) The hydraulic head must be measured with a tensiometer.
5) The hydraulic conductivity and the moisture content are both functions of the pressure head.

3.2. Flow Equation for Transient Unsaturated Flow in Porous Media

Using the equation of continuity for transient unsaturated flow, inserting the unsaturated form of DARCY's law, recalling the definition of the specific moisture capacity $C = d\theta/d\psi$, where θ ist the moisture content and noting that $h = \psi + z$, we obtain

$$\frac{\delta}{\delta x}\left(K(\psi)\frac{\delta\psi}{\delta x}\right)+\frac{\delta}{\delta y}\left(K(\psi)\frac{\delta\psi}{\delta y}\right)+\frac{\delta}{\delta z}\left(K(\psi)\left(\frac{\delta\psi}{\delta z}+1\right)\right)=C(\psi)\frac{\delta\psi}{\delta t}. \qquad (3.2)$$

This equation is the ψ-based equation of flow for transient flow through an unsaturated porous medium. It is often called RICHARDS equation, in honor of the soil physicist who first developed it (L. A. RICHARDS, 1931). The solution $\psi(x,y,z,t)$ describes the pressure head field at any point in a flow field at any time. It can easily be converted into an hydraulic head solution $h(x,y,z,t)$ through the relation $h = \psi + z$. This solution requires knowledge of the characteristic curves $K(\psi)$ and $C(\psi)$ or $\theta(\psi)$.

Monitoring in the unsaturated zone in this case means to get information about the time dependent and horizon specific water content and tension head for the calculation of the unsaturated conductivity. Measuring the flow rate through the unsaturated zone gives a controlling value for the calculations using the RICHARDS equation.

3.3. Hydrodynamic Dispersion

It is becoming increasingly common in the investigation of groundwater flow systems to view the flow regime in terms of its ability to transport dissolved substances. These solutes may be natural constituents, artificial tracers, or contaminants. The process by which solutes are transported by the bulk motion of the flowing groundwater is known as advection. Owing to advection, non-reactive solutes are carried at an average rate equal to the average linear velocity of the water. There is a tendency, however, for the solute to deviate from the ideal path that it would be expected to follow according to the advective hydrodynamic dispersion. It causes dilution of the solute. It occurs because of tortuosity of pore canals causing mechanical mixing during fluid advection and because of molecular diffusion due to the thermal-kinetic energy of the solute particles.

Mechanical dispersion is most easily viewed as a microscopic process. On the microscopic scale, dispersion is caused by three mechanisms. The first occurs in individual pore channels because the molecules travel at the different velocities at different points across the channel due to the drag exerted on the fluid by the roughness of the pore surfaces.

The second process is caused by the difference in pore size along the flow paths followed by the water molecules. Because of differences in surface area and roughness relative to the volume of water in individual pore channels, different pore channels have different bulk fluid velocities.

The third dispersive process is related to the tortuosity, branching, and interfingering of pore channels. The spreading of the solute in the direction of bulk flow is known as longitudinal dispersion. Spreading in directions perpendicular to the flow is called transverse dispersion. Longitudinal dispersion is normally much stronger than lateral dispersion.

Dispersion is a mixing process. Qualitatively, it has a similar effect to turbulence in surface water regimes. For porous media, the concepts of average linear velocity and longitudinal dispersion are closely related. Longitudinal dispersion is the process whereby some of the water molecules and solute molecules travel more rapidly than the average linear velocity and some travel more slowly.

When a tracer experiment is set up in the laboratory or in the field, the only dispersion that can be measured is that which is observable at the macroscopic scale. It is assumed that this macroscopic result has been produced by the microscopic processes described above. Heterogeneities on the macroscopic scale will cause additional dispersion to that caused by the microscopic processes.

3.4. Preferential Flow

Because understanding water and solute transport through the unsaturated zone is one of the keys in protecting our groundwater resources, many experiments have been carried out in order to brighten up our horizon about these topics. Unfortunately most of the present models mainly provide solutions for homogenous systems. They do not account for "preferential flow" like macropores or "fingered flow" (K. BEVEN & P. GERMANN, 1982, P. F. GERMANN, 1990, M. Th. VAN GENUCHTEN, 1994).

The main characteristic of preferential flow is that some of the water infiltrating into the unsaturated zone bypasses the major part of the matrix and quickly moves downwards. We distinguish two different forms of preferential flow: flow through macropores and fingered flow.

F. SCHEFFER et al. (1998) define flow through macropores like this: "A part of the water flows through crevice- and tube-like pores and bypasses water already existing in smaller pores". This description only accounts for big pores, also called secondary- or macropores with a diameter > 60 µm. But there exist many more definitions which have been collected by H. THEURETZBACHER (1997). Generally there seems to be agreement that macropores are characterized by the lack or very small impact of capillary potential and therefore are mainly influenced by gravity. G. M. AUBERTIN (1971) describes them as follows:

"A macropore is a large pore, cavity, passageway, channel, tunnel or void in the soil, through which water usually drains by gravity".

Besides this description which mainly accounts for the hydrologic features of macropores there are many attempts to measure the structure of these voids. But since one can seldomly find regular structures in nature these definitions of size are a more or less arbitrary, because the geometry, continuity or form of the macropores have a much bigger impact on the flow behaviour than this single parameter concerning their diameter (H. THEURETZBACHER, 1997).

The formation of macropores is mainly caused by biogenic or geogenic factors: these are the tunnels of animals or the roots of plants; their diameter ranges from 1 mm to > 5 cm and they are concentrated in the upper soil layers. Outstanding are the cavities made by earthworms which can lead almost vertically into depths of more than 1 m (F. SCHEFFER et al., 1998) and the tubes caused by roots. During their growth they compact the adjoining soil and when the plant dies the rind/bark rotts more slowly than the xylem and a very stable pipe-macropore develops.

Geogenic cavities mainly evolve because of expanding and shrinking processes during periods of wetting and drying. It is also possible that several generations of fissures nest into each other. Uneven wetting can also cause the appearance of shearing-

cracks. Sometimes macropores are created by selective chemical weathering or erosion. These forms are called "soil pipes" and can reach a diameter up to several meters (K. BEVEN, 1982, K. BEVEN & P. GERMANN, 1982, M. KIRBY & J. WILEY, 1980).

Macropores however do not represent a stable system; they are very sensitive to influences of various factors like climate/weather, plants, animals, mankind, ... They can develop in a very short period of time and exist over hundreds of years or be sealed or clogged during one high intensity rainfall (H. THEURETZBACHER, 1997).

In their work the authors G. A. DIMENT & K. K. WATSON (1985) give a historical abstract about occurrences of fingered flow during experiments and along with these they present results of their own studies and their assumptions about the reasons for the instability of the wetting front:

- increasing saturated hydraulic conductivity with depth,
- infiltration into a fine-over-coarse stratified profile,
- initial water content and its spatial distribution,
- sudden and/or gradual change of capillary potential,
- different compaction.

Of course there are some more like the infiltration rate or the flow rate. Another interesting fact is, that there seem to be different kinds of fingered flow: some have a saturated core and an unsaturated domain around the inner part whilst others continuously reduce saturation downwards.

4. Results from Experimental Sites

During the last five years co-ordinated ATH-research activities have been executed at different field sites. These sites have been selected according to the climatic and topographic conditions, according to representative soils and sediments and areas that typically may influence surface and groundwater quality. These areas have been investigated using predominantly either environmental tracers or artificial tracers and in most cases also other results applying traditional evaluations have been available. In this way also scale related questions have been discussed to regionalize local results.

4.1. Berlin Test Site (G. NÜTZMANN, W. STICHLER)

For more than eight years phenomena and effects of surface water pollution with phosphorus because of diffuse sources are studied in Berlin at the Institute of Freshwater Ecology and Inland Fisheries (H. LADEMANN & R. PÖTHIG, 1994, J. GELBRECHT et al., 1996).

Regional mass balance estimations for different European catchment areas showed the risks and significance of diffuse phosphorus leaching from soil and groundwater into surface water (H. BEHRENDT & A. BOEKHOLD, 1993). To understand the hydrogeochemical transport mechanisms and to model the processes of P-leaching in the unsaturated zone, experimental and theoretical investigations have been carried out (S. PUDENZ, 1998, T. TISCHNER, 2000). Among other things, a strong dependence of leaching from subsurface hydrological conditions, i.e. short-term vertical and lateral flow velocities have been detected. Consequently, there was a need for estimating these water flow components at the same field test site where chemical investigations are

carried out. But because the measuring of such processes under field conditions is difficult, it seems to be necessary to improve and complete the results using model calculations and tracer experiments.

The test site is located at a small river named Neuenhagener Mühlenfließ or Erpe, which contributes to the Spree river (Fig. 4.1). The Erpe is flowing through a pleistocen landscape consisting of hydraulically conductive sandy horizons in the unsaturated zone and in the unconfined aquifer (saturated hydraulic conductivity is between 4.5×10^{-5} ms^{-1} and 1.25×10^{-4} ms^{-1}) with a thickness of 10–30 m. At a distance of 40 m eastwards the relief increases and a boulder clay horizon is underlying.

The soil cover with a thickness between 0.15 and 0.45 m consists of fine and middle grained sands with a bulk density of 1.65–1.73 gcm^{-3}. Estimating the hydraulic properties of the unsaturated zone four horizons could be distinguished, where porosities are between 0.31 and 0.36, and saturated hydraulic conductivities are between 195 and 720 cmd^{-1}. The mean groundwater table lies in a depth between 170 and 200 cm below soil surface. An annual precipitation was observed from long-term measurements in summer with 331 mm, and in winter with 254 mm, the groundwater recharge of 180 mm has been calculated after M. RENGER et al. (1989). Many years this section was used to crop barley and rye, but since 1996 no agricultural production was carried out here and the soil surface is grass-covered.

In 1997 the research station was constructed for insitu experiments investigating phosphorus leaching, particularly in the soil and in the unsaturated zone. A complete description of the instrumentation, the research topics and the results are given in T. TISCHNER (2000).

As it is shown in fig. 4.2, ceramic suction cups as sampling devices are installed at six locations (I–VI) in different depths in the unsaturated zone, though it should be noted

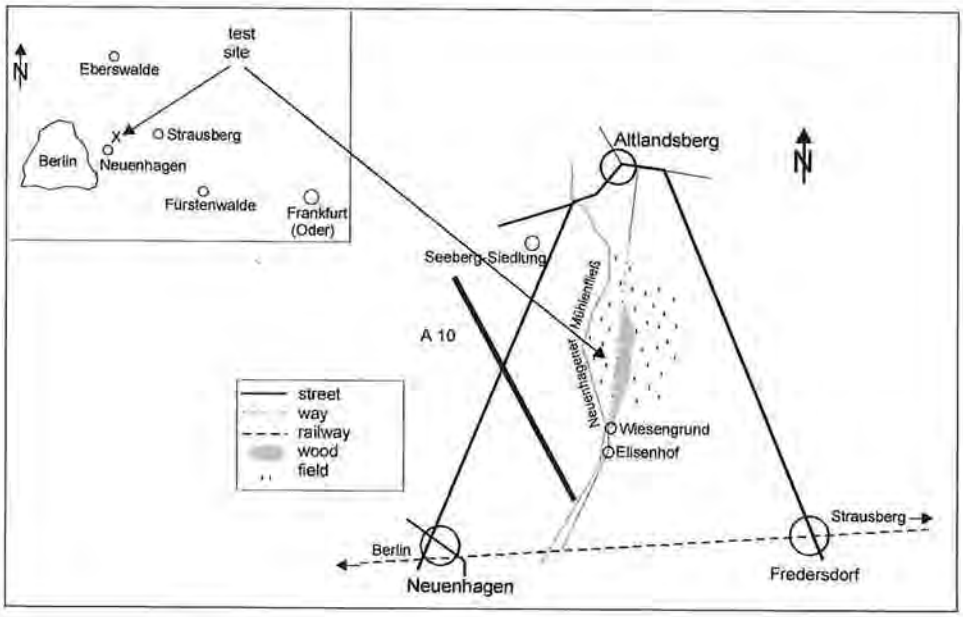

Fig. 4.1: Location map of test site Erpe at Neuenhagener Mühlenfließ, 25 km to the E of Berlin.
Lageskizze der Erpe-Versuchsfläche am Neuenhagener Mühlenfließ ca. 25 km östlich von Berlin.

that the devices are arranged in a transect line crossing the area of the location. Owing to their construction suction cups were held under a constant pressure of 0.4 bar, so that soil water can flow into the collectors continuously. This soil water samples were taken off weekly. At the same depths tensiometers are used to monitor pressure head in the unsaturated zone in intervals of 60 min. The amount of precipitation was measured at the test site automatically also, cumulating the values at every hour. Two observation wells (G4, G3) allow the sampling of groundwater inflow and outflow of the test site, and their water levels are also measured in one-week time intervals.

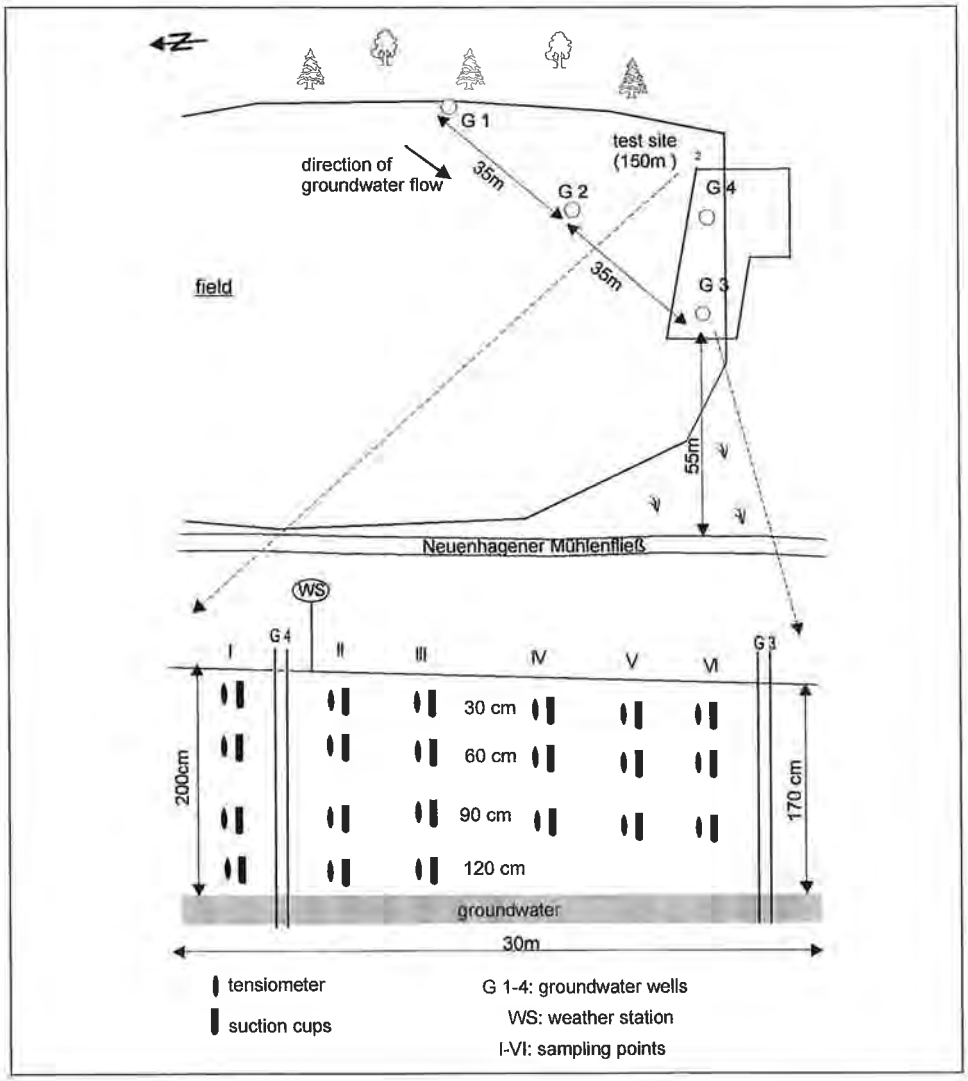

Fig. 4.2: Water sampling points at the test site: WS – rainfall collector, ceramic suction cups in depths of 30, 60, 90, and 120 cm below soil surface, groundwater observation wells G4, G3. Probenahmepunkte auf der Versuchsfläche: WS – Niederschlagssammler, Keramiksaugkerzen in den Tiefen 30, 60, 90 und 120 cm, G4, G3 – Grundwasserbeobachtungsrohre.

The period just before the tracer experiment on March 7, 1999 was characterized by daily fluctuations in temperature between –3 and +5° C, and the saturation of the soil profile was near the field capacity. There was the beginning of the vegetation period, the tufts of grass completely covered the soil surface which was under a small and incomplete snow cover.

In fig. 4.3 monthly sums of precipitation and evaporation are depicted, where evaporation was calculated with the help of PENMAN's formula. During the summer of 1999 there are three months without any precipitation, which considerably affects the effective infiltration rates, so that the surface water balance becomes negative.

Tracer injection was carried out in the morning of March 7, 1999. A dual tracer consisting of 60 g of sodium bromide (Br^-) and 0.5 l of 0.9986 atom-% of deuterium (δ^2H) was dissolved in 200 l water and equally distributed to the soil surface on a 10m² area around the location II during one hour. Thus, we have the initial concentrations of $c_0 = 300\ mgl^{-1}$ for bromide and $c_0 = 2.629$ PPM for deuterium.

The amount of irrigated water (20 mm) are corresponding to a normal spring rainfall event. Because of the actual climatic conditions on March 7, 1999 it could be assumed that evaporation doesn't occur during the tracer application.

As a result of that, a long stagnant period without detectable water movement in the unsaturated zone could be stated and soil water samples are not available from the beginning of July to the end of November 1999.

Figure 4.4 shows the normalized bromide breakthrough curves in different depths of the location II. The graphs show qualitatively plausible concentration curves with respect to the transient behaviour of tracer transport except the data from observa-

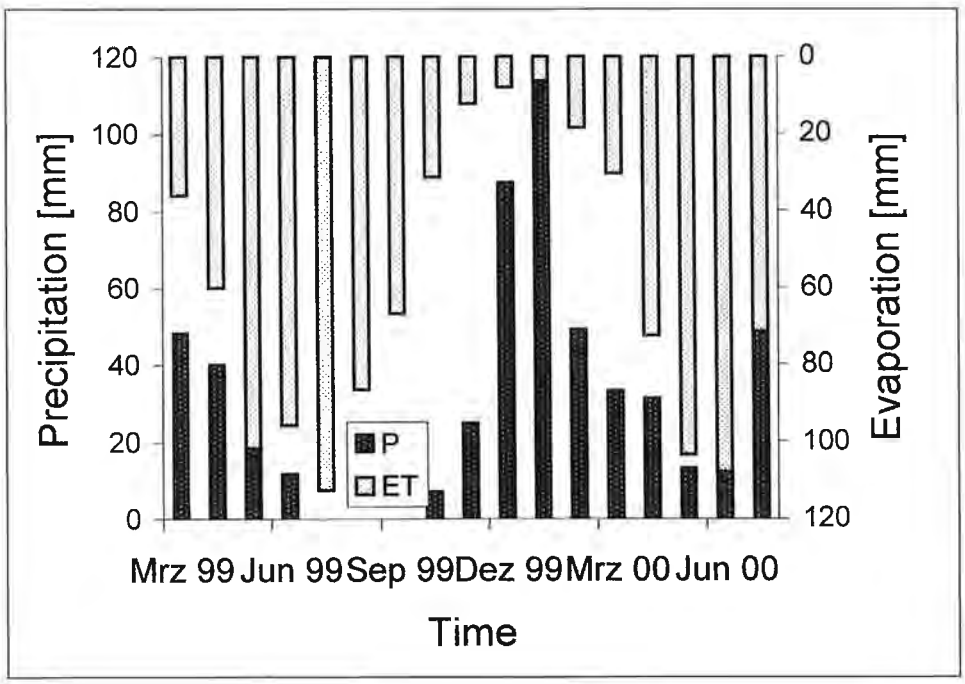

Fig. 4.3: Monthly values of precipitation and evaporation during tracer experiment.
Monatssummen für Niederschlag und Verdunstung während des Versuchs.

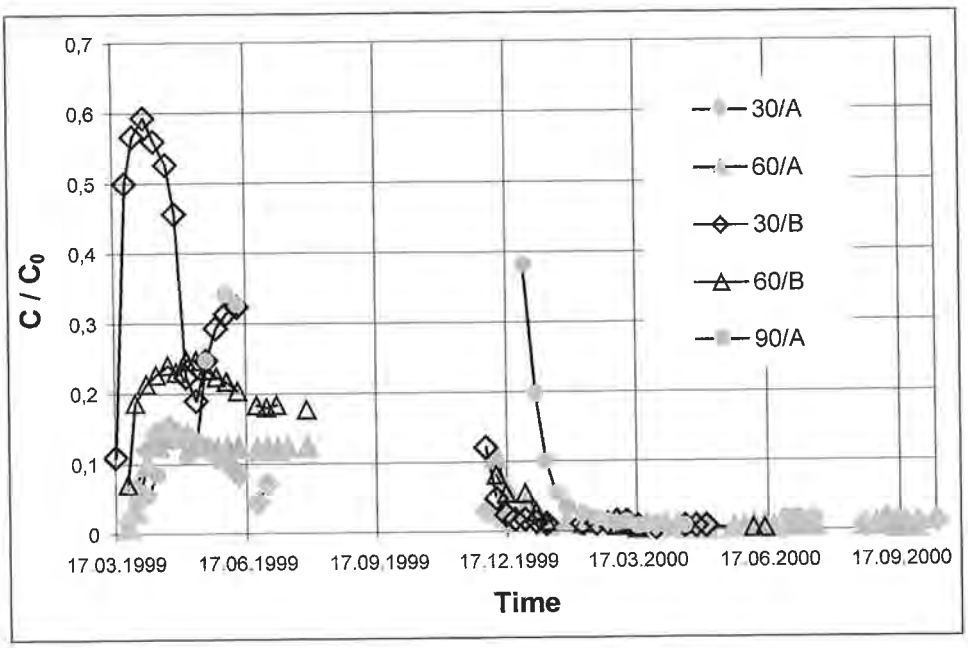

Fig. 4.4: Comparison of normalized bromide concentration breakthrough curves in 30, 60 and 90 cm depth below the location II. A and B denote different spatial positions of the suction cups at location area.
Vergleich normierter Bromiddurchgangskurven in den Tiefen 30, 60 und 90 cm unter dem Messpunkt II. A und B bezeichnen verschiedene Anordnungen der Saugsonden auf der Messfläche.

tion point 30/B. Here, a very rapid and steep breakthrough has been observed because of the fact that the contact between suction cup and soil matrix is not sufficient so that an artificial preferential flow along the cup occurs. Thus, these data has been ignored in further analysis. The arrival time of concentration peaks increases from 30–90 cm depth, but the maximum of c/c_0 also. This could be a sign of preferential flow due to the existence of macropores. The shapes of the breakthrough curves depend strongly on hydro-meteorological boundary conditions, which was discussed above: there are no data from July to November, but the concentration of the tracer remains approximately constant during this period.

Residence times and the velocity of water movement through the unsaturated zone are calculated from these results. The mean residence time belongs to more than three years and the mean flow velocity was between –3.5 and +3.8 cmd^{-1}. Observations in 120 cm depth showed only negligible small tracer signals up to now, and, of course no bromide was found in the upstream groundwater observation well.

Comparison of measured bromide data at the different locations (I–VI) doesn't allow drawing conclusions about lateral water and tracer fluxes during the experiment. Until now, at the locations III–VI bromide couldn't be detected. Due to the hydraulic properties of sediments in the different horizons of the test site classical reasons for the origin of lateral flow components do not exist in a theoretical sense (S. KRAUSE, 2000). But because of large differences in hydraulic conductivity during infiltration in the upper region of soils lateral flow could occur (P. K. ZUIDEMA, 1985).

In fig. 4.5 normalized deuterium breakthrough curves in different depths of the location II are depicted. In contrast to bromide the gradient of increased concentrations is more linear and less steep, and the differences between 30, 60 and 90 cm are not so large than in the case before. But similar to the bromide breakthrough the concentration peaks at 60 and 90 cm seem to be gradually higher than in 30 cm depth. This phenomenon couldn't be explained completely up to now, but on the one hand fluxes through macropores seem to be possible, and on the other hand evapotranspiration may effect soil water movement very strong, especially in dry periods during the tracer experiment. Residence times and the velocities of water movement calculated from these tracer curves are in the same range as shown before.

Using the method of J. FANK (1999) dispersivity coefficients have been calculated from bromide and deuterium breakthrough at several depths on location II as a basis for modelling the tracer transport.

The results summarized in tab. 4.1 show for both tracers an increase in dispersivity coefficients with depth and significant differences between both tracers. Because of investigations of G. NÜTZMANN et al. (1999) the dependence of dispersivity on water content may lead to the first finding, but at this time there is no evidence to support the second one.

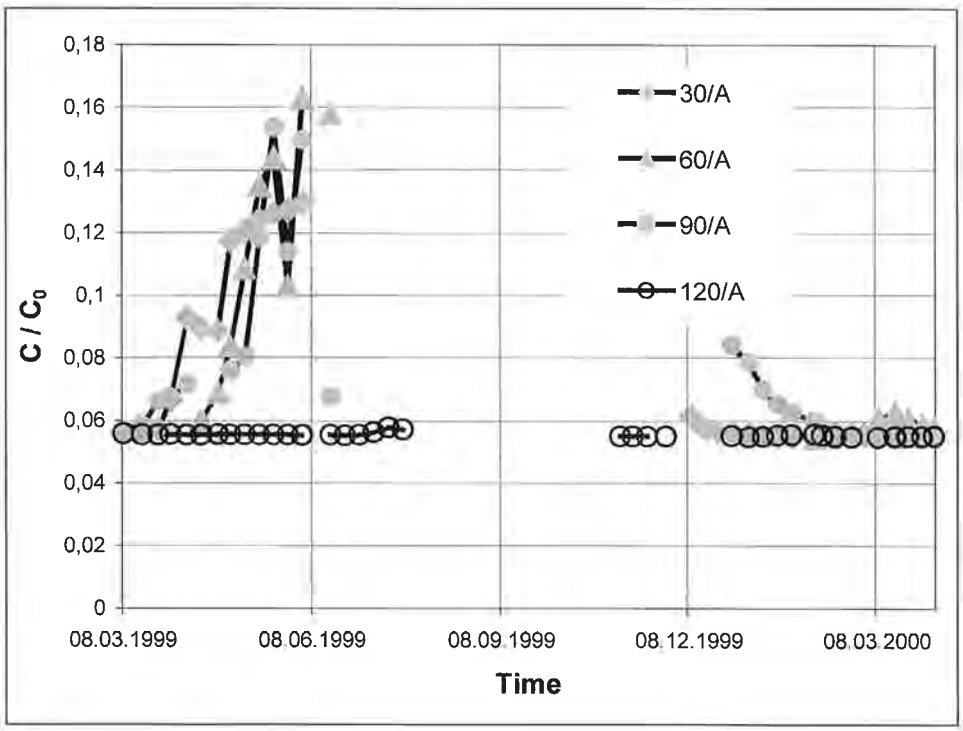

Fig. 4.5: Comparison of normalized deuterium concentration breakthrough curves in 30, 60, 90 and 120 cm depth below the location II. A stands for the position of suction cups on a transect line crossing the area of location II.
Vergleich normierter Deuteriumdurchgangskurven in den Tiefen 30, 60, 90 and 120 cm unter dem Messpunkt II. A bezeichnet die Position der Saugsonden auf einer Transekte quer über die Messfläche II.

Tab. 4.1: Dispersivity coefficients (α_L) evaluated for the 30, 60 and 90 cm depths at sampling point II from breakthrough curves.
Dispersivitätskoeffizienten (α_L) für die Messtiefen 30, 60 und 90 cm, berechnet aus den Durchgangskurven am Messpunkt II.

Measuring depth	Deuterium α_L [cm]	Bromide α_L [cm]
30 cm	2.75	0.43
60 cm	5.5	0.86
90 cm	7.5	2.5

To interpret isolated tensiometer and groundwater measurements as a first step a numerical model was applied based on the code HYDRUS2D (see J. SIMUNEK et al., 1996) to simulate unsaturated/saturated water flow during the tracer experiments (S. KRAUSE, 2000). Results agreed well to measured pressure head patterns and show a plausible flow component distribution. Next, estimated flow velocities and dispersivities resulted from breakthrough curves are used for model predictions of tracer transport based on particle tracking technique (G. NÜTZMANN et al., 2001).

The evaluation of the breakthrough curves from the dual tracer experiment at the Erpe test site leads to the following temporary conclusions:

- It was possible to detect the tracer breakthrough of bromide and deuterium at sampling point II (the area of application) in depths of 30, 60, 90 and 120 cm. At all other sampling points in the unsaturated zone tracer breakthrough doesn't occur, naturally.
- The mean residence time in the unsaturated zone under climatic boundary conditions from March 1999 to December 2000 at the Erpe test site was about three years, which results from mean flow velocities between –3.5 and +3.8 cmd^{-1}.
- The results of tracing experiments indicated that preferential flow may be possible and, together with evapotranspiration they effect water flow and tracer transport in the upper region of soil.
- Indications of a superposition of different flow components in the unsaturated zone are shown by the breakthrough curves, but their significance isn't clear at the moment.
- For modelling of water and solute transport in the unsaturated zone of the test site it will be necessary taking into account heterogeneous structures with respect to hydraulic properties and dispersivity depending on water saturation.

4.2. Test Site Leibnitz, Styria, Austria (J. FANK, W. BERG)

4.2.1. Introduction

Since the beginning of the 90th groundwater recharge mechanism through the unsaturated zone of shallow phreatic aquifer systems in Austria are investigated in an intensive way (P. NACHTNEBEL, 1994, J. FANK & T. HARUM, 1994, E. STENITZER, 1995, F. FEICHTINGER, 1995, J. FANK, 1999). Water movement and the residence time of percolation water in the unsaturated zone depends on the horizon specific water content and the hydraulic potential. These parameters are depending on meteorological parameters, vegetation, land use practices and the characteristic curves of the different compartments. Because the measuring of the latter ones in field applications is very diffi-

cult, it seems to be necessary to proof the results of hydraulic calculations using tracing experiments. Because bromide has very low concentrations in natural environments this salt often is used as a tracer. The results of tracing experiments with bromide can be used for the calibration of solute transport models.

The area of investigation, the so called Leibnitzer Feld is situated in the lower Mur valley, which is filled up with Quaternary gravel and sand with relatively high permeability (saturated hydraulic conductivity equals approximately 5×10^{-3} m/s) and a thickness of 10–15 m. They represent an important aquifer which is intensively used for common water supply of the region. The aquiclude consists of Tertiary strata with generally less permeability. The overburden of the aquifer varies between 1 to 2 m in the Alluvium of the river Mur and reaches up to 7 m under the Pleistocene erosional terraces. The soil cover with a thickness between 0.2 and 2.5 m consists primarily of loamy sands with high field capacities and high permeability under saturated conditions (> 100 cm/d) (M. EISENHUT et al., 1992). Because of the wavy surface of the overlaying loamy and sandy silica cambisoils can change their thickness locally within the range of decimetres (Fig. 4.6).

The mean annual precipitation is 949 mm with its maximum in summer and its minimum in winter, the mean annual air temperature comes to 9° C with the maximum of 19.2° C in July (observation period 1901 to 1980). The groundwater recharge (200–400 mm/y) in the central parts of the Leibnitzer Feld is mainly due to infiltration of precipitation water, especially to snow melt in February and March.

In 1991 an observation station of infiltration water was constructed. The main purpose of the investigations is to intensify the knowledge of the solute transport processes on the seepage path through the unsaturated zone depending on meteorological and soil conditions and the type of agricultural cultivation and to develop land use practi-

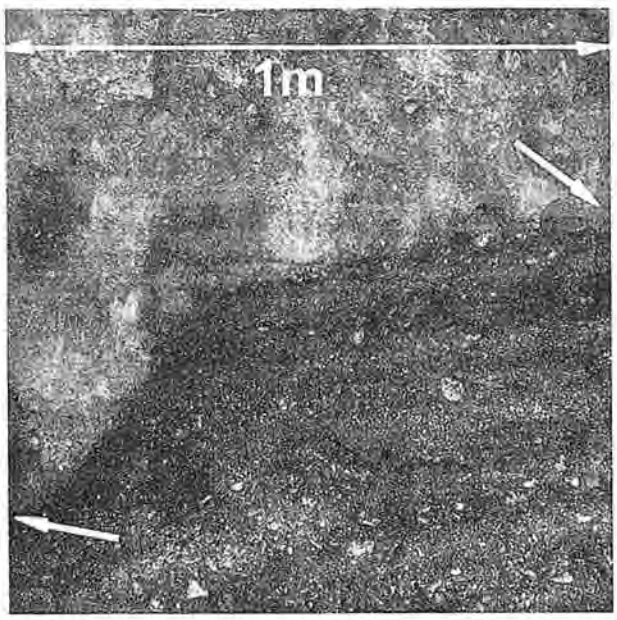

Fig. 4.6: Change of thickness of the topsoil within 1 m of horizontal distance.
Wechsel der Mächtigkeit des Bodens innerhalb einer Horizontaldistanz von 1 m.

ces with reduced impact of fertilizers and pesticides on the shallow groundwater system. A complete description of the research station, the investigations and their results is given in J. FANK (1999).

4.2.2. Tracing Experiments Using Bromide at the Research Station Wagna

In spring 1993 a combined tracer experiment has been carried out with the aim of comparison of infiltration velocities under disturbed and undisturbed soil conditions, comparison of solute transport and water movement, comparison of the mobility of the tracers used, comparison with the transport behaviour of contaminants from fertilization and verification of the model conceptions concerning solute transport in the unsaturated zone.

Suction cups as sampling devices are installed in different depths. Additionally monolithic field lysimeters are accessible for sampling in depths of 0.4, 0.7 and 1.1 m. Small field lysimeters are installed under disturbed conditions in deeper parts (1.5 and 3 m below surface) of the unsaturated zone (gravel and sands). An observation well allows the sampling of groundwater downstream the test area. The groundwater table at mean water conditions lies in a depth of 4.5 m below surface.

The period before the tracer injection on April 14, 1993 was characterized by a long dry weather period and a winter without snow cover. Nevertheless the saturation of the soil profile was near the field capacity. Due to the missing precipitation input there were nearly stagnant conditions in the system. The soil temperatures in all depths indicated that the soils had not been frozen for some weeks. The field with maize monoculture was fallow. At the other field there was the beginning of the vegetation period, the plants of rape were approximately 5 cm high and the leafs completely covered the soil.

The injection of the tracers was carried out in the evening of April 14, 1993. Six kilogramme of sodium bromide were diossolved and injected by sprinkler irrigation during 6 h on both fields (area 10.5 × 9 m on each test site). The regularity of distribution of the artificial rainfall over the irrigated area was controlled by 10 precipitation gages. The amounts of irrigated water (approximately 30–40 mm) are corresponding to a normal summer thunderstorm event.

The results of the evaluation of the breakthrough curves of bromide are summarized in tab. 4.2. The code of the sampling site shows the sampling device (3rd character: M = monolith, W = small field lysimeter with two suction plates, R = small field lysimeter with one suction plate, S = suction cup, G = lysimeter tank), the test field (4th character: R = right [maize monoculture], L = left [crop rotation, rape during the experiment], at the lysimeter tank as 5th character) and the sampling depth (numbers at the end of sampling site in 10 cm) below surface. The groundwater observation well is named GW, the sampling depth in this case is 4.5 m depth.

Figure 4.7 shows the bromide breakthrough curves in different depths on the maize monoculture test field at the research station Wagna. The soil water samples from different sampling systems show well comparable concentrations of bromide, depending on the different residence time in depth. The shape of the tracer curves depend on the hydro-meteorological boundary conditions: precipitation not used for evapotranspiration causes tracer movement downwards and results in concentration peaks of the breakthrough curves. During stagnant periods – if there are water samples available – the concentration of the tracer is nearly constant in time.

As a result of the tracing experiment it is possible to calculate residence time and the velocity of water movement through the unsaturated zone by comparing diffe-

Tab. 4.2: Results of the tracing experiment on April 14, 1993 at research station Wagna (J. FANK, 1999).
Zusammenfassung der Ergebnisse des flächenhaften Markierungsversuches vom 14. April 1993 am Versuchsfeld Wagna (J. FANK, 1999).

Sampling site	First appearance	Peak conc.		Center of gravity conc.		Center of gravity freight		Recovery rate [%]
		Date	[mg/l]	Date	[mg/l]	Date	[mg/l]	
LSML04	930416/10.10	930828/14.10	150.00	930930/16.20	43.87	931007/15.56	63.78	22.10
LSML07	930416/10.10	931118/12.15	58.04	931209/00.47	14.28	931213/01.36	20.76	17.22
LSML11	931023/21.00	931215/11.25	33.13	940217/17.19	8.38	940212/03.17	26.88	25.00
LSWL15	931028/11.05	940128/12.20	23.86	940417/05.26	6.95	940422/11.16	22.59	15.96
LSWL30	940425/12.10	941219/12.30	16.57	950106/03.41	2.65	950219/22.33	9.11	2.77
LSMR04	930416/09.50	931123/12.05	124.40	931111/16.40	33.13	931218/04.16	24.35	12.69
LSMR06	930416/09.50	931109/09.20	73.42	931112/07.58	19.85	931220/09.45	41.62	24.83
LSMR07	930416/09.56	931114/09.56	118.60	931123/13.37	26.09	931223/09.44	55.79	56.02
LSWR15	930423/20.20	940104/15.05	107.98	940201/20.27	23.98	940203/12.55	187.31	92.09
LSRR15	931029/10.05	931216/09.50	58.47	940220/05.05	16.06	940303/16.00	88.27	39.41
LSWR30	931227/14.30	940417/14.00	47.38	940903/03.24	11.62	940925/07.45	16.32	11.95
LSSL11	931025/10.20	931222/10.40	44.51	940104/01.43	10.31			
LSSR04	930418/11.05	930511/09.45	90.86	931014/11.10	31.50			
LSSR07	930425/14.35	931104/10.20	91.17	931117/22.47	23.16			
LSSR11	930423/11.30	931110/09.15	48.48					
LSSR20	930423/12.00	931119/10.50	57.82	940105/10.44	15.72			
LSGVL	930522/17.45	931116/12.05	124.30	940530/22.07	27.71	940719/04.50	153.95	73.05
LSGVR	930416/14.55	931116/10.30	149.10	940104/09.18	32.49	940119/00.58	230.36	78.96
GW	960105/16.40	960711/10.40	0.07					

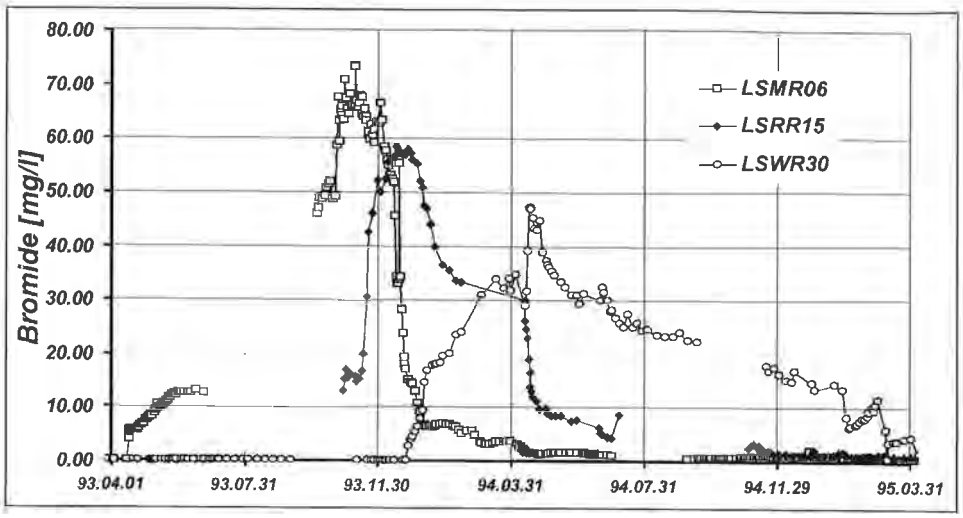

Fig. 4.7: Comparison of bromide concentration breakthrough curves in different depths (60, 150 and 300 cm below the plot under maize monoculture (fallow at injection time April 14, 1993; J. FANK, 1999).
Vergleich der Bromidkonzentrationsdurchgangskurven unter der Maismonokulturparzelle in unterschiedlichen Messtiefen (60, 150 und 300 cm; Brache zum Zeitpunkt der Einspeisung am 14. April 1993; J. FANK, 1999).

rent points of the breakthrough curves with date and time of tracer injection. The results are summarized in tab. 4.3. Under the boundary conditions at test site Wagna from spring 1993 to spring 1997 the mean residence time of bromide in the unsaturated zone was more then 3 y. The mean flow velocity in the unsaturated zone was about 1.4 m/y. The first appearance in the groundwater shows a residence time in the unsaturated zone of more than 2.5 y.

The movement of bromide through the unsaturated zone under different vegetation and cultivation types is shown in fig. 4.8. The mean velocity in the upper soil is significantly lower (0.6 and 1.3 m/y) than in the underlying gravel and sand (1.5 and 2 m/y). This results turns looking to the first appearance of the tracer. In the soil the maximum velocities are 85–150 m/y, to the sampling sites in the gravel and sand (–300 cm) they are between 2 to 4 m/y. Some sampling sites (suction cups) show preferential flow paths in the underlying gravel and sand as well.

The bromide recovery rate in tab. 4.2 shows strong inhomogeneity at the different sampling sites. The recovery rate at the lysimeter tanks (refilled with disturbed soil) is much higher (73–79 %) than the recovery rate under undisturbed conditions. The influence of vegetation and the different thickness of soil is shown in the differences of the recovery rate under crop rotation (16–25 %) and maize monoculture (40–50 %). In both test fields there are some sampling sites, which show influences of mistakes in the construction of the sampling devices (LSWL30, LSWR30, LSML04).

The evaluation of the breakthrough curves from the tracing experiment at the research station Wagna leads to the following conclusions:

– It was possible to detect the tracer breakthrough at different sampling sites in the unsaturated zone and in the groundwater observation well as well. The different

Tab. 4.3: Residence time and flow velocity of percolating water at the research station Wagna evaluated from the tracing experiment on April 14, 1993 (J. FANK, 1999).
Verweilzeiten und Sickergeschwindigkeiten im Bereich der Forschungsstation Wagna aus den Ergebnissen des Markierungsversuches vom 14. April 1993 (J. FANK, 1999).

Sampling site	Maximum velocity		Mean velocity	
	[days]	[m/y]	[days]	[m/y]
LSML04	1.72	85.12	175.96	0.83
LSML07	1.72	148.96	242.36	1.05
LSML	192.17	2.09	303.43	1.32
LSWL15	196.75	2.78	372.76	1.47
LSWL30	375.80	2.91	676.23	1.62
LSMR04	1.70	85.81	247.47	0.59
LSMR06	1.70	128.72	249.70	0.88
LSMR07	1.71	149.80	252.70	1.01
LSWR15	9.14	59.91	294.83	1.86
LSRR15	197.71	2.77	322.96	1.70
LSWR30	256.90	4.26	528.61	2.07
LSSL11	193.72	2.07	264.36	1.52
LSSR04	3.75	38.90	182.76	0.80
LSSR07	10.90	23.44	217.24	1.18
LSSR11	8.77	45.78	209.68	1.91
LSSR20	8.79	83.03	265.74	2.75
LSGVL	38.03	14.40	460.49	1.19
LSGVR	1.91	286.17	279.33	1.96
GW	995.99	1.65	1183.74	1.39

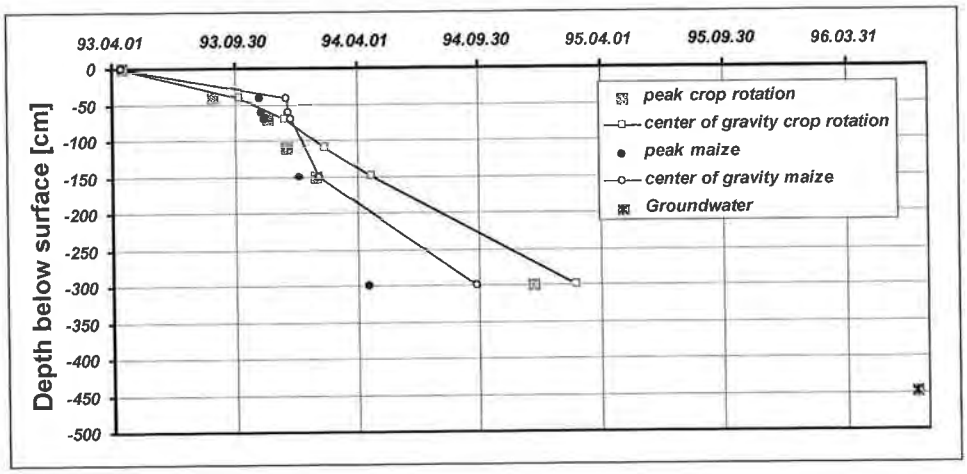

Fig. 4.8: Velocity of bromide transport in the unsaturated zone of the research station determined from the tracing experiment on April 14, 1993 (J. FANK, 1999).
Verlagerungsgeschwindigkeit von Bromid in der ungesättigten Zone im Bereich der Forschungsstation Wagna als Ergebnis des Markierungsversuches vom 14. April 1993 (J. FANK, 1999).

sampling devices lead to comparable results, although the different devices showed different results due to their construction principle.

- The mean residence time in the unsaturated zone under the hydro-meteorological boundary conditions between spring 1993 and spring 1997 at test site Wagna was higher than 3 y. That results to a mean flow velocity in the unsaturated zone of approximately 1.4 m/y. The maximum velocity is 1.65 m/y (residence time more than 2.5 y).
- The results of the tracing experiment indicated that there are preferential flow paths in the upper soil. Some sampling sites showed high velocities in the underlying gravel and sand as well.
- Infiltration rates and velocities are significantly reduced under fields with rotation of crops and short fallow periods. Therefore the type of soil cultivation is an important factor for groundwater recharge and quality.
- All breakthrough curves show indications of a superposition of different flow components. The superposition of breakthrough from systems with different porosity is clearly visible. For the modelling of the transport processes in the unsaturated zone it will be necessary to develop a combined model taking into account the processes of dispersion, diffusion, adsorption and temporary piston flow in a multi porosity system.

Using the method of J.-P. SAUTY (1977) J. FANK (1999) showed the possibility to derive the dispersivity of different parts of the unsaturated zone, the basis for modelling tracer transport. The analytical solution of the convection-dispersion equation (A. LENDA & A. ZUBER, 1970) was the basis to model different components of the tracer breakthrough, calibrating the specific yield. Modelling results were used to correct the measurements of groundwater recharge on small field lysimeters (J. FANK, 1999).

The tracing experiment at research station Wagna was used for validation of the soil water model SIMWASER and the nitrate transport model STOTRASIM (concepts of this model see chap. 5.2.). Using the calibrated model for nitrate transport (measurements of groundwater recharge and nitrate concentration in lysimeters were used for calibration – see fig. 4.9) the tracing experiment was simulated without any fur-

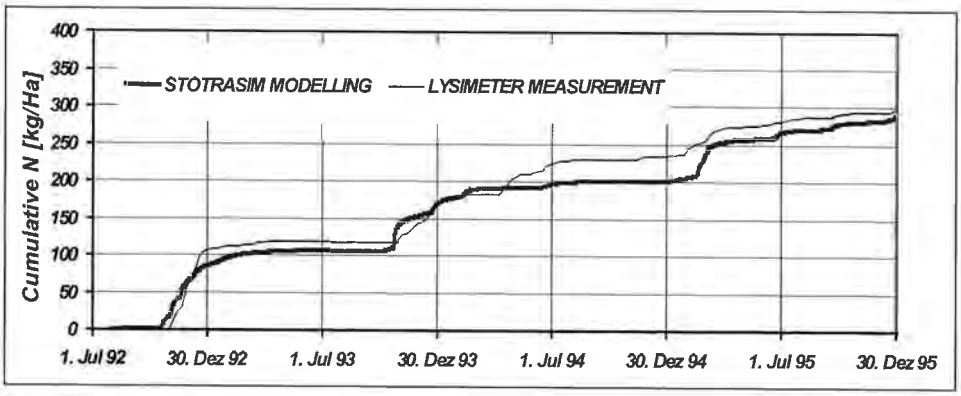

Fig. 4.9: Calibration of STOTRASIM (cumulative sum of N-leaching to groundwater) in 1.5 m below surface on the crop rotation plot.
Modellkalibration STOTRASIM (Summenkurven des N-Austrages ins Grundwassers) in 1.5 m unter Gelände auf der Fruchtfolgeparzelle.

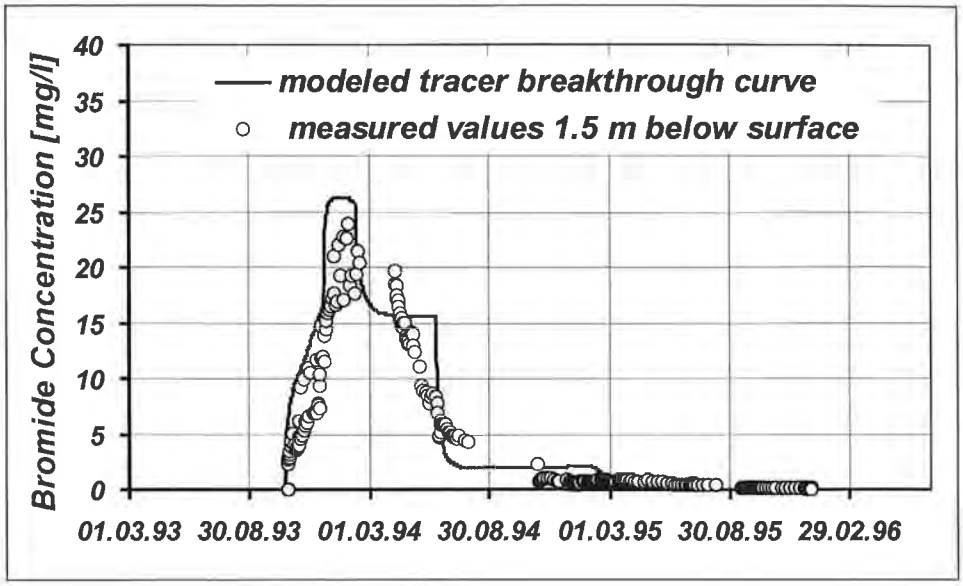

Fig. 4.10: Comparison of measured and modelled bromide breakthrough curves 1.5 m below surface at the crop rotation plot.
Vergleich zwischen gemessenen und modellierten Bromiddurchbruchskurven in 1.5 m Tiefe unter Gelände auf der Fruchtfolgeparzelle.

ther calibration, assuming that bromide is taken up by the plants with the water uptake and assuming no interaction of the tracer with the environment. The result of the simulation in comparison to the measured bromide concentration at the small field lysimeter LSWL15 (in a depth of 1.5 m below surface) is shown in fig. 4.10.

4.2.3. Preferential Flow in the Unsaturated Zone at Test Site Leibnitz

The evaluation of the bromide tracing experiment at research station Wagna showed a sharp reaction of the bromide concentration short time after the tracer injection in the shallowest observation points (Fig. 4.11). At the lysimeters in the soil cover (40 cm, 60 cm and 70 cm below surface) the tracer was detected only a few days after injection, at the field lysimeters in the gravel and sand (150 cm and 300 cm below surface) the first appearance of the tracer was detectable approximately two weeks (150 cm) or some months (300 cm) after tracer injection.

This results led to the conclusion, that in the upper part of the unsaturated zone preferential flow through macropore systems will happen. A second series of experiments was started to detect preferential flow in the unsaturated zone of the test area at research station Wagna. A second aim of this experiment was to detect the spatial variability of the thickness of the soil cover and the different kinds of preferential flow and their importance for solute transport.

Depending on the different soil types at test field Wagna, resulting from two different maps eight profiles have been located for detailed investigations of preferential flow in the upper part of the unsaturated zone (Fig. 4.12).

The investigations do not want to provide new modelling techniques. The aims were to introduce new techniques in visualizing preferential flow (H. THEURETZBACHER,

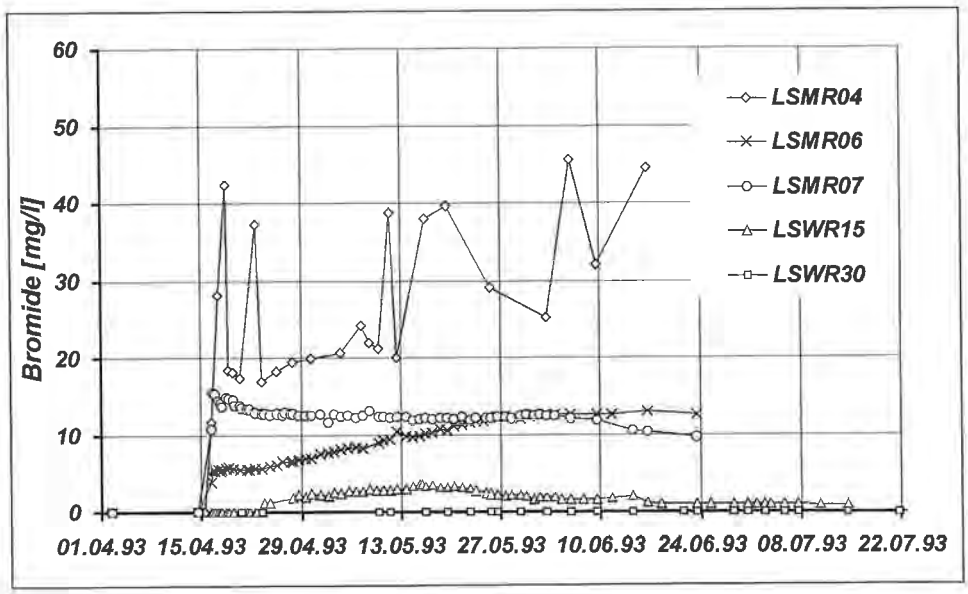

Fig. 4.11: Bromide breakthrough curves in different depths (40, 60, 70, 150 and 300 cm below surface) of the maize monoculture plot at research station Wagna during the first weeks after tracer injection (April 14, 1993).
Bromiddurchbruchskurven in unterschiedlichen Tiefen (40, 60, 70, 150 und 300 cm unter Gelände) der Maismonokulturparzelle der Forschungsstation Wagna während der ersten Wochen nach der Einspeisung (14. April, 1993).

1997) by using methods of remote sensing and satellite image classification (I. FORRER, 1997) in order to make understanding of bypass-flow easier and to show the possible effects and consequences.

Two tracers commonly used are chloride and bromide which have the disadvantage that they cannot be seen by the human eye and samples of a soil profile have to be taken in a regular grid. Dye tracers on the other side can easily be seen and samples taken only from coloured areas. This method also reduces the work in the laboratory. A dye tracer that is easily visible, is not toxic, whose derivatives are not toxic at any moment, whose transport behaviour is similar to that of water and whose solubility in water is very good can be found in Brilliant Blue FCF, also called Acid Blue 9, FD&C Blue No. 1 or C. I. Food Blue 1 (see fig. 4.13 for chemical structure). It is produced in technical grade and food grade and mainly used as a dye in toilet bowl cleaners. Since Brilliant Blue FCF is used in food many tests concerning its toxicity have been carried out.

The sprinkling apparatus has been constructed by H. THEURETZBACHER (1997) following the descriptions of H. FLÜHLER et al. (1994) and its purpose is to irrigate an area of 1 × 1 m as homogeneously as possible. This device is not intended to be a rain-simulator because it does not account for the size nor the impact speed of the drops.

In order to activate preferential flow the uppermost layer of the soil had to be almost saturated because the higher the intensity of the rainfall and the initial water content and the smaller the infiltration capacity the more water bypasses the matrix. To achieve these conditions irrigation was carried out with 40 mm, which equals a heavy

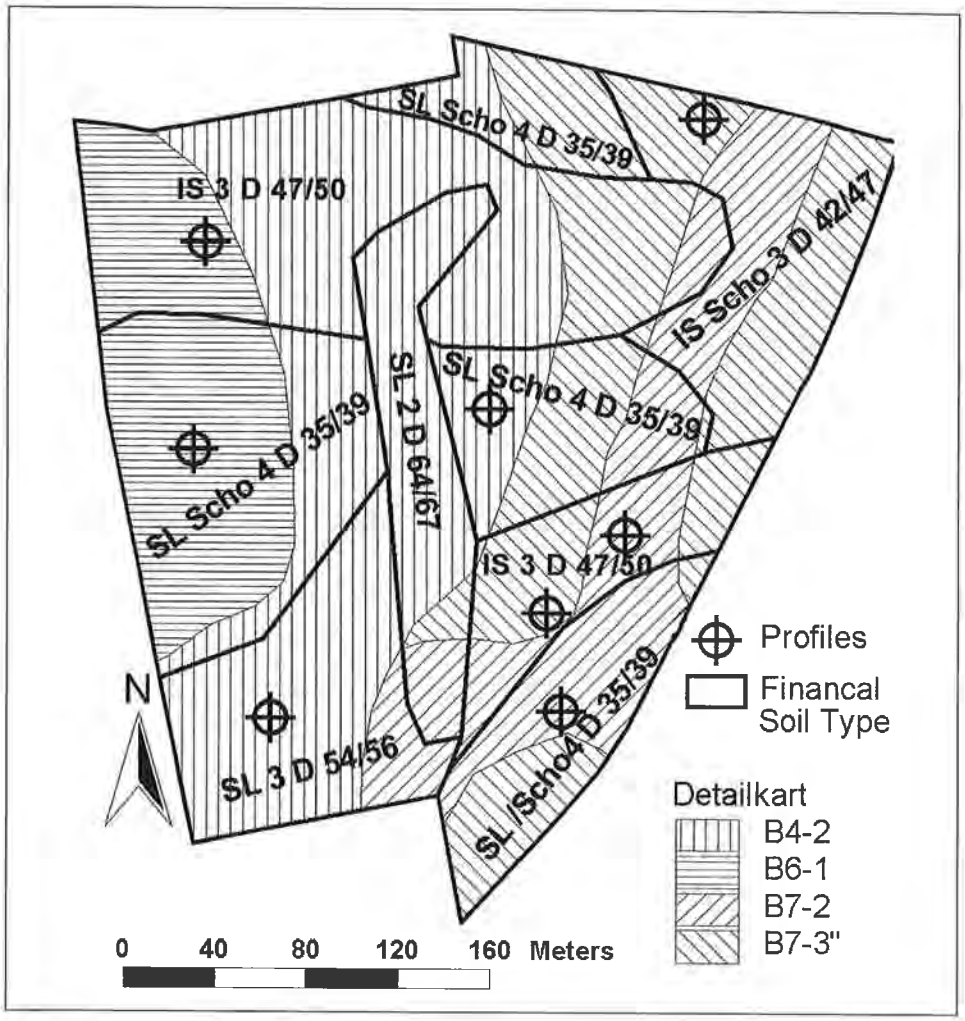

Fig. 4.12: Experimental site with the different types of soil and locations of profiles for the detection of preferential flow system.
Testfläche Wagna mit den unterschiedlichen Bodentypen und den Profilpunkten zur Erfassung des preferentiellen Flusses.

rain that occurs once or twice per year in this region. On one day during the field work we encountered a rainfall with 60 mm in one hour.

Before irrigation about 5 cm of the topsoil were removed to provide homogenous infiltration environment and a plane area over the whole spot. It was tried to choose locations that had not been compacted by heavy farming devices, because that would have reduced the infiltration capacity enormously. In 80 l of groundwater 1,000 g of Brilliant Blue FCF and 30 g of lithium bromide were dissolved. With a generator, a pump and the sprinkler apparatus the solvent was sprayed onto the plot. The irrigation was conducted intermittently and stopped when ponding occurred on the surface; the constant dispersion was controlled with eight cups.

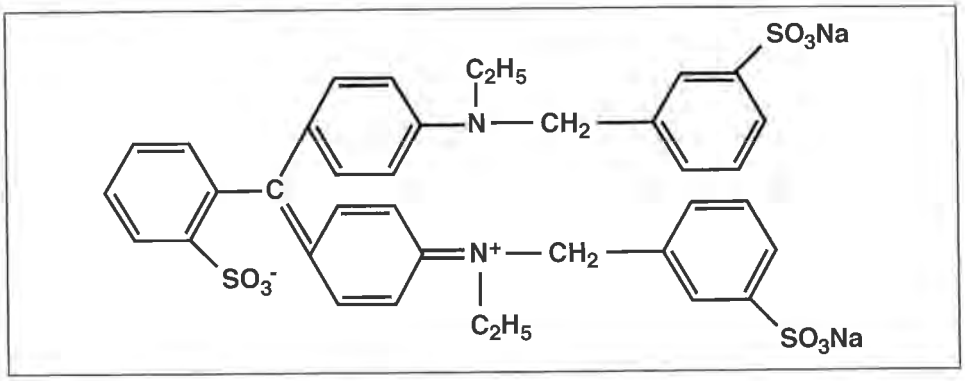

Fig. 4.13: Chemical structure of Brilliant Blue FCF.
Chemische Struktur von Brillant Blau FCF.

One day after the irrigation the excavation was carried out. On each plot six profiles of 1 × 1 m were prepared. The distance between the profiles was 20 cm. In regard to the digital post-processing the field work had to be carried out very carefully to achieve homogenous illumination on the profile. In order to accomplish optimal photo-quality two 800W spot-lights were used to illuminate the profile and a tarpaulin was mounted on poles to protect the plot from direct sunlight and a white sheet was laid into the trench to diffuse the spotlights evenly. Furthermore a grey frame with a measuring tape was attached to the profile to create a standard for the correction of illumination heterogeneity and geometric distortion during the post-processing. To determine the Brilliant Blue FCF concentrations in the soil, samples were taken of the stained parts of the profile. Immediately after sampling, the specimens were cooled and transported to the laboratory. Additionally soil cores were taken following a regular grid.

In the laboratory the samples were weighed, dried at 105° C for 24 h and weighed again to gravimetrically determine the water content. After that 8 ml of a 1 : 4 aqua dest : acetone solution was added to extract the dye. After 4 h of shaking and 48 h of decanting the solution was filtered at 0.45 µm. Because of the enormous light-absorption of the dye the specimens had to be diluted 1 : 10 and photometrically measured at a secondary extinction maximum. As a matter of fact some of the samples unfortunately showed degradation processes which lead to a change of their spectral properties and made them unusable for measuring purposes. Of course these samples were excluded from further processing. Additionally the concentrations of bromide, chloride, nitrate and sulphate were measured ion-chromatographically.

The colour negatives were scanned by Kodak and transferred onto Kodak PhotoCD with a resolution of 3072 × 2048 pixels. These non-orthogonal pictures were orthogonalized by an affine transformation using the measuring tape that was photographed with the soil profile (see fig. 4.14). For this procedure the images were imported into a Geographic Information System (GIS), whose main purpose is the processing of satellite images. Two separate algorithms are required for a geometric correction: first an algorithm that defines the spatial transformation itself and second, an algorithm for grey level interpolation. Special points, so called "ground control points", are needed to describe the spatial transformation over the entire image. GCPs are a subset of pixels whose locations are known in the distorted and corrected image. Polynomial equations are fitted to these GCPs using least squares. Although a higher order polynomial

describes more accurately the transformation in the vicinity of the GCPs, it may introduce enormous errors in those parts of the image further away from the GCPs.

The rectification process was performed with a 3rd order correction and the "nearest neighbour resample method" by using 40 points with known co-ordinates. The maximum geometric error of these 40 points fitting to the polynomial equation was less than two pixels, which corresponds approximately to one millimetre in nature. Furthermore the geometric correction served to decrease the spatial resolution of the images. This adjustment was necessary to reduce computing time and memory requirements.

Although great effort had been spent on illuminating the profile homogeneously, digital compensation for illumination had to be carried out. This was done by using the photographed grey scale and the "method of background subtraction". The trade-off of this procedure is the loss of a part of the dynamic range of the original data. This method used for grey scale images is not suitable for direct application to the red, green and blue colour planes because this operation produces colour shifts that alter the image. So the RGB-photographs had to be converted into the intensity, hue and saturation colour space, the described method applied to the intensity plane and the images converted back to RGB. Then a supervised classification was used to mark areas with the same concentration of the tracer (W. BERG et al., 1999). This method is calibrated by using training areas whose properties are known: this means that the concentrations

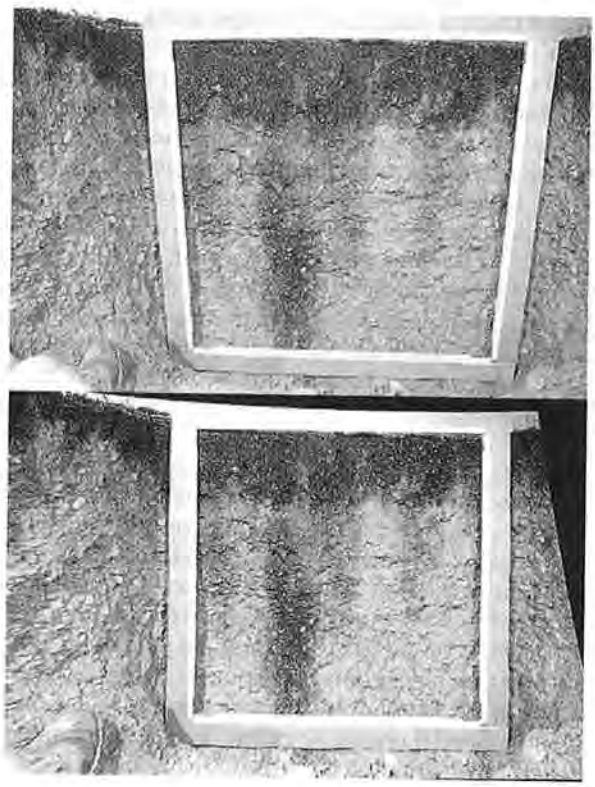

Fig. 4.14: Original and geometrically corrected image of a soil profile (1 × 1 m). Originalbild und geometrisch entzerrtes Bild eines Bodenprofils (1 × 1 m).

of the tracer acquired in the laboratory are linked to the spectral properties of the area where the specimen had been taken in the field. The algorithms of the GIS then search for areas with the same or similar properties and generate a new image that shows the results of this classification (see fig. 4.15 and fig. 4.16).

From the tracing experiments to detect preferential flow at test site Wagna following conclusions can be done:

- During the photographic documentation a lot of attention had been drawn to the light conditions, which have a great effect on the possibilities and the quality of post-processing. It is very important to reduce the influence of sunlight, the reflections from the soil profile or the colour scales as much as possible in order to get fine images.
- If there is a long period between soil sampling and the analysis in the laboratory the specimens should be frozen rather than only cooled, because in our case where it was not always possible to process the specimens right after the excavations some of them showed degradation of the dye and therefore were not of any use for further treatment.
- Another important fact that cannot be left aside is the requirement of hardware and software for "digital image processing". Although the final images need very little hard-disk space the steps in-between require a lot of memory and computing time. During processing one has to calculate at least 200 MB per image which leads to 9.6 GB as in this case where 48 images had to be processed.
- Nevertheless the information acquired is very precise and can be used for further analysis. As mentioned before, one pixel in the image corresponds to one square millimeter in nature.
- The very high correlation between the concentrations of Brilliant Blue FCF and lithium bromide shows that this dye can be used for examining the flow paths of water through the unsaturated zone. The results of H. M. FLÜHLER et al. (1994) are very similar.
- The comparison of the profiles reveals enormous heterogeneity and shows that the flowpaths vary from profile to profile: even if they are separated by 20 cm only.
- These heterogeneities showed clearly that with this scale of observation it is not possible to derive directly the existence or quantity of preferential flow from the soil type, because there are a lot of other parameters that have to be taken into account: such as the distribution of biomass, root density and agricultural land use, but it is a good basis for further investigations.
- In all profiles the tracer got below one meter in less than 24 h, at plot 4 even deeper than 1.7 m, whereby the mean transport velocity for these soils has been calculated with 1.5 m/y (see chap. 4.2.2.), which shows the importance of preferential flow primarily regarding the transport of highly toxic substances and their occurrence in groundwater.
- Furthermore these experiments are a good supplementation to the interpretation of so far unexplainable or unrealistic results of lysimeter studies. Besides this there is good conformity of the instability of the wetting front in sandy soils (Fig. 4.15) according to other studies on this subject. Figure 4.15 also shows that the plough horizon is more or less homogeneously stained and only some fingers are reaching to a depth of about one meter or more.
- In this context it is also interesting that different types of fingered flow were observed like mentioned by G. A. DIMENT & K. K. WATSON (1985): some had a saturated core and an unsaturated zone around it whilst others continuously reduce saturation downwards.

- On the contrary we have loamy soils (Fig. 4.16), where the plough horizon is not homogeneously stained and below that there are only very small coloured areas. These are macropores, mainly wormholes. Below that when reaching more sandy or gravely areas the tracers spreads again and almost homogeneously stains the material.
- Apparently the plough horizon seems to create some kind of barrier. Even in sandy soils as can be seen in fig. 4.15. It is most likely that the pores are smeared and sealed by ploughing. In any case the rapid structural change of the soil lead to horizontal flow and suppresses the vertical flow.
- At some sites the wavy surface of the underlying gravel could be observed very well: e.g. at the excavation plot in fig. 4.6, where the soil depth changed from the right side of the plot from about 40 cm below surface to about 85 cm below surface on the left side of the plot, within one meter of horizontal distance.

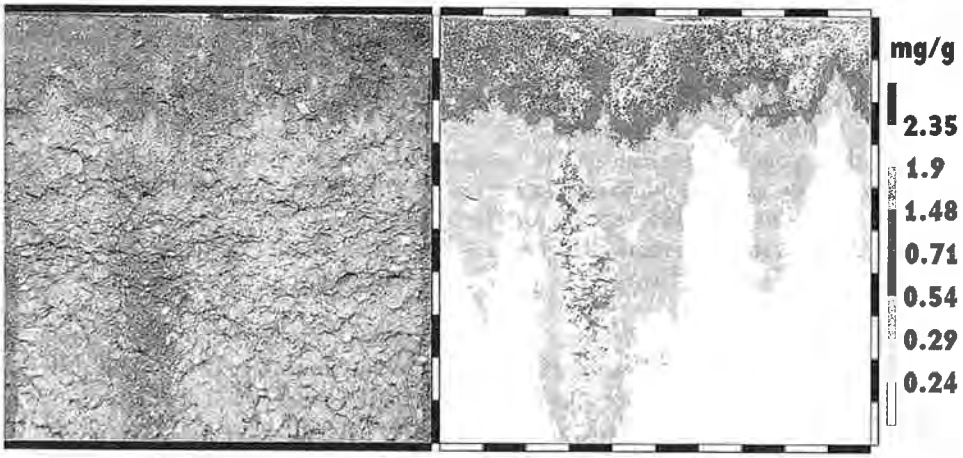

Fig. 4.15: Fingered flow in a sandy soil (1 × 1 m).
Fingerartiges Fließen in einem sandigen Boden (1 × 1 m).

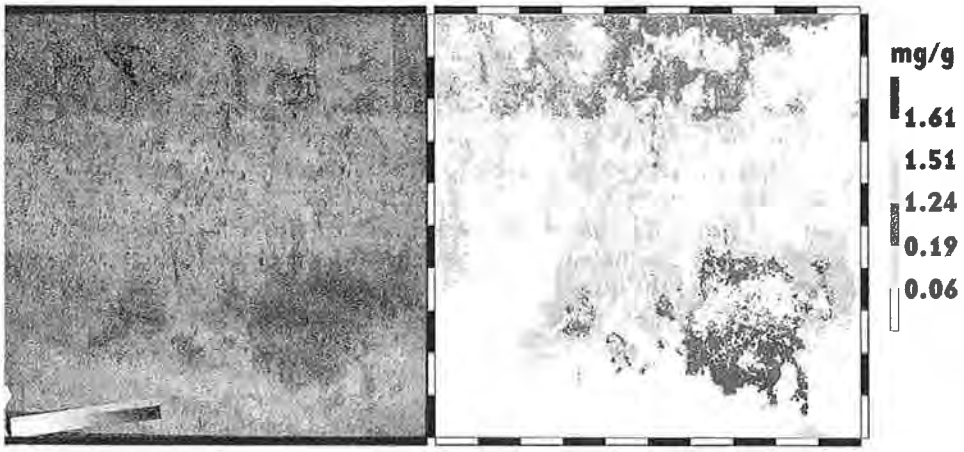

Fig. 4.16: Waterflow through wormholes in a loamy soil (1 × 1 m).
Wasserfluss durch Wurmgänge in einem lehmigen Boden (1 × 1 m).

4.3. Matrix and Bypass-Flow in Quaternary and Tertiary Sediments of the Agricultural Area of Scheyern, South Germany

(K.-P. SEILER, S. SCHNEIDER)

4.3.1. Introduction

The unsaturated zone between land and groundwater surface seems to have limited regulatory functions for water discharges as well as the fate of contaminants on the way to water resources. The main pool of contaminants is the effective root zone in arable soils. At the interface atmosphere and lithosphere, precipitation produces overland flow and partly evapotranspirates. The infiltrating water is either stored or percolates to neighbouring compartments as groundwater recharge or as interflow (see fig. 4.17). These discharge components transport pollutants either dissolved or carry it bound on particles (K.-P. SEILER & C. HELLMAIER, 2000), and may exert adverse impacts on ground- and surface waters.

Porous media often exhibit a variety of natural heterogeneities, such as shrinking cracks, macropores, interaggregate pores and destruction features from humans, animals and plants. All these structures close to the land surface may affect water and solute movement at the macroscopic level by creating widely different flow velocities, often referred to as slow matrix (D. HILLEL, 1971, R. A. FEDDES et al., 1988) and fast preferential or bypass-flow (D. R. SCOTTER, 1978, K. BEVEN & P. F. GERMANN, 1982, P. F. GERMANN, 1990, M. Th. VAN GENUCHTEN, 1994). These phenomena have been studied in structured (K. BEVEN & P. F. GERMANN, 1982) and seemingly homogeneous

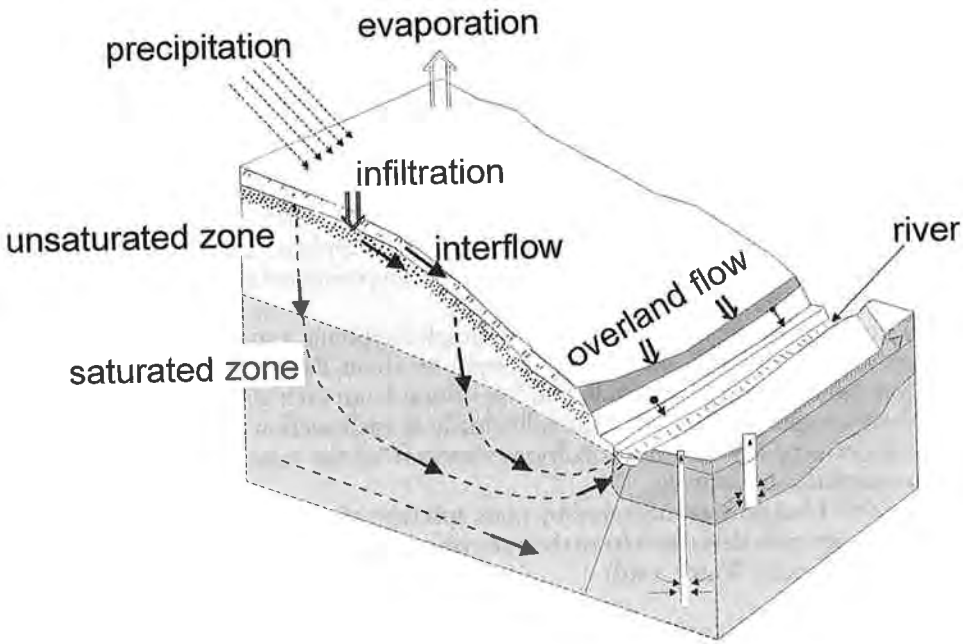

Fig. 4.17: Block diagram of a landscape with the four most important discharge components (evaporation, overland flow, interflow, groundwater recharge).
Blockdiagramm einer Landschaft mit den vier Hauptabflusskomponenten (Verdunstung, Oberflächenabfluss, Zwischenabfluss und Grundwasserneubildung).

coarse-textured soils (R. J. GLASS et al., 1989, R. S. BAKER & D. HILLEL, 1991). Fast flow leads to an apparent non-equilibrium situation with respect to the pressure head or the solute concentration (J. S. Y. WANG, 1991), and severely limits our ability to define initial boundary conditions of flow and reliable forecast of contaminant transport in unsaturated media.

Bypass-flow interacts with matrix flow by means of diffusion and incorporation into the matrix, or produces interflow in hilly terrains. However, it is not well understood:

- how much of the infiltrating water consists of bypass-flow,
- what is its penetration depth according to the type of sediment, its weathering history, its bioturbation, shrinking and swelling and the intensity of the infiltration process itself and,
- how its interaction with matrix flow is governed by capillary force gradients and the respective hydraulic conductivities or by surface tensions along solid surfaces prevailing under dry weather conditions before the infiltration event; both may prohibit or favour the incorporation of bypass- into matrix flow at very low or high pre-existing water contents, respectively.

In order to answer some of these questions, several deuterium tracer experiments were conducted at natural lysimeter installations to analyse and assess different flow components.

4.3.2. Method of Determination of Bypass-Flow

In field experiments areas of melting snow covers ranging from 50–100 m² were traced with deuterium (^2H). The ^2H-tracer is non-reactive, does not undergo significant isotope fractionation in winter (low evaporation) and does not change ion balance of soil water. Deuterium breakthrough has been observed in natural lysimeters (Fig. 4.18) at 10, 20, 50, 90, 130 and 180 cm below the traced surface using three suction cups for water sampling at each observation depth.

Suction cups have been positioned at the end of a 2-inch drilling in 3 m horizontal distance from an accessible vertical shaft (Fig. 4.18); these drillings are full-tubed till 2.7 m from the shaft wall and the conditioned suction cup was introduced at the end of the 0.3 m free standing drill into a predrilled hole applying a diameter lower than the cup itself. The three cups at each depth have been positioned at a horizontal distance of 0.5 m from each other.

Water from the unsaturated zone was sampled applying a suction, which exceeded the prevailing tension in the respective depth by about 100 hPa; the prevailing mean tension dated from a shaft installation 5 m distant from each water sampling shaft.

Water sampling was performed individually at each suction cup most of the year; only under very dry weather conditions waters from the same sampling depth have been sampled cumulatively.

The $^2H/^1H$-ratio was measured by mass spectrometry and concentrations are expressed as per mille deviations from the international standard V-SMOW (Vienna-Standard Mean Ocean Water, vstd).

$$\delta^2H = \frac{^2H/^1H_{sample} - ^2H/^1H_{vstd}}{^2H/^1H_{vstd}} \cdot 1000\ [‰], \qquad (4.1)$$

whereby negative δ-values indicate lower concentrations than the standard and vice versa.

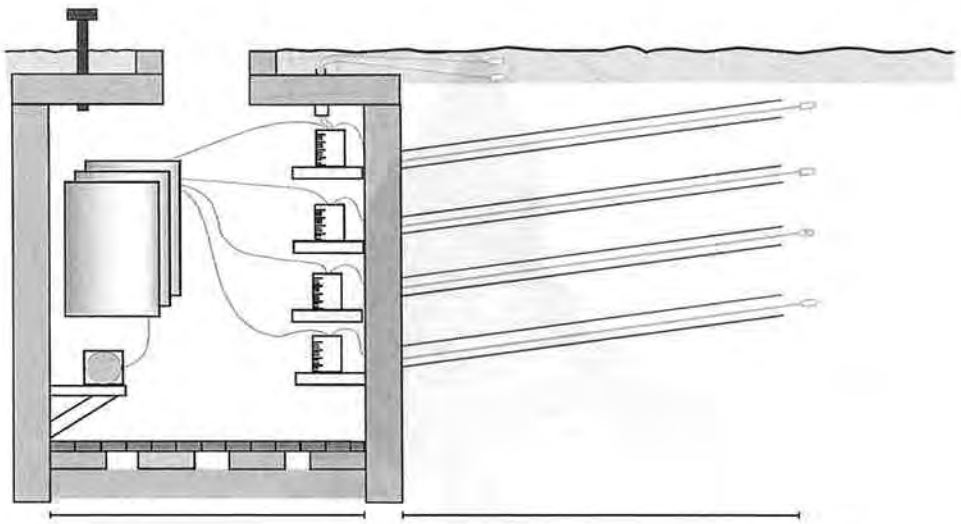

Fig. 4.18: Design of a natural lysimeter with suction cups, which were located 3 m away from the shaft wall in the unsaturated zone. At each depth three suction cups at horizontal distances of 50 cm have been installed in the 30 cm freestanding end of a tubed horizontal borehole. Skizze eines Naturlysimeters mit Saugkerzen, welche 3 m von der Schachtwand entfernt in der ungesättigten Zone situiert sind. In den jeweiligen Messtiefen wurden drei Saugkerzen im Horizontalabstand von 50 cm am 30 cm langen freiliegenden Ende einer verrohrten waagrechten Bohrung installiert.

4.3.3. Results on Bypass-Flow and Interflow

Tracer experiments have been performed once at eight sites in Scheyern during the years 1995 to 1998. These tracer experiments have been observed throughout 3–4 y in three replicates each depth. Tracing instantaneously the melting snow of areas of 50–100 m^2 over Loess, sand and gravely sand produced for percolation water a DIRAC signal along a hydraulic potential plane. Applying the well known advection dispersion theory (R. A. FREEZE & J. A. CHERRY, 1979) homogeneous flow transforms the DIRAC signal into a GAUSSian distribution of the concentrations at defined time steps throughout the extent of the profile; this, however, has never been observed (Fig. 4.19) in eight experiments performed in the study area.

The evaluation of tracer breakthrough curves clearly indicates, that flow in the unsaturated zone is not homogeneous; contrary, a detailed evaluation showed that it is dominated by different forms of slow matrix flow, and superimposed at the beginning of the tracer experiments by positive and thereafter by negative peaks in the breakthrough curve (Fig. 4.20), which all must be attributed to bypass-flow occurring during storm events. The observation (Fig. 4.20) and interpretation of deuterium breakthrough (W. KÄSS, 1998) at similar or different depths clearly documents this lack of homogeneity in the flow.

It becomes evident from breakthrough curves of deuterium experiments that matrix flow ranges at 0.7–1.2 m/y in Loess and Tertiary sands/gravels, respectively. Infiltration ranged from 150 mm/y in the Loess and at 200 mm/y in the Tertiary sand/gravel site. Contrary to matrix flow, bypass-flow has been evaluated to range between

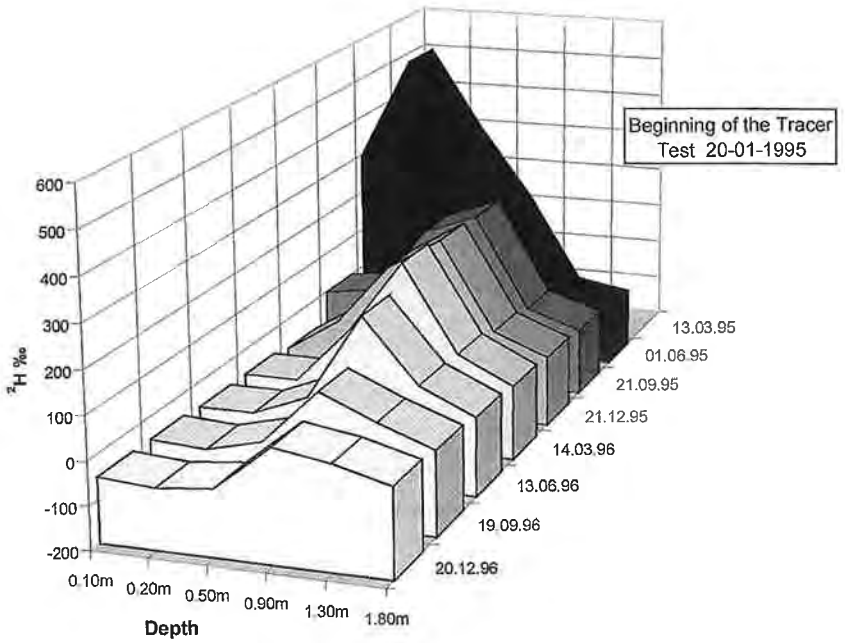

Fig. 4.19: Concentration distribution of deuterium throughout the profile at given time intervals. Verteilung des Deuteriumgehaltes im gesamten Profil bei gegebenen Zeitintervallen.

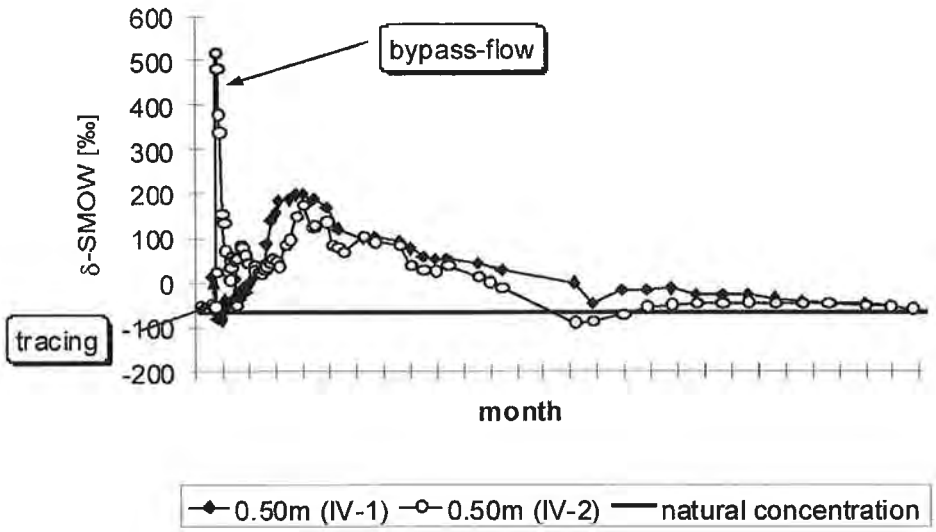

Fig. 4.20: Breakthrough curves of deuterium, observed by extracting water from the same sampling depth through three suction cups 50 cm distant from one another, documenting slow matrix and fast bypass-flow in Loess.
Durchgangskurven für Deuterium in den von drei in 50 cm Abständen angelegten Saugkerzen gewonnenen Wasserproben; sie zeigen einen langsamen Matrix- und raschen Bypass Flow im Löß.

0.7 m/d and 2 m/d in all studied sediments and may approach flow velocities of overland flow; it was observed till depths of 1 m in Loess, 1.5 m in Tertiary sands and deeper than 3 m in Quaternary gravels.

Standard calculations of seepage velocities based on tensiometer- and TDR-observations from respective installations 5 m distant from water sampling installations do not allow to differentiate between slow and quick flow. Such a differentiation, however, was possible through ^2H-experiments, if tracer concentrations in the breakthrough exceed the mean of natural annual ^2H-concentrations by at least two orders of magnitude, because bypass-flow contributes only minimally to matrix flow at each individual infiltration event (chap. 2.).

Results on bypass-flow have been related by mathematical modelling to the generation mechanism of discharge components (interflow and groundwater recharge), K.-P. SEILER & D. BAKER (1985), and have been quantified on a larger scale than shafts analysing the discharge from transient and perennial creeks in the catchment. The analysis of discharge was based on hydrograph methods to distinguish between direct and indirect runoff and on the analysis of the natural environmental stable isotope information during storm events allowing to calculate mixing ratios between storm and pre-storm waters (M. G. SKLASH et al., 1976) and to differentiate between contributions of interflow to overland discharge having similar flow velocities and contributing both to direct runoff.

K.-P. SEILER & D. BAKER (1985) have shown that permeability changes along interfaces may favour lateral flow of seepage according to the inclination of the interface and the differing hydraulic conductivities along it (capillary barrier concept). A tracer result from the unsaturated zone as compared to the saturated zone is shown in fig. 4.21. During infiltration events such interfaces transform fast seepage flow into fast lateral or interflow (in hilly terrains), and thus enhance direct runoff. Most of these interfaces are of anthropogenic, rock dilatation, or, in the environment of formerly glaciated areas, of permafrost origin, and parallel morphology.

Using hydrograph analysis it was demonstrated on the catchment scale of the study area that discharge (200 mm/y) produce about 21 % of direct and 75 % of indirect runoff. Analysing direct discharge using environmental stable isotopes leads to less than 7 % of flow with weak contact to solid surfaces or stored water and thus equalling to the environmental isotope or chemical signature of precipitation (overland flow), and more than 14 % of quick flow was in close contact with solids and reservoirs exceeding by its water contents the infiltration (interflow); in areas without baseflow this discharge component equals to the environmental isotope or chemical signature of matrix flow. The missing 4 % of runoff are within the error bare or may be interpreted as bypass-flow that joint matrix flow.

The mean annual interflow of more than 14 % varied in between none and over 60 % of individual infiltration events, and depends on initial hydraulic conditions at the soil surface as well as on the intensity, duration and quantity of rainfall events. Based on the analysis of a time period of 8 y, only precipitation exceeding 2–4 mm/d produced overland and interflow, and interflow was highest under very wet (snow melt conditions) and very dry pre-storm conditions; in between this two extreme conditions it was less pronounced; this is attributed to a predominance of gravity forces in wet respectively surface tension of dry sediments, which both favour bypass-flow.

Bypass- and interflow mostly seem to be strongly associated with human, animal and plant activities in the effective rote zone. Consequently, hydrograph analysis demonstrated, that the inverse value of the dry weather recession factor for direct runoff,

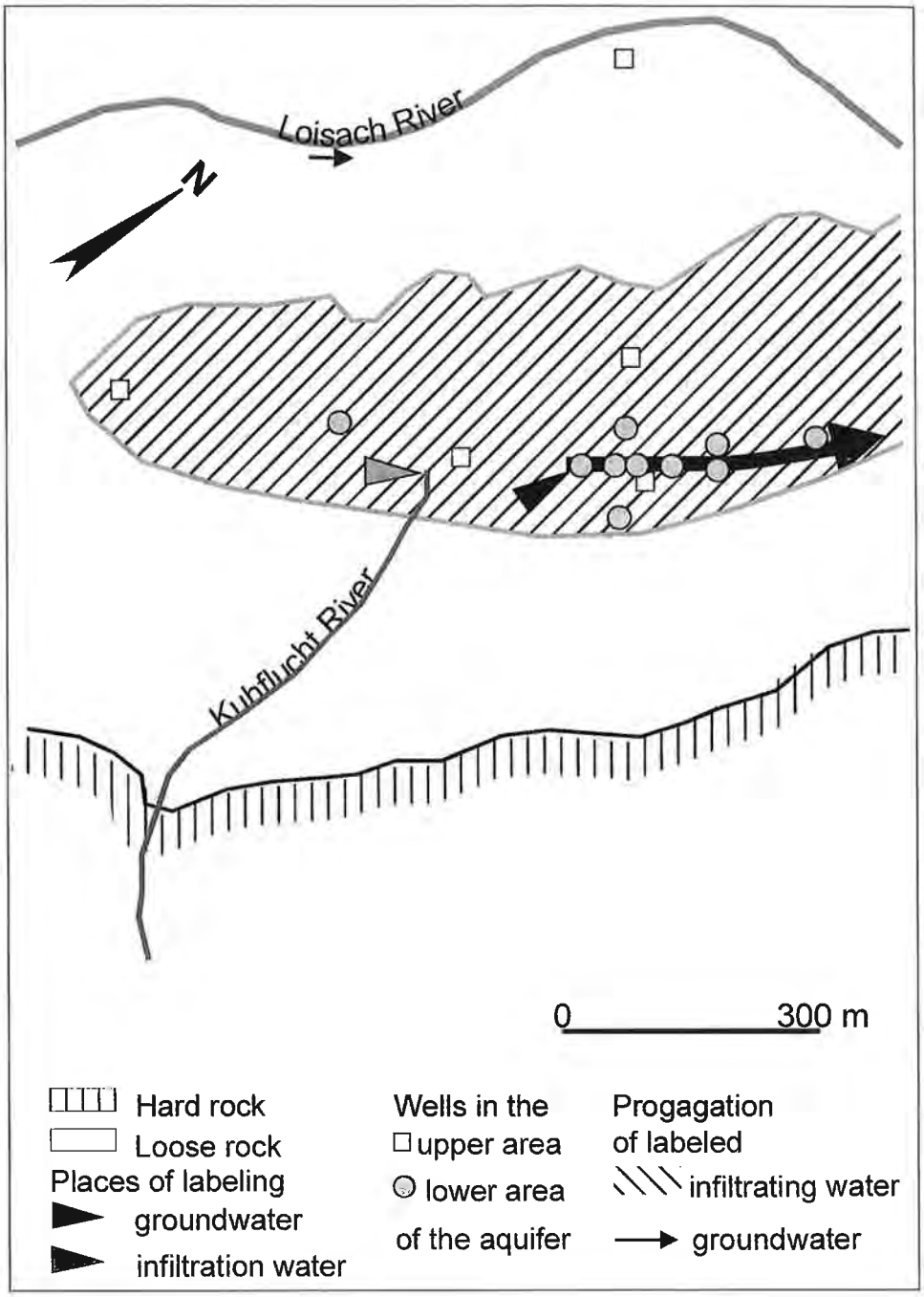

Fig. 4.21: Comparison of results of a tracer experiment executed over a river cone through the unsaturated zone (hatches area) with a tracer input into groundwater (arrow).
Ergebnisse eines Markierungsversuchs in der ungesättigten Zone (schraffiert) und einem Tracerinput in das Grundwasser (Pfeil).

which represents in areas without groundwater outflow the mean residence time, was shorter in the vegetation period (30 d) than during winter season (60 d).

As compared to crops in the study area, mean residence times of interflow were found to be lowest in grasslands, medium in arable lands and highest in forest areas, and in all the above mentioned areas seasonal variations were observed.

4.3.4. Conclusions

Flow in the unsaturated zone is often so inhomogeneous that sampling on fixed points delivers more reliable results for scaling up in a catchment than sampling by coring and extracting water from soil samples or unsaturated sediments. Only mass transport studies contribute to distinguishing between different forms of seepage flow like bypass- and matrix flow; whereas classical hydraulic observations in the unsaturated zone do hardly as well. The velocities of bypass-flow are in the same order of magnitude as overland flow and, in hilly terrains, turns into lateral or interflow at hydraulic interfaces paralleling morphology.

Interflow and overland flow reduce groundwater recharge. Agricultural activities in hilly terrains influence predominantly infiltration and overland flow; contrary, groundwater recharge is mainly influenced by geologic structure and texture properties of the sediments (H. BEHRENS et al., 1980). Changing agricultural activities therefore predominantly impact the contribution of discharge to overland and interflow and lesser impact on groundwater recharge. Only changes from crop into grassland will change groundwater recharge on a long run.

Since matrix flow is too slow to recognize changes of land use on the groundwater quality in short times, the analysis of export processes in the effective root zone (K.-P. SEILER & C. HELLMAIER, 2000) or in the direct runoff deliver quick information on both small and large scales of a catchment as compared to respective changes in the groundwater quality.

Acknowledgements

The scientific activities of the FAM Research Network on Agroecosystems are financially supported by the German Ministry of Education and Research (BMBF 0339370). Overhead costs of the Research Station of Scheyern are funded by the Bavarian State Ministry for Science, Research and the Arts.

4.4. Experimental Field Site Sinji Vrh (M. VESELIČ, B. ČENČUR CURK, B. TRČEK)

4.4.1. Introduction

Fractured and karstified rocks are very heterogeneous and complex in terms of their geometry and void topology. This results in parameter variability and large uncertainities reflecting complicated hydraulic, mechanical, thermal and chemical processes. Therefore, detailes studies of these processes have to be performed on a macro scale, at experimental field sites (B. ČENČUR CURK, 1997). Such experimental field site was planned (M. VESELIČ, 1995) and equipped at Sinji Vrh in the western part of Slovenia (Fig. 4.22).

The main goal of the in situ-experimental studies at experimental field site Sinji Vrh (EFS Sinji Vrh) was the study of flow and solute (pollutant) transport in fractured and karstified rocks, particularly in the unsaturated zone and its epikarstic zone. These results

Fig. 4.22: Location of the experimental field site Sinji Vrh (EFS Sinji Vrh).
Lage des Testgebietes Sinji Vrh (TG Sinji Vrh).

were compared with monitoring of the karst aquifer outflow 600 m below the experimental field site in Hubelj spring. Regionalization of study results could enable us to determine vulnerability, which is a prerequisite for sustainable groundwater management.

4.4.2. Site Description

The experimental field site Sinji Vrh is located in the western part of Slovenia (Fig. 4.22) at the edge of the Trnovski Gozd plateau (mean altitude of 900 m a.s.l), which is an overthrust (Trnovo nappe) of carbonate rock over Eocene ($E_{1,2}$) flysch. This area is composed of Jurassic (Lias–Dogger) limestone, which passes laterally into crystalline dolomite. The beds dip in general towards SW and dip angle changes between 30° and 60°. This territory is crossed by the subvertical Avče fault with a Dinaric direction (NW–SE).

The area was divided according to permeability of their lithological characteristics in several hydrogeological units (J. JANEŽ, 1997). Well permeable aquifers with fractured and karstic porosity are formed in limestones of Upper Triassic to Upper Cretaceous age. Permeable rocks with fractured porosity are built by Upper Triassic dolomite. Well permeable sediments and rocks with intergranular porosity are built by coarse grained to block shaped Quaternary periglacial breccias on slopes and cover the impermeable flysh rocks. The geological profile of the Trnovski Gozd plateau is presented in fig. 4.23 (J. JANEŽ, 1997).

The groundwater horizon lies extremely deep and appears on the surface at the lowest point of the impermeable flysh border in karstic spring Hubelj. Water generally flows out of the bedplanes, widened by corrosion (J. JANEŽ, 1997). In dry periods the spring outlet is at 240 m a.s.l. and the minimum discharge is 0.185 m^3/s. At high waters the water level rises up to 40 m and the disharge increases up to 59.5 m^3/s. The mean discharge is 3.03 m^3/s (M. PETRIČ, 1997). The catchment area of the Hubelj spring are carbonates of Trnovo Plateau and can be estimated at about 50 km^2.

4.4.3. Field Research Studies

The specific characteristics of fractured and karst aquifers can be understood only on the basis of integrated results of different research methods. Therefore several research methods were used at the experimental field site Sinji Vrh and are listed in tab. 4.4.

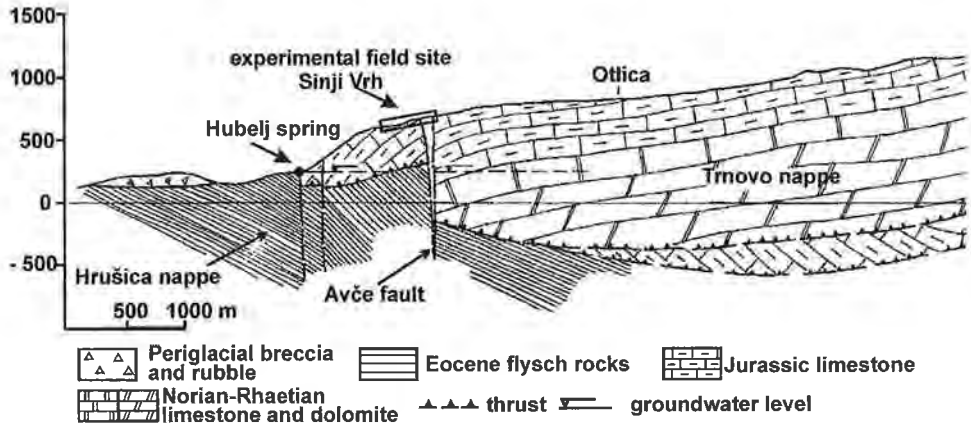

Fig. 4.23: Geologiocal cross-section of Trnovo plateau (J. JANEŽ, 1997).
Geologischer Schnitt durch das Trnovo Plateau (J. JANEŽ, 1997).

4.4.4. Experimental Design

The experimental field site in the unsaturated zone of fractured and karstified rock presents a 340 m long artificial research tunnel, 5–25 m below the surface (Fig. 4.24). The tunnel direction is nearly constant running SW–NE (N66°E). The surface is covered with grassland and small beech forests which usually cover outcrops. The unsaturated fractured and karstified limestone has a negligible matrix porosity and very high fracture density with some greater conduits (B. CENČUR CURK & M. VESELIČ, 1999).

Tracer experiments were performed at the north-western part of the research tunnel, where the distance to the surface is 10–15 m (Fig. 4.24). An agrometeorological station (Fig. 4.25) has been installed on the surface, where precipitation, evaporation, air temperature, air moisture, wind speed and direction (both at two levels) are continuously measured.

From the structural analysis and detailed fracture mapping (1 : 20 scale) we were able to properly position injection holes, which were positioned above the tunnel (Fig. 4.24, 4.25). The injection holes were drilled through the soil cover in order to avoid interaction between tracer and soil. A plastic tube was inserted in order to prevent their colapse and chemical reactions between the injected tracer and the soil. For the special tracer experiment (P4; tab. 4.4) one injection hole was drilled into soil, another to the soil rock interface and one into fractured rock (K. WITTHÜSER & B. ČENČUR CURK, 2000). On the meadow an area of 150 m^2 was used for fertilization experiment (Fig. 4.25). For that purpose suction cups in two levels (depth of 15 and 45 cm) were installed in the karstic soil above the research tunnel. The soil is a typical karstic soil (calcaric brown soil) with characteristic deeper pockets extended along weak zones like fractures in the underlying rock. In a 0.7 m deep soil profile the Ah-horizon has a thickness of 15 cm and B-horizon a thickness of 55 cm. In the latter an upper horizon with more roots and higher organic content can be distinguished.

For tracing tests and fertilization experiments a special water collecting structure was made and installed into the research tunnel. Each segment of the construction consists of metal girders on which a plastic sheet was tightened. Special funnels were made

Tab. 4.4: Field research studies at experimental field site Sinji Vrh.
Feldforschungen im Testgebiet Sinji Vrh.

Completed studies	• **Petrographical, lithological, structural, karstological studies** • **Pedological study** • **Hydrogeological study** • **Geophysical studies:** ➢ geoelectric tomography of the tracer experiment area ➢ ground penetrating radar technique (GPR) of the area above the research tunnel • **Laboratory tracer tests** of carbonate material under saturated and unsaturated conditions with NaCl and uranine tracer • **Tracer experiments** within an intensively fractured rock test area: ➢ NaCl field tracer experiments with tracer injection beneath soil cover within a fractured rock test area under saturated (P1) and unsaturated conditions (P2) ➢ uranine, NaCl, KCl, $MnCl_2$, $CuSO_4 \cdot 5H_2O$, $NiSO_4 \cdot 6H_2O$ field tracer experiment (P3) with tracer injection beneath soil cover within a fractured rock test area ➢ tracer experiment (P4) with injection in the soil, at the soil-rock interface and in the fractured rock with different tracers ($MnCl_2$, $NiSO_4$ and uranine) • Two **fertilization experiments** (G1 and G2) with fertilizer calcium ammonium nitrate spreading on soil cover within the fractured rock test area
Continuous studies	• **Hydrometeorological measurements:** temperature, wind speed and direction at two levels (0.5 and 2 m), relative humidity, evaporation and rainfall recording
Studies under way	• **Isotope and hydrogeochemical study** concerning basic physical and chemical parameters, DOC, isotope composition of oxigen, deuterium and carbon in precipitation, soil atmosphere, unsaturated zone water and aquifer outflow water (the karst spring Hubelj); long term (monthly) and short term observations (storm event) are included • **Agrohydrologic study** on lysimeter with recording of climatologic data and dynamics of migration of nitrogen and phosphorous compounds into the underground • **Modelling:** water flow and solute transport model evaluation of the obtained NaCl, uranine and other field tracer tests data from tracer injection beneath soil cover within the fractured rock test area
Planned studies	• **Geophysical study** of the research facility area by seismic "crosshole" measurements, additional ground penetration radar measurements and geoelectrical surface mapping • **Microbiological study:** tracing with phages and study of biochemical processes and related microorganisms • **Isotope and hydrogechemical study** of additional fast flow monitoring during new storm events • **Continuous monitoring of:** ➢ soil conditions in different depths (T, moisture content, soil atmosphere) ➢ water inflow rates in the research tunnel, especially in the areas supported by concrete (crushed zones) • **Tracer experiments:** NaCl, uranine and other field tracer tests with tracer injection beneath soil cover within a poorly fractured rock test area • **Modelling** water flow and solute transport model evaluation of the obtained NaCl, uranine and rhodamine field tracer tests data from tracer injection beneath soil cover within the poorly fractured rock test area on the basis of integrated results of all applied research methods

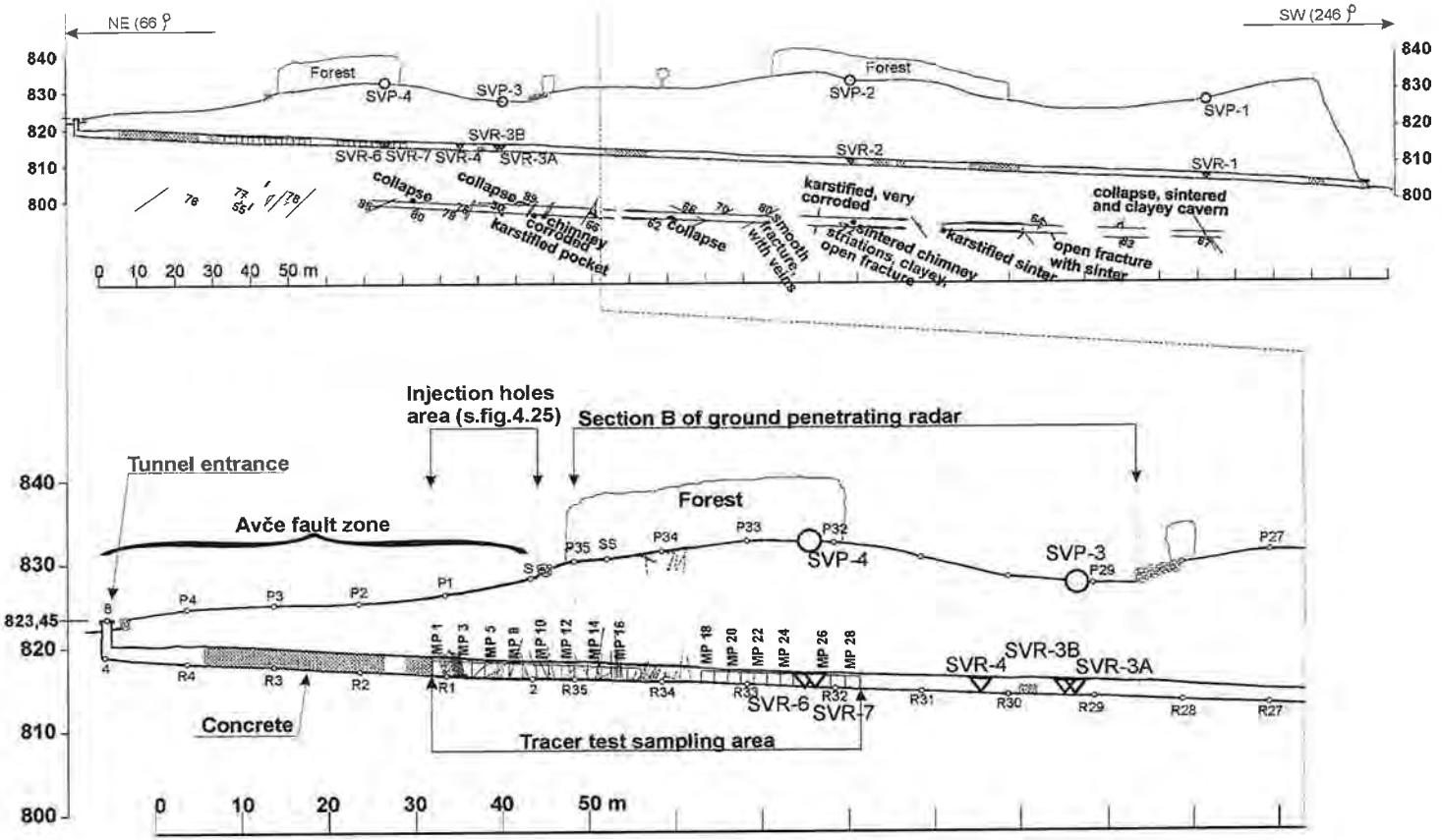

Fig. 4.24: Longitudinal cross-section of the research tunnel with sampling points for tracer experiments (MP1–MP28) and isotope study (SVP-1 to SVP-4 and SVR-1 to SVR-7).
Längsschnitt durch den Forschungsstollen mit Messstellen für die Tracerversuche (MP1–MP28) und Isotopenstudien (SVP-1 bis SVP-4 und SVR-1 bis SVR-7).

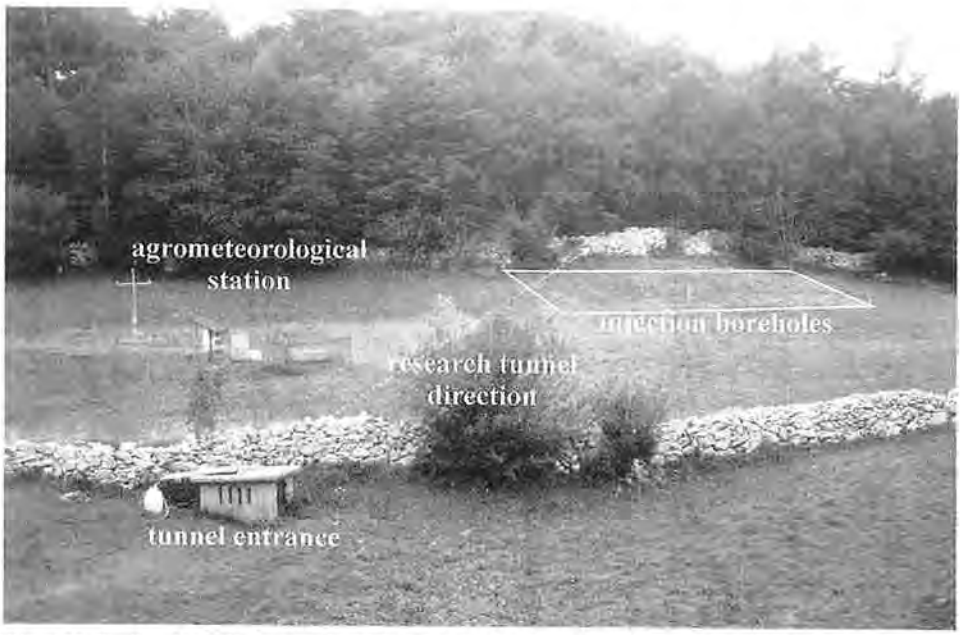

Fig. 4.25: Surface installations at the EFS Sinji Vrh – agrometeorological station, injection holes area (inside rectangle) and fertilization area (a rectangle).
Obertägige Einrichtungen in TG Sinji Vrh – agrometeorologische Station, Injektionsbohrungen (im Rechteck) und das gedüngte Gebiet (Rechteck).

to collect water in narrow sampling containers (Fig. 4.26). The water seeping from the ceiling of the research tunnel is gathered in 1.5 m long segments with a gathering surface of 2.2 m². The total length of the collecting area is 49 m with interruption of 7 m due to dry rock and the total number of segments is 28 (MP1–MP28; fig. 4.24). For the special tracer experiment (P4; tab. 4.4) water was sampled also from two subhorizontal boreholes (approximately 1.2 m length and 55 mm diameter) drilled with core into both sides of the tunnel walls perpendicular to the tunnel axis. The boreholes were drilled into an area (MP5; fig. 4.24), which showed in previous tracer experiments the shortest travel times and the highest recovery of tracer (B. ČENČUR CURK & M. VESELIČ, 1999). The sampling devices in the boreholes are built of one half of plastic pipe (∅ 40 mm) separated into several sampling chambers with separate outlets. The sampling system is pressed by a tube against the top of the boreholes to ensure a correct position and to avoid bypassing of water. The subhorizontal boreholes allow a gravity driven sampling of the different chambers (K. WITTHÜSER & B. ČENČUR CURK, 2000).

The isotope and hydrogeochemical study includes sampling of precipitation and water from the unsaturated zone (in the research tunnel) and aquifer outflow (Hubelj spring). Eight sampling points (SVR-1 to SVR-7; fig. 4.24) were constructed in the research tunnel in such a way that the collected water is prevented from being influenced by external effects and to enable measuring of discharge (Fig. 4.27). Above the sampling points in the tunnel, there was also monthly monitoring of soil conditions at depth of 50 cm in four sampling stations (SVP-1 to SVP-4; fig. 4.24) concerning the measurements of soil temperature, moisture content and partial pressure of CO_2 and the sampling of soil atmosphere for ^{13}C-isotope composition of soil CO_2.

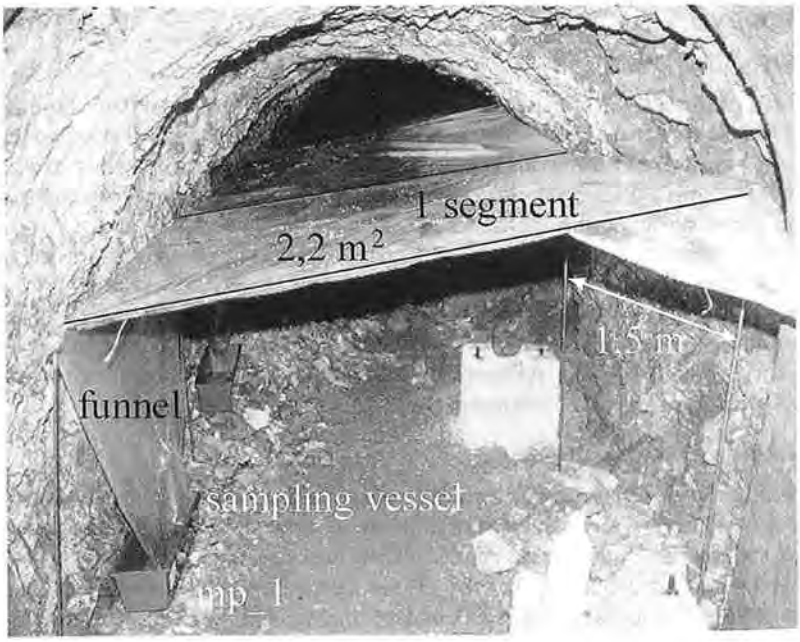

Fig. 4.26: Construction for collecting water samples in the research tunnel (B. ČENČUR CURK et al., 2000).
Probenahmeeinrichtung im Versuchsstollen (B. ČENČUR CURK et al., 2000).

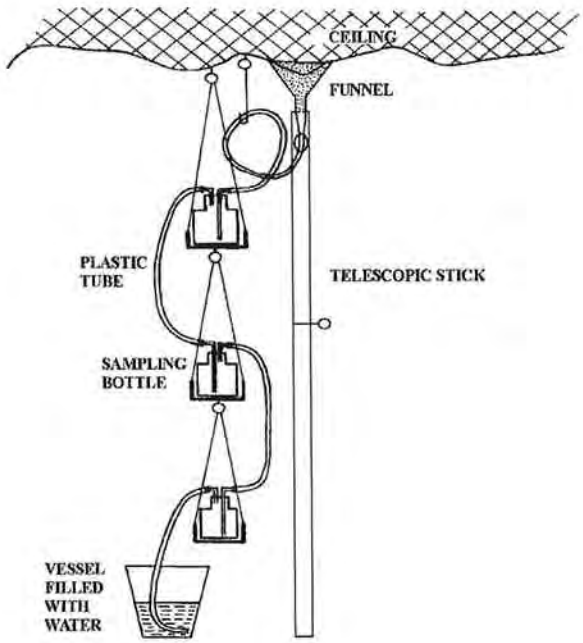

Fig. 4.27: The sampling point for water collection in the research tunnel for isotope studies (B. TRČEK et al., 2000a).
Probenahmeeinrichtung für die Isotopenstudien (B. TRČEK et al., 2000a).

4.4.5. Results

4.4.5.1. Structural Study

The area of the NE-part of the tunnel is crossed by the subvertical Avče fault (Fig. 4.24) with a Dinaric direction (NW–SE), where the rock is crushed and fractured. Within the broader fault area numerous accompanying subvertical faults (they are streching in NNW–SSE and NNE–SSW directions) are present, branching from the main fault plane and repeatedly joining it (J. ČAR, 1997).

The main fracture and fault strike of the surface rocks and within the tunnel is NNE–SSW (dip direction and dip angle: 295/80 and 115/85), the subordinate dips are 85/80–90, 185/85 and 140/80 (M. VESELIČ et al., 1998). The Jurassic limestone of the tracer experiments area is composed of 99 % calcite and has a south-westerly dip direction and a gentle dip (of 5°–30°). At sections where the tunnel is supported by concrete (Fig. 4.24) crushed zones are assumed.

4.4.5.2. Geophysical Measurements

The results of the ground penetrating radar (GPR) investigations of subsection B (Fig. 4.24) indicated from hydrogeologic point of view the depth of pronounced rock desaturation, the near surface fast vertical flow and drainage areas as well as the areas of retained water (B. TRČEK et al., 2001). It is assumed that the limestone is mainly dry up to 3 m below the surface (Fig. 4.28), except in areas of karst channels where the dry zone is deeper. Below the depth of 3–5 m a relatively saturated area was detected, which presents a storage within the unsaturated zone (epikarstic zone). Geoelectrical tomography indicates 1.5 m thick subsurface clay zone and very fractured (crushed) limestone at the Avče fault area (Fig. 4.24, 4. 28). On the hill a compact limestone zone with surface clay-filled fractures is detected.

4.4.5.3. Tracer Experiments

In the first tracer experiment (P1) the tracer NaCl has appeared only in two segments (MP4 and 5; fig. 4.24). The tracer appeared almost immediately after the injection and the maximal concentration appeared after 2 h (Fig. 4.29). This phenomena was due to a very high rate of saturation (snow melting). The peak values after the first tracer breakthrough occurred because the meadow above the tunnel was additionally watered and subsequently, it started to rain. It must be noted that only the addition of new fresh water (either from watering or raining) results in additional rinsing of pollutants, provoking a temporary rise in their concentration. We believe that the tracer is retained (and gradually rinsed) in the small fractures of the overlaying rock mass cover. This experiment indicated only one fast conduit where water runs faster than in the total conductive part of the rock. This phenomenon indicates that the conduit (large fracture/fault) does not reach the bottom of the weathered subsurface zone or even lower. This conduit presents a drainage to the surrounding fractured system. The first peak was fitted with the single fissure dispersion model (SFDM) (P. MALOSZEWSKI et al., 1999, P. MALOSZEWSKI & A. ZUBER, 1990, A. WERNER, 1998a, b). The vertical dispersion in MP4 was 5 m^2/h with mean flow velocity 0.93 m/h and in MP5 6.2 m^2/h with mean flow velocity 0.96 m/h. From the comparison of the data with literature (W. KÄSS, 1998) the values are typical for fractured and karstified rocks.

Determination of one fast conduit is not enough to design a flow in fractured rock in general, but we should be aware that such direct and fast paths exist in karst and are very important in determining potential pollutant locations (B. ČENČUR CURK &

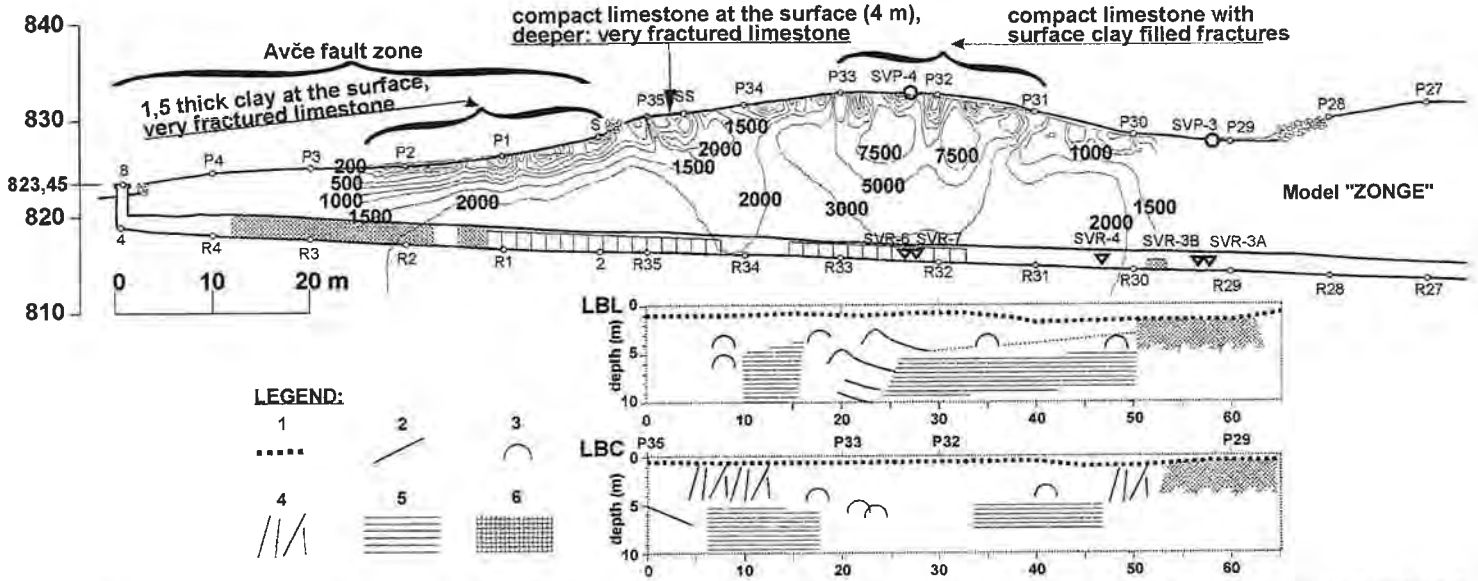

Fig. 4.28: Geoelectrical tomography longitudinal profile above the tunnel axis and interpreted GPR longitudinal profiles (LBL: 5 m to the S and LBC: above the tunnel axis) of subsection B (see fig. 4.24). Legend: 1 – boundary of surface weathered layer, 2 – discontinuity, 3 – observed karst feature, 4 – fractures, 5 – area of chaotic signals (partly saturated rock), 6 – area where clay prevails (after B. TRČEK et al., 2000b).
Geoelektrischer Längsschnitt über dem Versuchsstollen und interpretierter Radarlängsschnitt (LBL: 5 m südlich der Stollenachse und LBC: über der Stollenachse). Legende: 1 – Grenze der Verwitterungszone, 2 – Diskontinuität, 3 – beobachtete Karsterscheinung, 4 – Klüfte, 5 – Gebiet der chaotischen Signale (teilweise gesättigte Zone), 6 – vorwiegend tonige Bereiche.

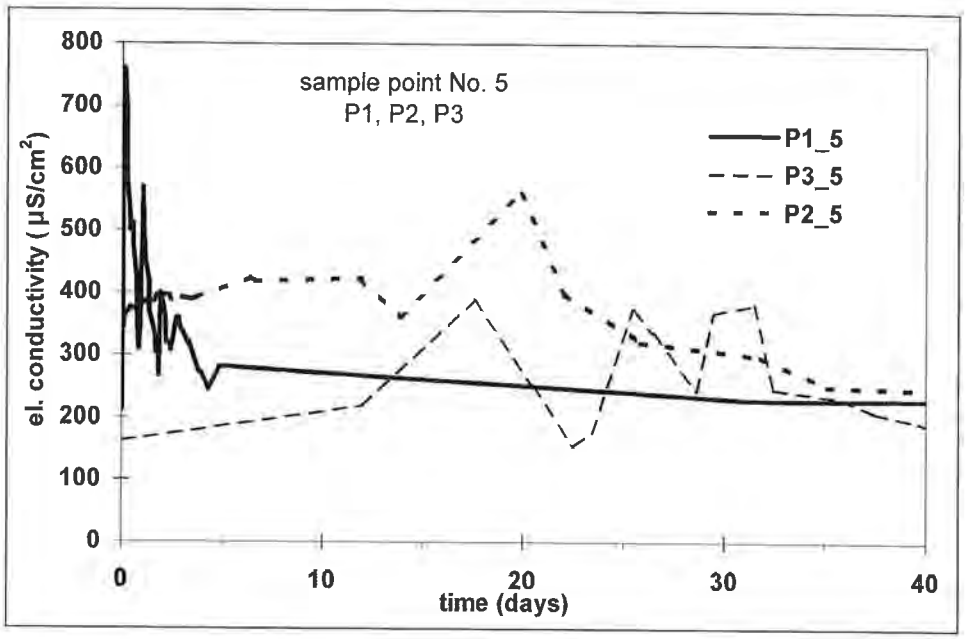

Fig. 4.29: Specific electric conductivities of water samples at sampling point MP5 for tracer tests P1, P2 and P3 in variable saturated rock (B. ČENČUR CURK & M. VESELIČ, 1999).
Spezifische elektrische Leitfähigkeit (ELF) an der Messstelle MP5 bei den Traserversuchen P1, P2 und P3 bei unterschiedlicher Sättigung (B. ČENČUR CURK & M. VESELIČ, 1999).

M. VESELIČ, 1999). This experiment was the first evaluation of flow conditions in the research area.

For the second tracer test (P2) additional injection holes were drilled (for a total number of 29) in order to obtain more dispersed flow and the influx caused by rock stratification. The injection was carried out in spring 1997. The tracer NaCl appeared in more segments approximately three weeks later (Fig. 4.29). The next rinsing of the tracer was caused by autumn rain after five months of the tracer injection. The tracer was retained in the small fractures of the system. In the smallest voids the water is in general present also in unsaturated stage of rock because of capillary pressure. In the case of almost dry rock also the smallest voids have to be filled up with water, after that larger voids fill up and the percolation threshold is reached. This is also confirmed by the first peak in the tracer experiment P3, which occures 17 d after the tracer injection and 10 d after the first rain event (Fig. 4.29). The experiment was carried out in the same season; oscillations were more evident due to a greater variability of precipitation conditions.

The multitracer experiment P3 (Tab. 4.4) was performed in spring 1998. This experiments have shown three main flow velocities. The fast flow of karst conduits was detected already in previous experiments and was confirmed by uranine peak after 25 d (MP5 in fig. 4.30). The crushed zone conducts water, yet a system of fractures presents a storage zone where the flow is not so fast (MP8 in fig. 4.30) and a retardation is observed – the first peak appeared after 58 d. Fractured zones present even slower flow and higher dispersion of the tracer. It should be pointed out, that uranine was injected into nine injection holes (each 1.5 g), which caused an overdose in fast pathways

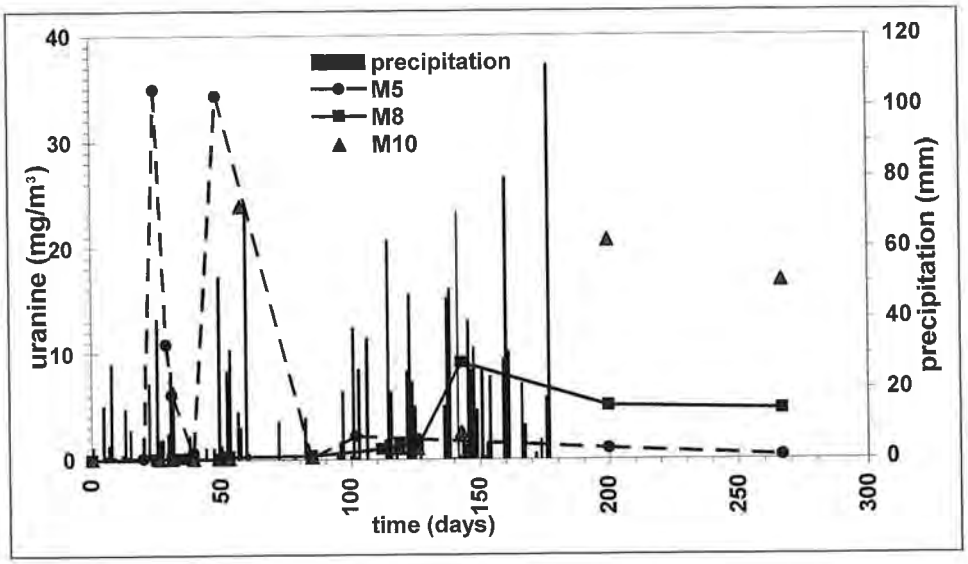

Fig. 4.30: Uranine concentrations in water samples at sampling points MP5, MP8 and MP10 for the multitracer test P3 (B. Čenčur Curk, 2001).
Uraninkonzentrationen in den Messstellen MP5, MP8 und MP10 beim Multitracerversuch P3 (B. Čenčur Curk, 2001).

and crushed zones such as MP4, MP5 and MP10. In other segments where the system is not so high conductive concentrations reached up to 2 mg/m³.

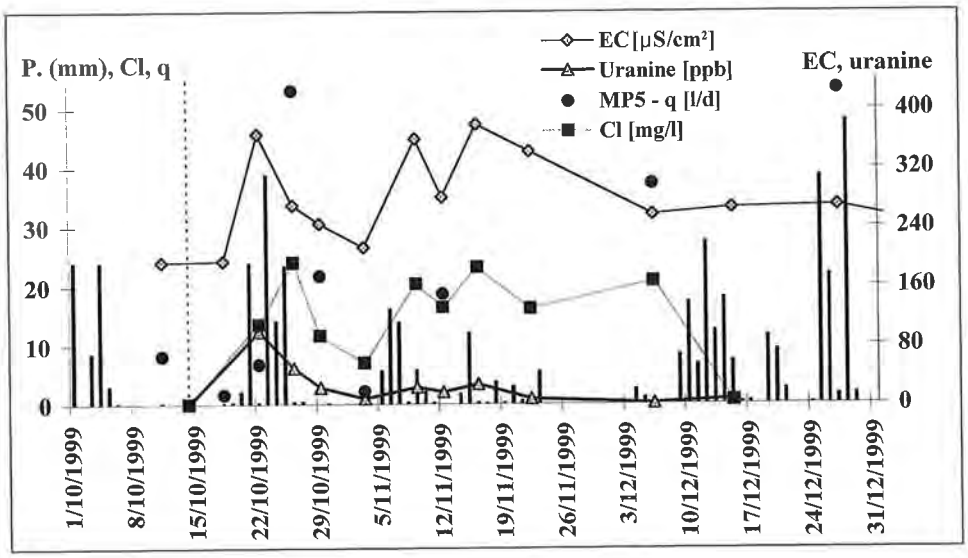

Fig. 4.31: Precipitation, flow rate, specific electric conductivity and tracer concentrations at sampling point MP5 for tracer test P4 (B. Čenčur Curk, 2001).
Niederschlag, Durchfluss, ELF und Tracerkonzentrationen in der Messstelle MP5 beim Tracerversuch P4 (B. Čenčur Curk, 2001).

The last tracer experiment (P4) was performed in autumn 1999 where tracers were injected into different depths: in the soil (0.1 m below surface: $MnCl_2$), at the soil-rock interface (0.23 m below surface: $NiSO_4$) and in the fractured rock (0.65 m below surface: uranine).

The chlorine peak appeared 12 d (0.8 m/d) after the injection and 5 d (1.9 m/d) after the rain event (Fig. 4.31). The sulphate and uranine peaks appeared 8 d (travel velocity 1.2 m/d) after the injection and 1 d (9.5 m/d) after the rain event (Fig. 4.31), which shows no retardation of tracer at soil-rock interface. However a short delay of chloride ions was observed due to passing the soil cover, where the velocity is 9.5 m/d (K. WITTHÜSER & B. ČENČUR CURK, 2000).The tracer was retained in soil and upper part of the weathered rock until the first heavy rain flushed it away. Before the rain event a problem of sample quantity is often present, therefore the first sample after rain already contains the highest tracer concentrations. Calculations were performed according SFDM and other models. The results and conceptual model of the fractured zone are in print (B. ČENČUR CURK, 2001).

4.4.5.4. Fertilization Experiments

In the first fertilization experiment (G1) the nitrate ion appeared in water samples of almost all sampling points after approximately 30–35 d (Fig. 4.32), which was 5 d after the heavy rain (July 4, 1998; 51.7 mm), followed by more or less constant rain (B. ČENČUR CURK & M. VESELIČ, 1999). The first precipitation event (Fig. 4.32) after fertilization dissolved the mineral manure and rinsed it into the soil.

The highest nitrate concentration (15.1 mg/l) appeared at the measuring point MP5 (Fig. 4.32), where one fast channel with strong fluxes exists and was confirmed also in

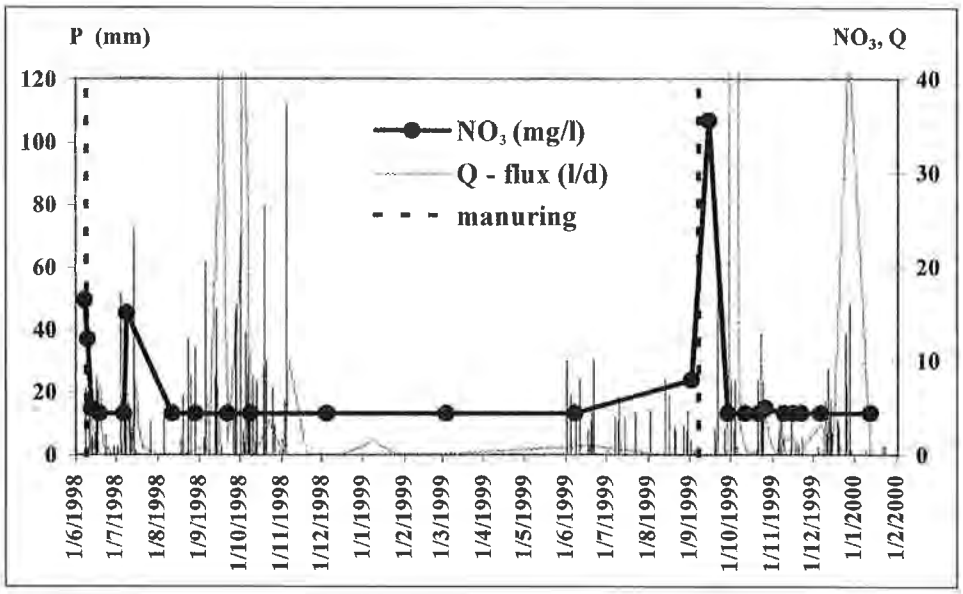

Fig. 4.32: Precipitation events and NO_3^--concentrations (detection limit 4.4 mg/l) in sampling points MP5 for fertilization experiments G1 and G2 (M. KARAHODŽIČ, 2000).
Niederschlag und NO_3^--Konzentrationen (Nachweisgrenze 4,4 mg/l) in der Messstelle MP5 bei den Düngeversuchen G1 und G2 (M. KARAHODŽIČ, 2000).

former tracer experiments and by mapping of discontinuities. Concentrations of NO_3^--ion were smaller than a natural background in springtime (before fertilization on June 8, 1998), when a mineralization in soil proceeds and is rinsed by precipitation water in spring.

The second fertilization experiment (G2) was performed in order to obtain more relevant data on nitrate percolation through the soil cover. For this reason vacuum lysimeters were installed into the soil cover and more isotope analyses were performed. The nitrate appeared one week after one huge precipitation event (September 9, 1999; 68.8 mm), about 22 d after the fertilization (Fig. 4.32). The isotope data $\delta^{15}N$ confirmed, that the nitrate source was the mineral manure applied on the meadow (B. ČENČUR CURK et al., 2000). The nitrate transport along the fast channel at measuring point MP5 was quicker and appeared after 8 d. In some measuring points another rinse of the manure was detected (MP21 and 10). After a huge precipitation in next spring (March 3, 2000; 85.1 mm) the nitrate was rinsed again – it was retained in the microfractures of the unsaturated zone.

In spite of the fact, that the meadow has not been manured for 15 y, the nitrate ion appeared after 30–35 d in the first fertilizing. Plants consumed a major part of the nitrate and only a small portion was retained in the soil cover, which is not very thick (50–100 cm) and contains a great amount of rubble.

4.4.5.5. Isotope and Hydrogeochemical Study

Isotopic and hydrogeochemical investigations based on the long-term (a one and a half year's period of the monthly baseflow monitoring) and short-term (detailed monitoring during an extreme storm event in the middle of July 2000) observation period. The most important data were obtained during the storm event because they enable a description of flow system with components of fast and slow response and provided additional information about the mixing processes and the residence times of water in the near surface unsaturated zone.

Two days before the observed storm event there was precipitation of about 70 mm, which caused a slight rise of Hubelj's discharge from 0.4–1.8 m^3/s. The heavy rain event lasted from 00.30 to 05.00 h on July 11 (85 mm), and from 02.00 to 05.00 h on July 12 (18 mm). This was an extreme event because it resulted in the Hubelj's discharge increase from 0.6m^3/s–24 m^3/s, which was an unusual discharge for summer time. The delay between the start of the precipitation event and the maximum discharge response was 3 h in the research tunnel and 5 h in 600 m lower lying Hubelj spring. The fastest discharge response in the tunnel was observed at the sampling point SVR-3A. Later, responses were at sampling points SVR-7, SVR-4 and SVR-3B (Fig. 4.33).

Sampling points SVR-3A and SVR-3B lie below the edge of a doline (accompanying fault zone of Avče fault) at a distance of 1 m (Fig. 4.24) fixed to the limestone layer that is quite karstified. SVR-3A showed the fastest and the highest discharge response. When its discharge almost stopped after 24 h (before the heavy rain on the second day), water started to flow at SVR-3B. There seem to be at least two kinds of drainage flow. The first one is through karst channels and/or wider fractures and the second one is most probably a laminar flow through the thiny fractured rock matrix. The results of ^{13}C-isotope and DOC-composition of sampled water in fig. 4.33 manifest these differences with maximum and minimum values. Values of other two sampling points are in between. The limestone around SVR-7 is layered and fractured. The direction of layers is the same as in GPR-profile LBL (Fig. 4.28) at a distance 20–30 m up dip. The limestone around SVR-4 is very fractured and crushed what is also observed in fig. 4.28.

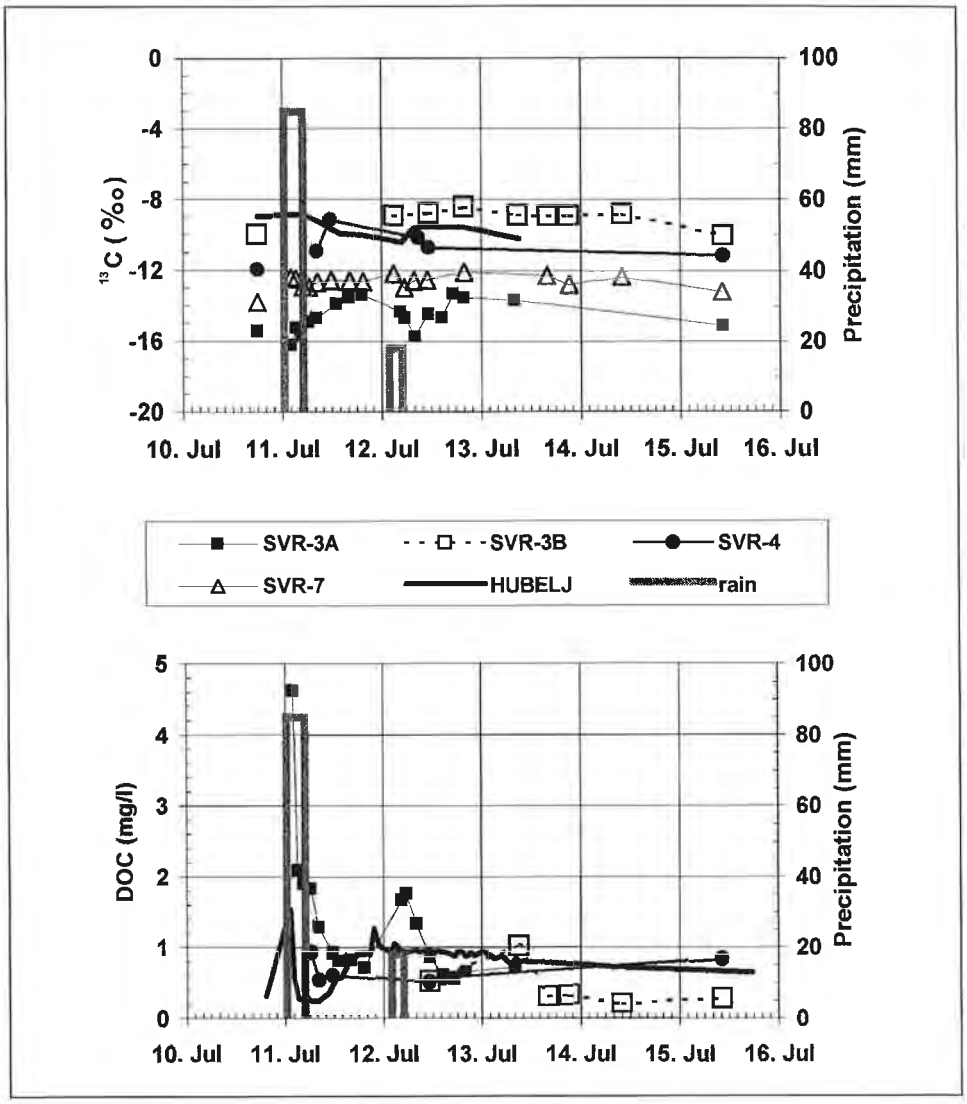

Fig. 4.33: ^{13}C-isotope and DOC-composition of water sampled during storm event (B. TRČEK, 2001). ^{13}C- und DOC-Gehalt in den Wasserproben während des Gewitters im Juli 2000 (see B. TRČEK, 2001).

On the basis of isotopic and GPR-results presented in fig. 4.28 and 4.33 we could say that a flow from fractured limestone is sampled at SVR-4 and SVR-7. The drainage of SVR-7 most probably presents a flow through wider fractures that are connected with karstified area in a background what could be also observed in GPR-profile LBL in fig. 4.28.

Unfortunately results of ^{18}O- and ^{2}H-isotope composition are not available yet. Figure 4.34 presents only first results of ^{18}O-isotope composition of baseflow samples. Nevertheless, described differences could be already noticed. The different residence

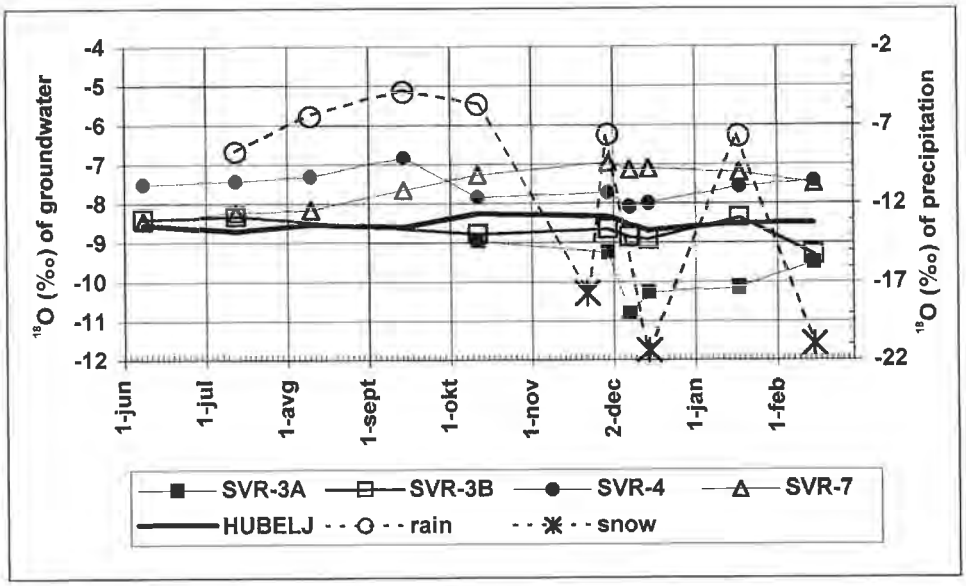

Fig. 4.34: ^{18}O-isotope composition of monthly water samples (B. TRČEK, 2001).
^{18}O-Gehalt in den monatlichen Wasserproben (B. TRČEK, 2001).

times of water could be expressed, but results of ^{2}H-composition will show if there are some evaporation effects.

The isotopic and hydrogeochemical results express different kinds of flow in the unsaturated zone. Values of the ^{18}O- and ^{2}H-isotope composition of water sampled during storm event will show major deviations resulting from single precipitation event, because the first values of analysed precipitation samples significantly deviate from mean precipitation values. The fastest flow was unfortunately not sampled, but its locations were registered during the storm event and could be included in further investigations.

Different kinds of flow are mixed in the outflow from the aquifer in Hubelj spring (Fig. 4.33 and 4.34). We could not evaluate parts of single flow yet.

4.4.6. Conclusions

The tracer experiments had shown different flow velocities. The fastest flow in karst conduits or large fractures/faults has no storage capacity and the smallest dispersion. The intermediate flow velocity in the crushed and higly fractured zone has storage capacity, which causes a retardation. Tiny fractured zones present more slow flow with higher dispersion of the tracer. The fractured and karstified rock could be seen as discrete conduits within higly fractured rock. Latter could be considered as permeable matrix, since the rock (limestone) matrix porosity is negligible (1 %) and the system could be modelled with double porosity model (continuum of conduits and continuum of dense fractured rock) either with hybrid model (discrete conduits and continuum of dense fractured system).

The fertilization experiments have shown very high horizontal flow velocities since the time difference in peaks of all segments was very small. This could be due to confirmed fact that under the soil an epikarst zone exists with temporary perched subsurface saturated zones, which was detected also by georadar measurements, which

were carried out in very dry season, and have shown relatively saturated areas below the depths of 3–5 m.

Another reason for high horizontal flow velocities are the bedding planes which dip from 10–30° and conduct water. Bedding planes were detected both with georadar and geoelectrical tomography measurements (Fig. 4.28). The depth of the epikarstic zone basis was not detected, therefore its influence is still a point of discussion, since the water seemingly flows uphill due to topographical conditions.

The results of isotopic and hydrogeochemical investigations gave some additional information about the drainage system, flow system and transport phenomena in the unsaturated zone. Results of ^{18}O- and ^{2}H-isotope composition will provide more complete explanation of the researched area and directives for further long-term and short-term observations. They will enable a differentiation of flow components by their mean residence time and thus allow for a better description of flow velocity distribution within the unsaturated zone.

Integrated results of all the above research will yield a knowledge of the flow and pollutant transport mechanism, which would enable us to predict the pollutant transport in fractured and karst aquifers. On this basis more precise protection areas of water resources could be determined and the impacts of potentially environmentally harmful activities could be detected.

The results of nitrate propagation have shown, that thin autochtonous soil cover on karstic rock is not enough to retain the nitrate and prevent pollution of karst groundwater. However, the maximum nitrate concentrations (up to 16 mg/l in G1 and up to 36 mg/l in G2) were smaller than some values of natural background and limits for drinking water.

Therefore the usage of allowed fertilizers in standards measures have to be advised and applied in agricultural practice. Further detailed studies with this respect are needed within the frame of the research on karstic aquifer vulnerability.

Acknowledgements

We express sincere thanks to Prof. Dr. K.-P. SEILER and Dipl.-Phys.W.STICHLER (GSF, Germany) for analyses of DOC, ^{18}O and ^{2}H and their valuable suggestions. We acknowledge the financial support from the Ministry of Science and Technology of the Republic of Slovenia for research projects under the research grants No. J1-7172-94, J1-0462-98 and L2-1310-98, for doctoral sholarship for B. ČENČUR CURK (S21-210-005/15249/97) and B. TRČEK (S21-215-007/13034/97) and for joint projects with Ministry for Physical Planning of the Republic of Slovenia, under the research grant No. V2-8575-96. This work was supported also by the International Atomic Energy Agency under the research grant No. 11519.

4.5. Lysimeter Study on Infiltration Processes in the Sandy Soil of the Great Hungarian Plain

(D. RANK, W. PAPESCH, V. RAJNER, K.-H. STEINER, Z. VARGAY)

4.5.1. Introduction

In the context of scientific-technologic co-operation between Austria and Hungary infiltration processes are studied at the lysimeter station Komlos near Kecskemet. Target of the work is a better understanding of the seepage in the sandy soil of the Great

Hungarian Plain and the assessment of the groundwater recharge from local precipitation. A further target of the study is the investigation of the role of adhesive water in the water transport. For this purpose several tracer experiments were carried out at the lysimeter station.

As the first step heavy rain events were simulated (D. JAYAWARDENA et al., 1997, D. RANK et al., 1997, A. P. BLASCHKE et al., 2000). The cylinder lysimeters have a depth of 60 cm (A), 110 cm (B), 160 cm (C) and 260 cm (D) respectively and a surface of 1 m^2. The bottom consists of a slightly inclined steel plate. The seepage water flows through a pipe from the deepest point of the lysimeter into the sampling container. Eight tracer experiments were performed in the period July 1996/August 1997. Tritium, ^{18}O, NaCl and NO_3 were used as tracers.

The soil in the investigation area predominantly consists of fine sand (Fig. 4.35) with very meager vegetation. Within the area of the lysimeter station there is no vegetation at all, here the top layer was replaced by a 10 cm thick sand layer. Hydraulic conductivities of about 2.10^{-4} to 1.10^{-5} m/s were estimated from the grain size distribution. The sand consists mainly of quartz with some carbonate and feldspar (Tab. 4.5). Total porosity amounts to 39 %.

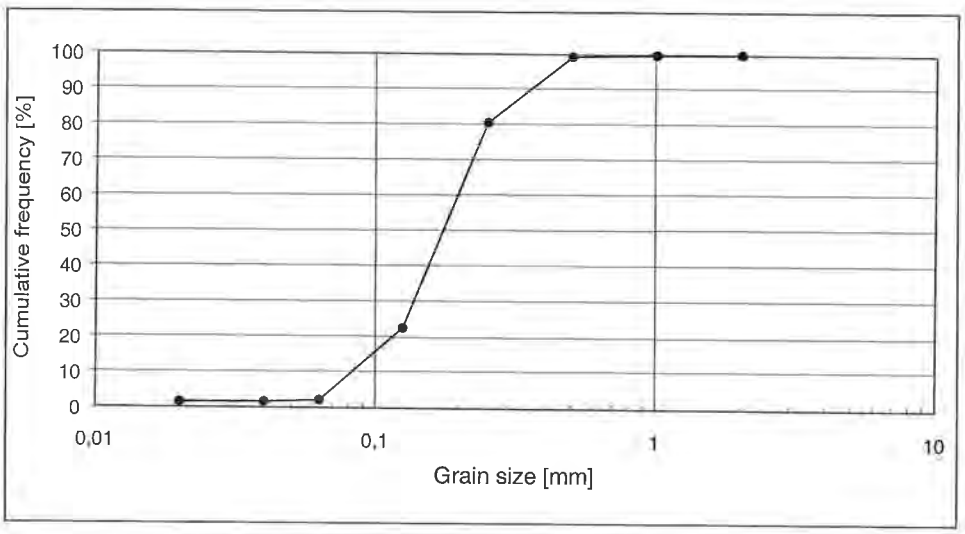

Fig. 4.35: Grain size distribution (cumulative curve) in a soil sample from the investigation area Komlos. Summenkurve der Korngrößenverteilung in einer Bodenprobe aus dem Untersuchungsgebiet Komlos.

Tab. 4.5: Mineralogical composition of a soil sample from the investigation area Komlos. Mineralogische Zusammensetzung einer Bodenprobe aus dem Untersuchungsgebiet Komlos.

Minerals	Mass [%]	Minerals	Mass [%]
Quartz	56	Dolomite	7
Plagioclase	11	Muskovite/Illite	3
Kalifeldspar	10	Chlorite	3
Calcite	9	Hornblende	< 2

4.5.2. Tracer Experiments

4.5.2.1. Principle Considerations

The investigations were mainly based on the measurement of the isotope ratios of hydrogen and oxygen in water, since these ratios are molecule properties of the water and thus are not influenced by the surrounding geological material like dissolved substances.

The first tracer experiment with water with low $\delta^{18}O$ (–14.55 ‰) pursued two targets. First the characteristics of the lysimeters should be roughly investigated by applying water with a $\delta^{18}O$-value deviating strongly from that in the lysimeters (~ –8 ‰), so that the main experiment with tritium tracing (2nd experiment) could be exactly calculated. Further, applying ^3H-free water should reduce and homogenize the ^3H-content of the water in the lysimeters in order to make the evaluation of the ^3H-experiment easier. Additionally a low ^3H-level permits the use of a relatively low ^3H-concentration.

Most important result from the first experiment was that the seepage water at the bottom of the lysimeters contained a very high portion of former adhesive water. For this reason a larger number of experiments than planned earlier (two experiments) had to be taken into account to achieve a reasonable recovery of the tracer.

Experiment 2 (^3H-tracing) is to be regarded as main experiment, which permits also a quantitative evaluation.

The ^3H-concentration of the irrigation water was chosen in such a way that it exceeded the previous concentration in the lysimeters by at least a factor 100. On the other side the ^3H-concentration of the irrigation water should be kept as low as possible to reduce the risk of contaminating the lysimeter site (underground laboratory) and water samples due to inevitable splash-water losses. The ^3H-content of the water in the lysimeters before the experiment was below or about 10 TU. About 1,500 TU were chosen as injection concentration, thus allowing to detect a portion of less than 1 % of the traced water. As base water the same water with low ^{18}O- content was used like for experiment 1. The used ^3H-concentration is several orders of magnitude below the maximal admissible concentration for drinking water (~ 300,000 TU). The total applied ^3H-activity amounted to approximately 8.10^4 Bq.

The following experiments served above all to increase the recovery of the injected ^3H. Additionally, NaCl and NO_3 were tested as tracers.

4.5.2.2. Experimental Procedure

Approximately one month before the start of the experiments the cocks at the base of the lysimeters were opened, so that the seepage water could run out. At the same time the lysimeters were covered with a plastic foil and thus the influence of evaporation and precipitation was prevented. In this status the lysimeters remained during the entire duration of the investigations. The foils were only removed for a short time to apply the irrigation water at the beginning of each experiment. Eight experiments were performed in the years 1996 and 1997 (July 2, August 21, October 10 and November 7, 1996, April 24, June 5, July 17 and August 20, 1997). Each time 100 l of traced water were applied to the four lysimeters within few minutes (3–5) and thus a heavy rain event with 10 cm precipitation depth was simulated. Table 4.6 contains the characteristics of the water applied in the experiments. In experiment 3 also NaCl was used as tracer (1 g/l), in experiment 4 also nitrate (water from a dug well with 88 mg/l NO_3).

Tab. 4.6: Isotopic characteristics, conductivity and nitrate content of the irrigation water.
^2H-, ^3H- und ^{18}O-Gehalt sowie Leitfähigkeit und Nitratgehalt des aufgebrachten Wassers.

Experiment No.	δ^2H [‰]	^3H [TU]	$\delta^{18}O$ [‰]	NO_3 [mg/l]	Conductivity [µS/cm]
1	−106.2 ± 1.0	0 ± 0.2	−14.55 ± 0.1	0	(534–600)
2	−106.2 ± 1.0	1,487 ± 24	−14.55 ± 0.1	0	600
3	−106.2 ± 1.0	0 ± 0.2	−14.55 ± 0.1	0	2,540
4	−61.5 ± 1.0	10.8 ± 0.5	−8.34 ± 0.1	88	796
5	−106.2 ± 1.0	0 ± 0.2	−14.55 ± 0.1	0	(534–600)
6	−106.2 ± 1.0	0 ± 0.2	−14.55 ± 0.1	0	(534–600)
7	−106.2 ± 1.0	0 ± 0.2	−14.55 ± 0.1	0	565
8	−106.2 ± 1.0	0 ± 0.2	−14.55 ± 0.1	0	534

A different infiltration behaviour of the lysimeters could be observed during irrigation. While the applied water in the lysimeters B (110 cm), C (160 cm) and D (260 cm) had completely infiltrated at the latest after a half hour, the infiltration process in lysimeter A (60 cm) lasted for 1.5–2 h. This indicates the occurrence of a state of saturation in lysimeter A. Also the maximum of discharge of lysimeter A lies within this period.

4.5.3. Results

4.5.3.1. Discharge

Figure 4.36 (see page 64–65) shows the discharge and the cumulative discharge of the four lysimeters for the experiments 1–4. The hydrograph curves from the different experiments show a similar shape – strong rise in the initial phase followed by a flatter decrease, they differ however in the detail, particularly by the occurrence of discontinuities. This result refers to the well-known fact that the percolation of the unsaturated zone is not a continuous process.

In lysimeter A the discharge begins already after few minutes, in lysimeter B after approximately 2 h and in lysimeter D only after approximately 20 h. The highest discharges amount to 6–8 ml/s in lysimeter A, in lysimeter D they are below 0.4 ml/s. Main cause for the differently high discharge maxima in the individual experiments are probably variations in temperature.

One would expect that the cumulative discharge at the end of an experiment corresponds with the irrigated quantity of water (100 l). Table 4.7 contains the actually measured values.

For the lysimeters B, C and D the water balance can be regarded as satisfying, in lysimeter A a deficit of approximately 10 % occurs. This is attributed to leakage in the top of the lysimeter and must be taken into account in the calculations.

Tab. 4.7: Cumulative discharge (l) from the lysimeters A, B, C, D after the experiments 1–4.
Gesamtabfluss (l) aus den Lysimetern A, B, C, D nach den Versuchen 1–4.

Lysimeter	A	B	C	D
Experiment 1	96.5	110.0	102.5	109.0
Experiment 2	84.1	94.7	109.8	94.8
Experiment 3	86.2	96.4	100.2	89.5
Experiment 4	90.2	106.3	106.3	109.1
Sum	357.0	407.4	418.8	402.4

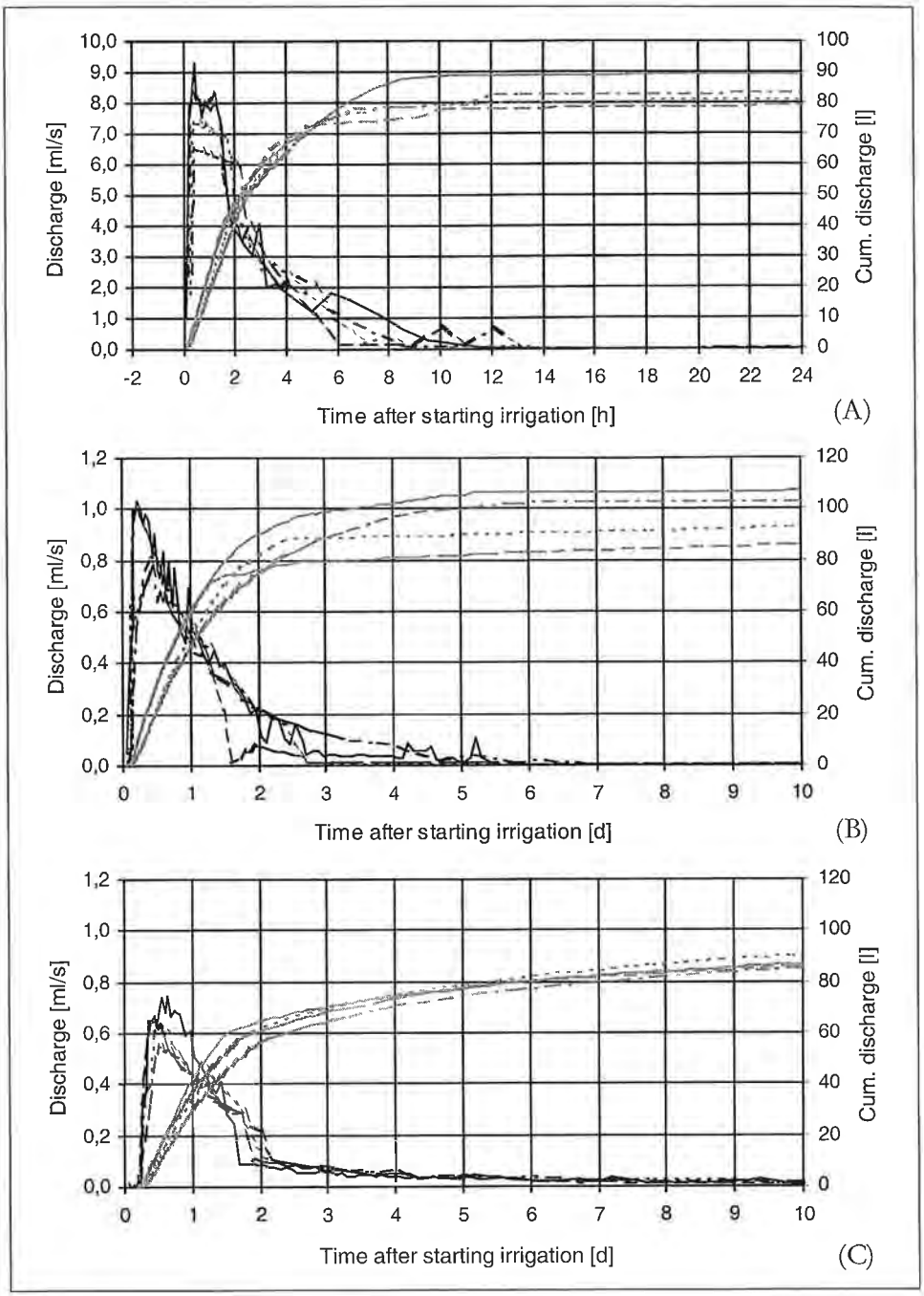

Fig. 4.36: Discharge and cumulative discharge of the lysimeters A, B, C and D; experiments 1–4. (Continuation p. 65.)
Abflussganglinien und Abflusssummenlinien der Lysimeter A, B, C und D bei den Versuchen 1–4. (Fortsetzung S. 65.)

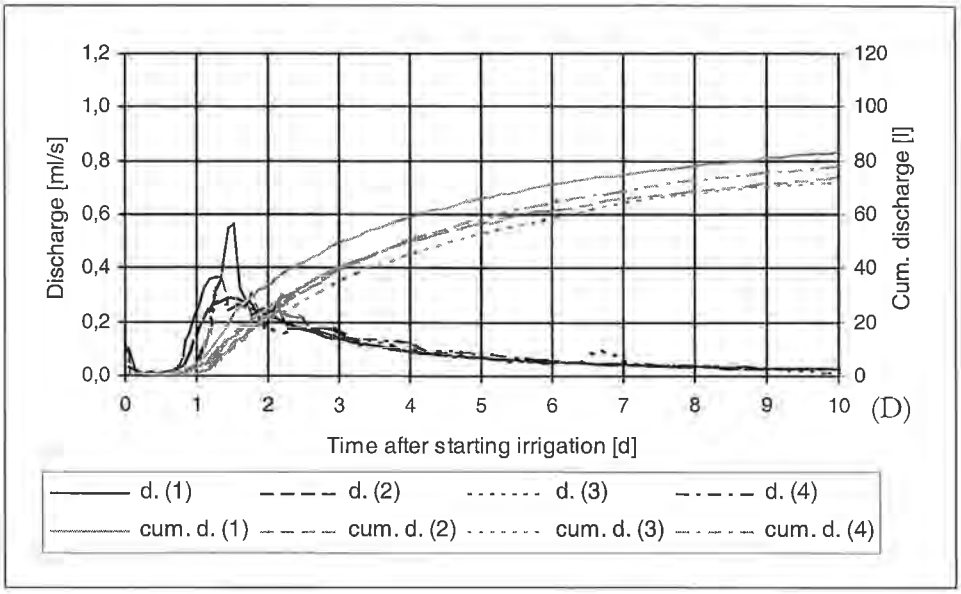

4.5.3.2. Isotope Measurements

The results of the ^{3}H- and ^{18}O-measurements are summarized in fig. 4.37, 4.38, 4.39 and 4.40. The course of the isotope concentrations in the discharge from lysimeter A differs basically from those in the other lysimeters. In B, C and D the expected steps occur during the discharge of the main quantity of water – in the deeper lysimeters C and D delayed only during the following experiment. For example, the ^{3}H-content of the discharge of B, C and D (Fig. 4.37) rises monotonously – in steps – up to a maximum (= passage of the tracer front) and drops thereafter – also again in steps – monotonously. Similarily pronounced is monotonous falling of the ^{18}O-content – also again in steps – during the experiments 1–3 (B) and 2 - 4 (C, D) respectively (Fig. 4.38). The further course of the ^{18}O-concentration is determined by the use of irrigation water with higher ^{18}O-content in experiment 4. The interpretation however is similar. These concentration courses correspond to a front passage – with corresponding dispersion – including the former adhesive water. The courses for lysimeter A however show maxima (Fig. 4.37, experiments 2, 3 and 4, fig. 4.38, experiment 4 and 5) and minima (Fig. 4.37, experiment 4 and 5, fig. 4.38, experiments 1 and 2) during the discharge of the main quantity of water. The reasons for this are discussed in the following in greater detail.

4.5.3.2.1. Lysimeter A

Figures 4.41 and 4.42 show the discharge hydrographs and the isotope concentration curves from the experiments 2–4 (^{3}H) and 1–4 (^{18}O) respectively for the first 12 h after irrigation. First the slightly inclined plateaus during the maximum discharge are noticeable, which obviously reflect a state of saturation. The inclination corresponds obviously to the decrease of the water level over the lysimeter body, until complete infiltration of the irrigation water into the lysimeter body abruptly ends the state of saturation (end of the plateau) and the discharge rapidly decreases. A closer view of the position of the ^{3}H-maxima during the different experiments shows that the maximum is achieved in experiment 2 (^{3}H-tracing) at the end of the discharge of the main

quantity of water (after approximately 10 h), in experiment 3 – highest value – much earlier (approximately 2 h after start of experiment) and that in experiment 4 the ^{3}H-maximum moves to the beginning of the experiment (Fig. 4.41).

A summary of these experimental results leads to the following conceptual model about the water movement in lysimeter A (Fig. 4.43): A saturated zone is formed in

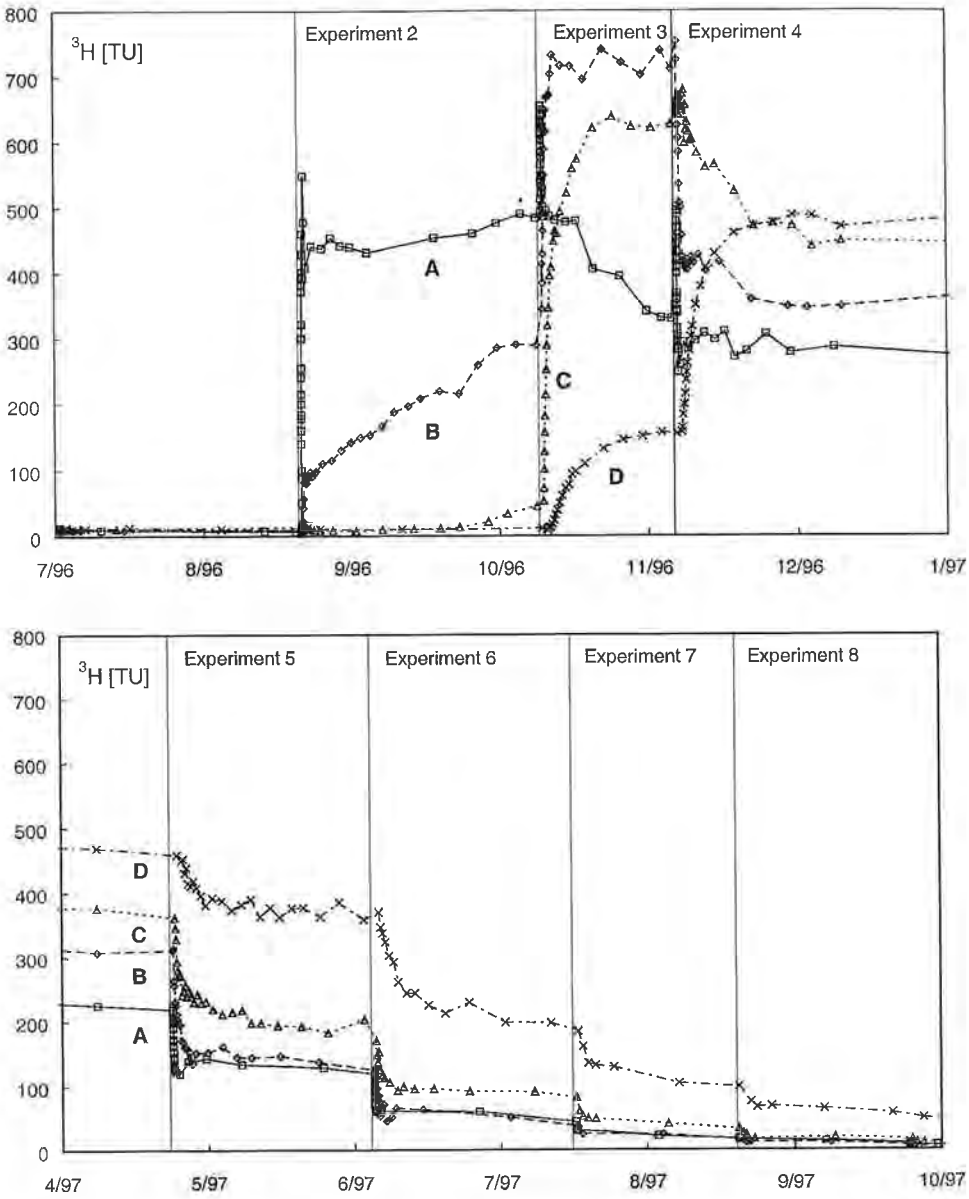

Fig. 4.37: Tritium content in the discharge of the four lysimeters; experiments 1–8.
Tritiumgehalt im Abfluss der vier Lysimeter; Versuche 1–8.

the upper part of the lysimeter body after irrigation. Air displaced by the infiltrating water can escape first through the outlet at the bottom of the lysimeter. With the increase of the discharge – few minutes after the irrigation – a saturated zone is formed also at the bottom of the lysimeter, the remaining air in the lysimeter cannot escape any longer. Preferential flow paths (Fig. 4.43, center) and a more or less stationary sta-

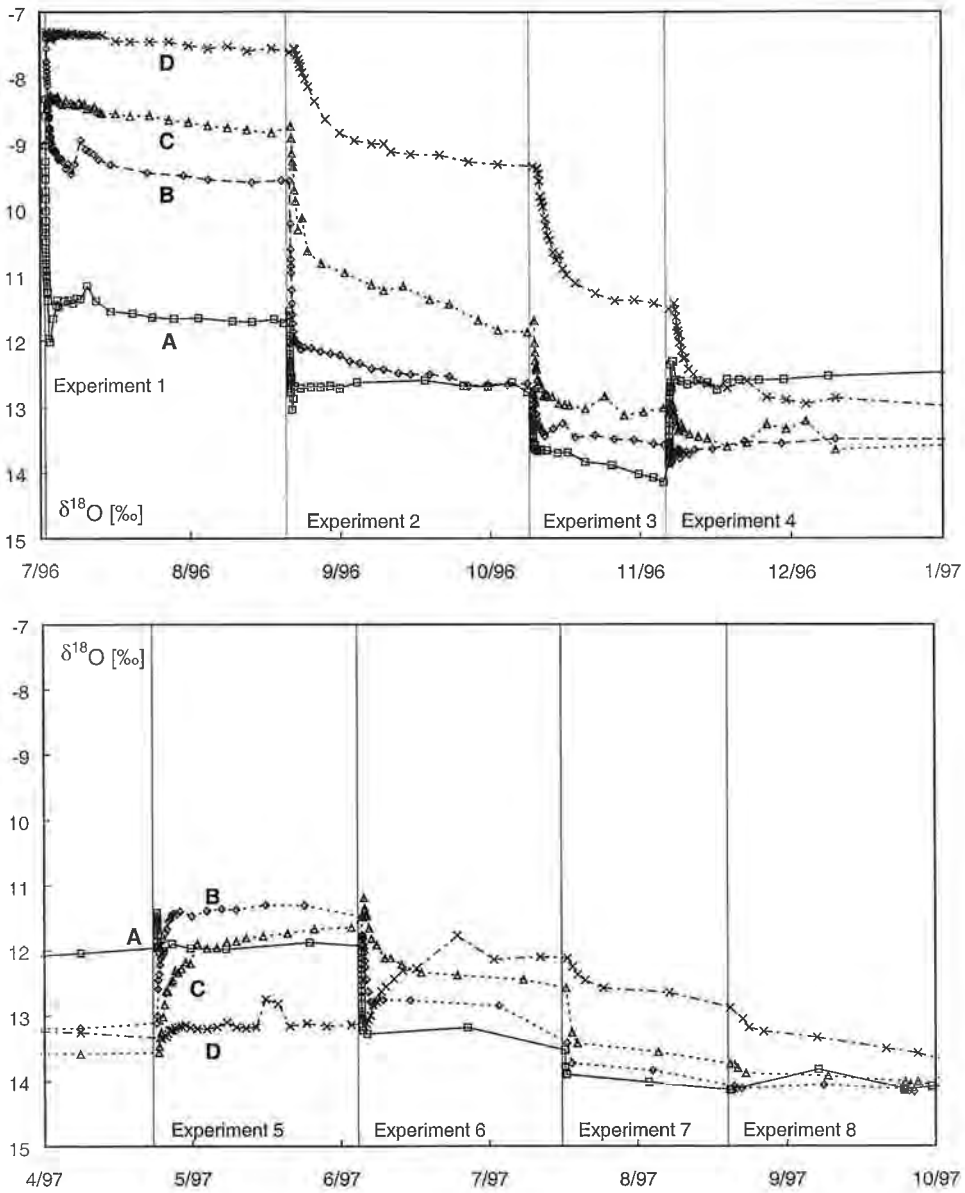

Fig. 4.38: Oxygen-18 content in the discharge of the four lysimeters; experiments 1–8.
Sauerstoff-18-Gehalt im Abfluss der vier Lysimeter; Versuche 1–8.

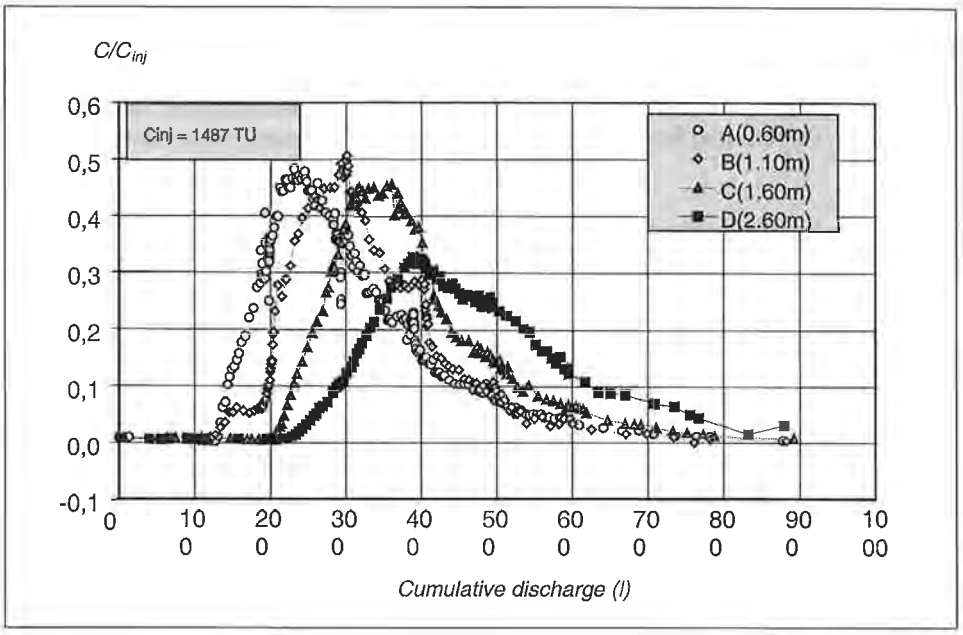

Fig. 4.39: Relative ^3H-concentration in the lysimeter discharge as a function of the cumulative discharge. Verlauf des ^3H-Gehaltes im Lysimeterabfluss in Abhängigkeit vom Gesamtabfluss.

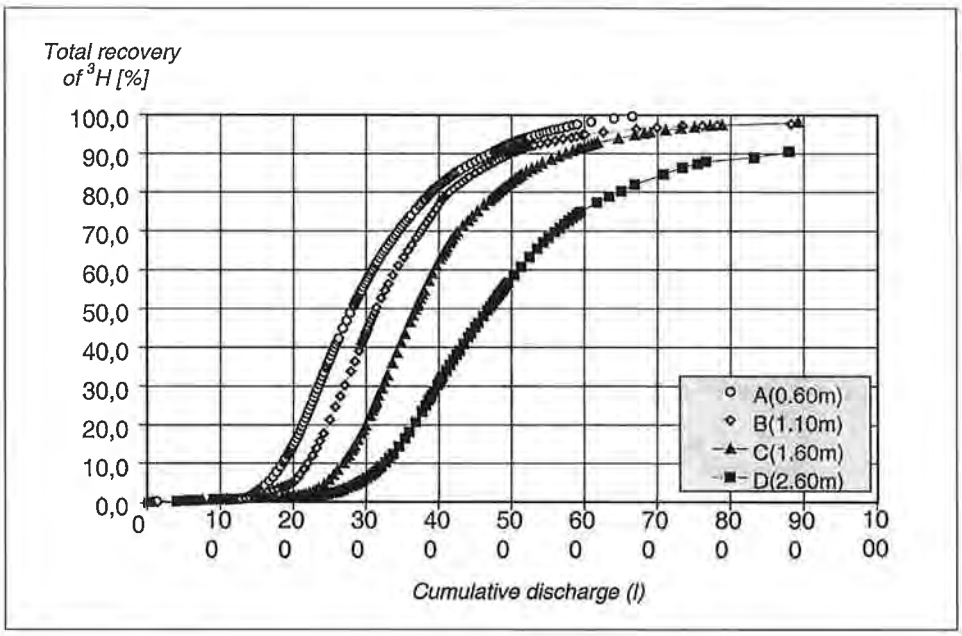

Fig. 4.40: Total recovery of ^3H as a function of the cumulative discharge. Ausgebrachte ^3H-Menge in Abhängigkeit vom Gesamtabfluss.

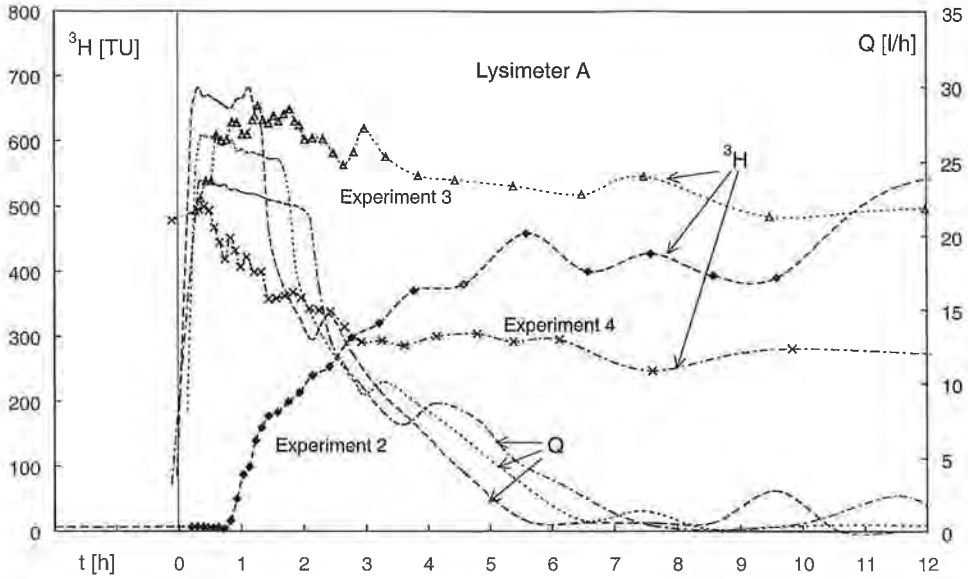

Fig. 4.41: Lysimeter A, experiments 2–4: ^{3}H-content in the discharge and discharge hydrograph for the first 12 h after irrigation.
Lysimeter A, Versuche 2–4: ^{3}H-Gehalt im Abfluss und Abflussganglinie für die ersten 12 h nach der Beregnung.

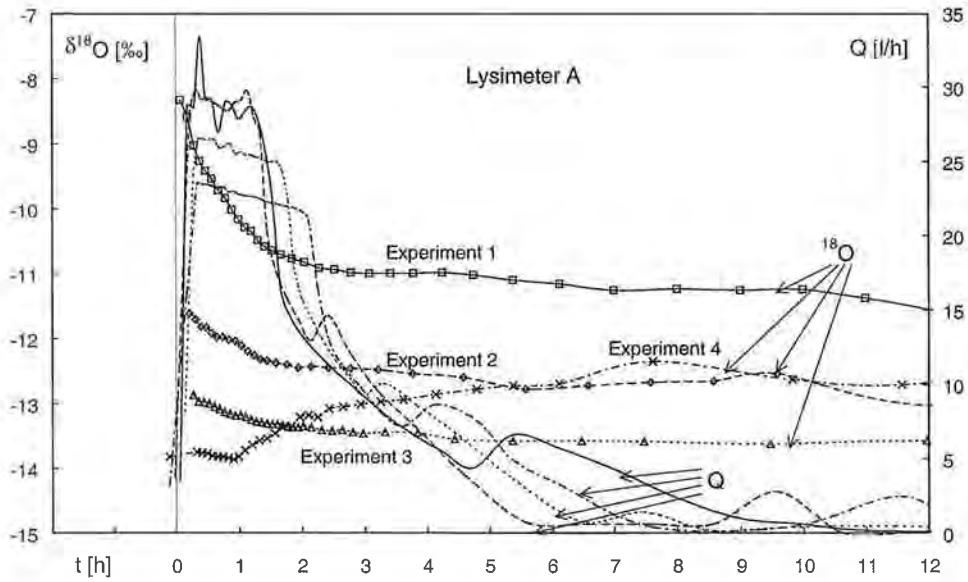

Fig. 4.42: Lysimeter A, experiments 1–4: δ^{18}O in the discharge and discharge curve for the first 12 h after irrigation.
Lysimeter A, Versuche 1–4: ^{18}O-Gehalt im Abfluss und Abflussganglinie für die ersten 12 h nach der Beregnung.

tus (plateau of the discharge curves) develop. These preferential flow paths are however not to interpret as macropores (e.g. wormholes), since the isotope concentration in the discharge indicates a large portion of former adhesive water with low ^{3}H-content (see e.g. fig. 4.41, experiment 2). This is also confirmed by the relatively small recovery of the traced water after the tracing experiment (Tab. 4.8). That is, these preferential flow paths are to be regarded as part of the matrix (C. J. RITSEMA et al., 1993), the water movement in these flow paths is again in form of a front. The seeping water mixes continuously with the adhesive water and a part of the mixture propagates.

The distribution of the dry soil bodies is probably coincidental and might change from experiment to experiment and achieve also different extents. If one assumes that at the end of the plateau of the discharge curve (= end of the state of saturation) there is still as much water in the lysimeter as necessary for maintaining saturation conditions, then the volume of the dry bodies in the lysimeter can be estimated from the effective porosity and the cumulative discharge at this time. The residual water mass is approximately 45 l, the effective porosity approximately 15 % (total porosity 39 %, adhesive water 24 %) and the total volume of the lysimeter body approximately 600 l. From this an air volume of about 45 l results, i.e. approximately half – once more, once less – of the usable pore volume remains dry during the saturation phase. The saturation flow in the preferential flow paths is breaking down after the complete infiltra-

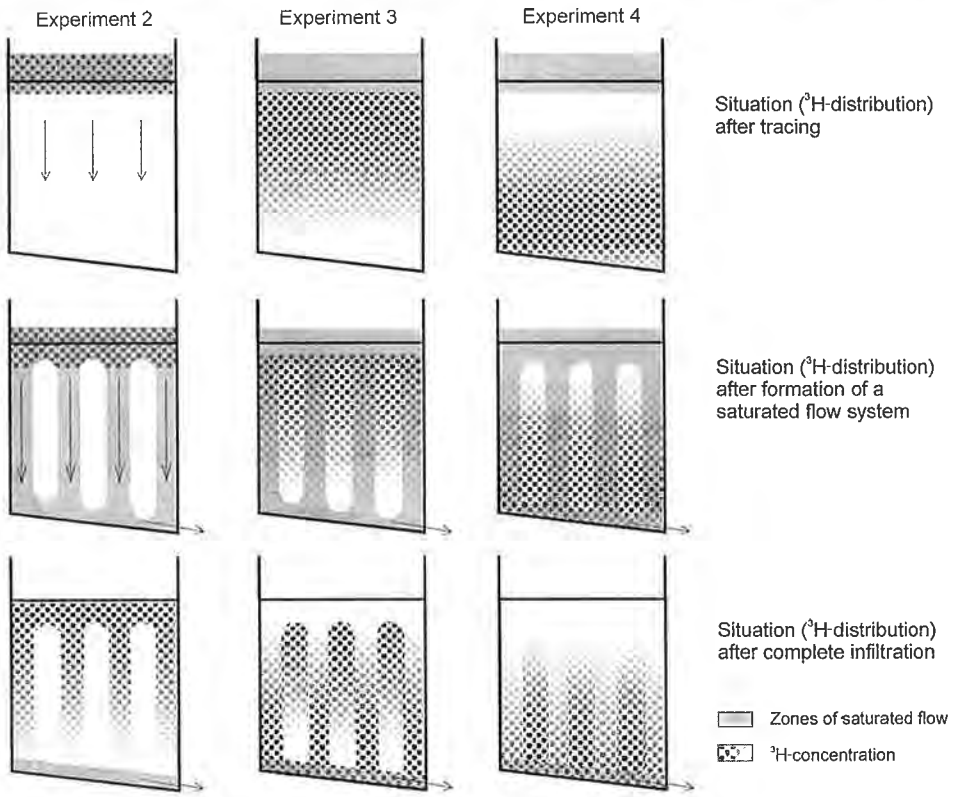

Fig. 4.43: Conceptual model of the formation of preferential flow paths in lysimeter A. Modellvorstellung zur Ausbildung bevorzugter Fließbahnen im Lysimeter A.

tion of the irrigated water. The entrapped air can again escape and gradually percolation takes place again in the entire cross section of the lysimeter. Thus former adhesive water from the air-filled parts arrives at the discharge and dilutes additionally the water coming from the tracing experiment (reaching the lower part of the lysimeter over the preferential flow paths). This leads to a decrease of the tracer concentration in the discharge, although the major part of the tracer is still in the lysimeter.

The different positions of the three maxima in the ^{3}H-concentration curve are easy to explain on the basis of the following considerations. In experiment 2 (^{3}H-tracing) the applied tracer is at the surface of the lysimeter. It will thus last a certain time until a part of the traced water – diluted with former adhesive water – arrives at the discharge over the preferential flow paths. At the beginning of experiment 3 the centre of the ^{3}H-plume has shifted downward, with the highest ^{3}H-concentration however within the upper part (Fig. 4.43, top centre). The way to the outlet is shorter and the dilution along the preferential paths smaller, therefore the ^{3}H-maximum in the discharge is achieved earlier and is higher than in experiment 2 (Fig. 4.43, centre centre). The ^{3}H-free water from experiment 3 already follows on the preferential flow paths. At the beginning of experiment 4 already a large part of the injected tritium has passed the lysimeter and the centre of the ^{3}H-plume has continued to shift downward. Water with high ^{3}H-concentration arrives directly at the outlet with the formation of preferential

*Tab. 4.8: Recovery of traced water (^{3}H) irrigated in experiment 2. * Correction factor 100/84.1 = 1.19. Ausgebrachte Gesamtmenge des beim Versuch 2 eingegebenen ^{3}H-markierten Wassers. * Korrekturfaktor 100/84.1 = 1.19.*

Amount of traced water [l]				
After experiment	Lysimeter			
	A (corr.*)	B	C	D
1				
2	11.1 (13.2)	5.1	0.9	0.7
3	44.6 (53.0)	43.2	24.0	4.5
4	66.1 (78.6)	77.9	66.8	30.5
5	75.4 (89.7)	89.5	83.6	55.1
6	80.2 (95.4)	94.3	91.8	74.0
7	82.6 (98.2)	96.4	95.6	84.4
8	83.7 (99.5)	97.4	97.4	89.7
End of project (98/11/04)	84.3 (100.2)	97.9	98.2	94.7
^{3}H-content (TU)	1.7	4.0	6.3	24.3

flow paths. In the course of the further experiments the ^3H-content decreases continuously, since the highest ^3H-concentrations are found at the bottom of the lysimeter.

4.5.3.2.2. General Conclusions from the Isotope Concentration Curves

The ^3H-tracing in experiment 2 proves as that one, which offers the best conditions for a quantitative evaluation. The following general considerations for all lysimeters refer therefore essentially to the results of the ^3H-measurements. As already mentioned, the course of the isotope concentration curves points out that the irrigation water infiltrates in form of a front – with corresponding dispersion – into the lysimeter body. There is no indication of a more-velocities mechanism, which can be found in more fine-grained soils. The formation of preferential flow paths in lysimeter A has other reasons. It is remarkable that the discharge consists mainly of former adhesive water, while the main quantity of the irrigated water appears only with considerable delay in the discharge. For example only approximately 13 % of the applied water appear in the discharge of lysimeter A (Tab. 4.8). The ^3H-concentrations in the discharge amount to maximal 30 % (lysimeter D) to 50 % (B) of the input concentration. That is, that also during the maximum of the breakthrough curve the predominant part of the discharge consists of former adhesive water and irrigation water from the following experiments. This can be explained only in such a way that the infiltrating water mixes with the available adhesive water and a part of the mixture propagates, while the other part remains as adhesive water. In this way the tracer concentration in the wetting front decreases continuously (current dilution by adhesive water). The part of the traced water remaining as adhesive water is only activated with the propagation of the wetting front in the next experiment.

4.5.3.2.3. Further Remarks on the Analysis of the Isotope Concentration Curves

The ^3H-results of lysimeter A were corrected for the losses of water in the following manner: The reason of the water deficit in lysimeter A is obviously a leakage in the uppermost part of the lysimeter. The leakage is therefore essentially effective until the irrigated water has infiltrated into the lysimeter body. Therefore only the loss of traced water during experiment 2 (^3H-tracing) influences the total amount of the injected tritium. The cumulative discharge in experiment 2 amounted to 84.1 l (Tab. 4.7), therefore a factor of 100/84.1 was used for the correction. Because of the small depth of the lysimeter A other factors (e.g. temperature, time) do not play an as important role for different total discharges as in the deeper lysimeters. So this correction factor seems to be realistic.

Remarks on the course of the ^{18}O-curves: The ^{18}O-content of a water sample reacts very sensitively to evaporation. If thus a sampling container is exposed for a longer time and not adequately isolated from the ambient air, as it can occur during longer sampling intervals, the ^{18}O-content of the water sample can rise. Some samples were eliminated, for which such an alteration of the ^{18}O-content was obvious (check by deuterium measurement). Slight short-term ^{18}O-peaks between the tracer experiments (Fig. 4.38) are probably due to such effects.

The irrigation water with high $\delta^{18}O$ ($\delta^{18}O = -8.34$ ‰) applied in experiment 4 caused a temporary rise of the ^{18}O-content in all lysimeters, with a corresponding time shift in the deeper lysimeters. However completely different ^{18}O-distributions were present in the different lysimeters at this time, so that this tracing is not suitable as well for evaluation as experiment 1 or as the ^3H-tracing in experiment 2.

The limits of error for the $\delta^{18}O$-values are below $\pm$ 0.1 ‰. The limits of error for the ^3H-values lie within the expansion of the symbols used in the diagrams or go scarcely beyond that.

4.5.3.3. Conductivity and Nitrate Measurements

The conductivity measurements after the application of 1 mg/l NaCl in experiment 3 furnished similar concentration curves as the ^{3}H-curves after experiment 2. The conductivity is influenced however obviously also by the filling material of the lysimeter, so that a quantitative evaluation was not possible. For many years the lysimeters were exposed to precipitation and evaporation, their outlets being closed.

The nitrate tracing in experiment 4 did not deliver evaluable results. The reason for this is not clarified so far. However, from the results the conclusion can be drawn that the nitrate is transported with the same velocity as the other tracers.

4.5.4. Conclusions

- Experiments simulating heavy rain events clearly showed the difference between propagation of the wetting front and the movement of individual water molecules in the unsaturated zone of a sandy soil in the Hungarian Plain. The discharge consists to a high proportion of former adhesive water, which is displaced by the infiltrating rain water. In the case of a contamination of the unsaturated soil zone, this causes a strong – temporary – retention of the dissolved material only by the seepage mechanism, even without adsorption. Only after applying 500 (lysimeter A) to 800 mm (lysimeter D) water, about 90 % of the injected tracer were recovered.
- The intensive participation of the initially adhesive water in the percolation process leads to the fact that the correlation between the isotope concentrations of single precipitation events and the newly formed groundwater ist very weak. Also the determination of the seasonal infiltration distribution from the isotope content of groundwater appears thereby problematic.
- There is no indication of a typical more-velocities mechanism, which can be found in a more fine-grained soil (macropores, micropores).
- There is evidence of temporary formation of preferential flow paths in a more or less homogeneous sandy soil after heavy rain events, at least when the depth to water table is small. The reason is not the existence of macro- and micropores like in more fine-grained soils, but the distribution pattern of the entrapped soil air. This air cannot escape as long as the water saturation of the uppermost soil layer continues after a rain event.
- The results of the tracer experiments serve as database for a mathematical modelling of the seepage process at the Technical University of Vienna. The models reported in the literature did not bring a satisfying agreement with the experimental results. The work is not final yet (A. P. BLASCHKE et al., 2000).

5. Modelling Concepts (G. NÜTZMANN, J. FANK, F. FEICHTINGER, E. STENITZER)

5.1. Introduction

Models for flow and transport in the subsurface, and, especially in the unsaturated zone are developing at a rapid pace since the late seventies of the 20th century. There are different ideas and personal views of what models are and what they are presumed to be. In general, it is assumed that such models are or will become regulatory as well as research tools, and that they can ultimately be scaled up to represent the significant

features of reality. Thus, in the process of model developing there are several questions of interest, like: How can we make models relate better to the field scale processes? How precisely do we need to know parameter values? Which level of complexity and which scale is needed?

Regarding to philosophy of modelling, K. ROTH et al. (1990) tried to distinguish some categories to classify field scale models:

- stochastic versus deterministic models (purely or with spatially variable parameters),
- black-box models versus models with a variable degree of process resolution,
- physically based versus empirical models,
- research versus management models.

Because of the fact that a model cannot be categorized in isolation from its objective, one has to focus to the main subject of the present study, which is concerned with tracer transport in variably saturated porous media at a field scale. Here, soil physicists increasingly developed stochastic models to approximate spatial distribution of model parameters regarding the field soil variability in water flow and solute concentrations (K. ROTH et al., 1990, D. RUSSO & G. DAGAN, 1993). Because of the lack of data in the most practical cases and the predictive intention deterministic models are widely applied, and additional, some hybrid categories may be defined by combining both model types also.

In general, the spatial variability of the controlling parameters of an unsaturated/saturated flow and transport system is not purely random, and it can often be shown that some kind of correlation exists in the spatial distribution of these parameters. Thus, subsurface flow and transport could be considered as a deterministic rather than a stochastic problem, and, only when uncertainties associated with these estimates are too high, a reverse action should be the case.

Based on the theory of multiphase flow in porous media the governing equations of fluid flow and species transport have been derived (see S. M. HASSANIZADEH & W. G. GRAY, 1979a, b) and reduced to a set of non-linear partial differential equations describing the main physical and chemical phenomena of solute transport in variable saturated porous media (H.-J. DIERSCH, 1980, G. NÜTZMANN, 1998). Referring to the transport of an ideal and/or reactive tracer, the mechanisms of advection, dispersion, diffusion, ad/desorption and some kinds of reaction kinetics have been applied in this theoretical considerations.

In addition to advection (at average velocity), mechanical dispersion, and molecular diffusion, several other phenomena may affect the concentration distribution of a tracer or a solute as it moves through a porous medium. The tracer, or more common, a solute may interact with the solid surface of the porous matrix in the form of adsorption of tracer particles on the solid surface, deposition, solution of the solid matrix, ion exchange, etc. All these phenomena cause changes in the concentration of a tracer in a flowing liquid. Decay and chemical reactions within the liquid also cause tracer concentration changes.

In general, variations in tracer concentration cause changes in the liquid's density and viscosity. These, in turn, affect the flow regime (i.e., velocity distribution) that depends on these properties. We use the term "ideal tracer" when the concentration of the latter does also not affect the liquid's density and viscosity. At relatively low concentrations, the ideal tracer approximation is sufficient for most practical purposes describing water transport in the unsaturated zone.

Similar to the model of saturated flow problems, the complete deterministic model of a pollution problem in the unsaturated zone consists of the following items:

1) Specification of the geometrical configuration of the closed surface that bounds the problem area, with possible segments at infinity.
2) Specification of the dependent variable(s) of the pollution problem, i.e., the concentration c(x,t) of the specific constituent or constituents under consideration. In the case of interacting constituents, the concentration of each of them is a state variable and we need information on how they interact with each other. Recalling that in all dispersion equations, the velocity appears in both the advective flux and as a building block of the dispersion coefficient, we must have information on v(x,t). This information can either be provided as part of the input to the pollution problem, or we may construct a model in which the velocity is another state variable for which a solution is sought.
   If changes in concentration affect the water's density, the latter becomes another state variable to be solved for, and we need information on the relationship between density and concentration.
3) Statement of a partial differential (balance) equation, for every relevant species. Balance equations, in terms of the various state variables of the problems, as listed in 2) above, are also required for every extensive quantity that is relevant to the problem.
4) Specification of the numerical values of the (transport and storage) coefficient that appear in 3). Of special interest here is the information on the dispersivity and on the coefficient of molecular diffusion in the porous medium under consideration.
5) Statement of the numerical values of the various source and sink terms that appear in 3).
6) Statement of initial and boundary conditions that the state variables appearing in 2) have to satisfy within the considered domain at $t = 0$, and on its boundaries at $t > 0$, respectively.

To describe the movement of water in the unsaturated zone any kind of models can be used describing the movement of ideal tracers. Solution of the continuity equation and the advection-dispersion equation for transport of solute in the unsaturated soil, subjected to appropriate initial and boundary conditions, has to be approximated as well as the time derivatives of both flow and solute transport equations. Most of this models assume that:

- the soil is stable, isotropic, isothermal, and that DARCY's law applies in both saturated and unsaturated zones;
- the solute is assumed to be inert with respect to its environment, so that interaction with the soil matrix is ignored and therefore the effect of tracer accumulation on water flow, adsorption and exclusion is neglected.

In real applications to predict groundwater recharge or the leaching of substances to groundwater much more attention has to be paid on the main processes influencing movement of water and solutes in the unsaturated zone: precipitation, evaporation, root water uptake depending on different plants, soil horizons, interaction of the solutes with the environment.

A more detailed discussion of numerical methods for simulation unsaturated flow and transport processes could be found in P. S. HUYAKORN & G. F. PINDER (1983) and G. NÜTZMANN (1998).

5.2. Transport Codes and Applications

5.2.1. One-Dimensional Models

5.2.1.1. Saturated/Unsaturated Transport Code SUNTRA

The code SUNTRA enables to simulate one-dimensional unsaturated/saturated water flow and solute transport in heterogeneous porous media (G. NÜTZMANN, 1991). The governing equation for transient saturated-unsaturated water flow in a vertical soil column without sinks and sources is given by the RICHARDS equation

$$\frac{\delta\theta}{\delta t} - \frac{\delta}{\delta x}\left[K(\theta)\left(\frac{\delta h}{\delta x} + 1\right)\right] = 0, \tag{5.1}$$

where

θ = the volumetric water content,
h = the pressure head,
K = the hydraulic conductivity,
x = the vertical distance taking on positive values upwards, and
t = the time.

The most common initial and boundary conditions for the one-dimensional flow simulations are

$$\begin{aligned} h &= L - x, && t = 0,\ 0 \le x \le L, \\ -K(\theta)\left(\frac{\delta h}{\delta x} + 1\right) &= 0 && t > 0,\ x = L, \text{ and} \\ h &= h_{gw}(t), && t > 0,\ x = 0, \end{aligned} \tag{5.2}$$

where

x = 0 = the bottom of the column,
x = L = the top of the soil, and
h_{gw} = the actual groundwater level in the column.

In SUNTRA, the solution of the RICHARDS equation was obtained from a GALERKIN finite-element method (G. NÜTZMANN, 1991). As shown by the authors M. Th. VAN GENUCHTEN & D. R. NIELSEN (1985) the water retention relation

$$\Theta(h) = \frac{(\theta - \theta_r)}{(\theta_s - \theta_r)} = \left[\frac{1}{1 + (\alpha|h|)^n}\right]^m, \tag{5.3}$$

with

Θ the effective water saturation ($0 \le \Theta \le 1$),
θ_s the saturated water content,
θ_r the residual water content, and
α, m, n the shape parameters

has great flexibility in describing retention data from various soils. At the same time, it has a simple inverse function and permits the derivation of closed-form analytical expressions for $K(\Theta)$ when combined with the predictive theory of Y. MUALEM (1976).

This model can be written in the form

$$K_r(\Theta) = \sqrt{\Theta}\left[\frac{f(\Theta)}{f(1)}\right]^2, \tag{5.4}$$

where $K_r(\Theta)$ is the relative hydraulic conductivity, K/K_s, or

$$Kr(\Theta) = \sqrt{\Theta}[I\xi(p,q)]^2 \tag{5.5}$$

which is the general expression for variable m and n. Here, $I\xi(p,q)$ is the incomplete beta function with $\xi = \Theta^{1/m}$, $p = m + 1/n$, $q = 1 - 1/n$ (M. Th. VAN GENUCHTEN & D. R. NIELSEN, 1978). A simple expression of unsaturated hydraulic conductivity results from this equation, if the parameter m of the water retention relation is connected to n via $m = 1 - 1/n$. The resulting two parameters (α,n) water retention function holds for porous media with moderate values of n from 1.01–7. Then, the equation for the relative hydraulic conductivity becomes

$$Kr(\Theta) = \sqrt{\Theta}[1 - (1 - \Theta^{1/m})^m]^2, \quad m = 1 - 1/n, \quad 0 < m \leq 1. \tag{5.6}$$

Both models have been implemented in the SUNTRA code to describe a wide range of soil types (G. NÜTZMANN et al., 1998).

Numerical solution of the flow equation results in spatial and temporal distribution of water content and velocity, which is used for solving the convection-dispersion equation in the form

$$\theta R\left(\frac{\delta c}{\delta t} + \lambda c\right) + q\frac{\delta c}{\delta z} - \frac{\delta}{\delta z}\left(\theta D_d \frac{\delta c}{\delta z}\right) - Q^* = 0, \tag{5.7}$$

where

c is the concentration of a solute,
R is the coefficient of retardation,
λ is a constant of decay,
D_d is the hydrodynamic dispersion coefficient, and
Q^* stands for a sink/source term.

For modelling transport of a conservative tracer, one has to assume that $\lambda = 0$. (e.g. there is no decay) and $R = 1$, which means that sorption doesn't occur. For non-conservative tracers, the SUNTRA code allows to choose for three sorption models containing the isotherms of HENRY, LANGMUIR, and FREUNDLICH.

In unsaturated porous media, the dispersion coefficient depends on both water velocity and water content, which leads to the following formulation

$$D = D(v,\theta) = \alpha(\theta)v + D_m\,\tau, \tag{5.8}$$

where

α[L] is the dispersivity depending on water content,
D_m[L^2T^{-1}] stands for the diffusion coefficient, and
τ[L^2L^{-2}] is the tortuosity factor.

As an example of applicability of SUNTRA, simulation of sodium chloride breakthrough in tracer column experiments are shown in fig. 5.1, 5.2 and 5.3. These experiments were carried out to estimate the dependence of dispersivity from water content.

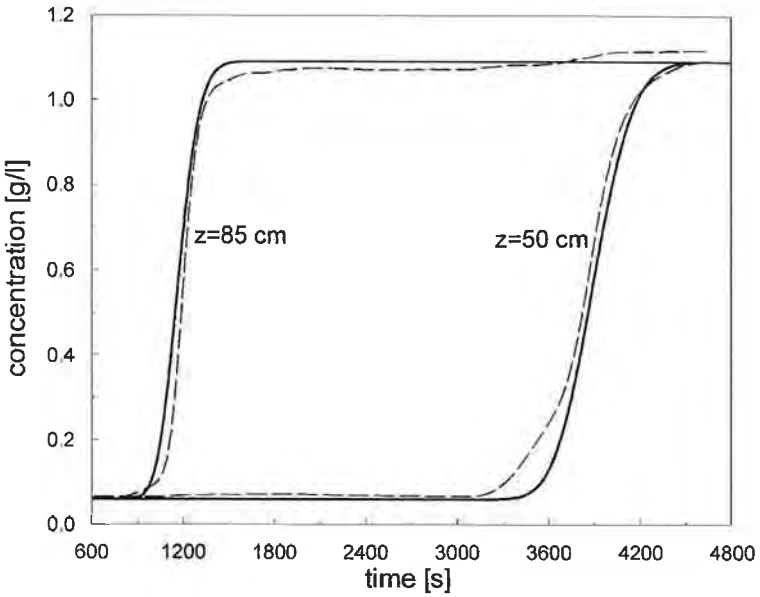

Fig. 5.1: Comparison of simulated and measured tracer breakthrough in a saturated porous medium (dashed lines – measured, continuous lines – simulated breakthrough).
Vergleich von simulierten und gemessenen Tracerdurchbruchskurven im gesättigten porösen Medium (gestrichelte Linien: Messung; durchgezogene Linien: Simulation).

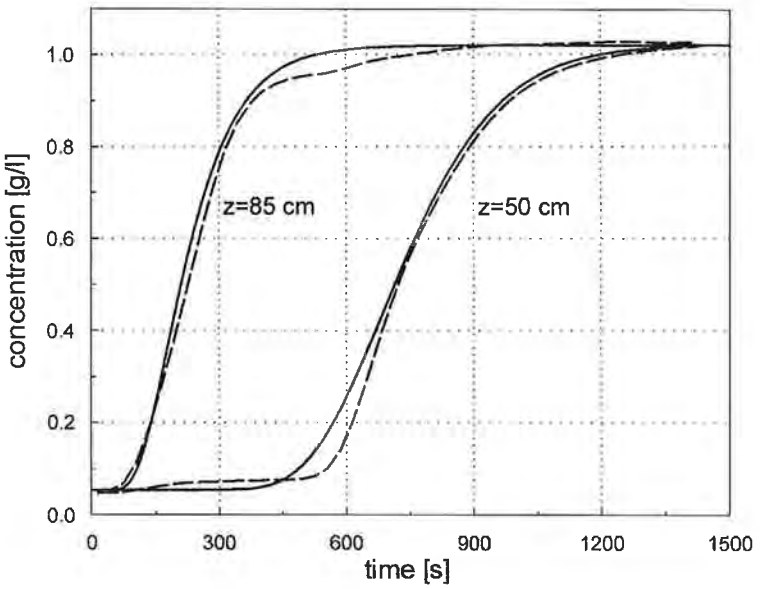

Fig. 5.2: Comparison of simulated and measured tracer breakthrough in an unsaturated porous medium (dashed lines – measured, continuous lines – simulated breakthrough).
Vergleich von simulierten und gemessenen Tracerdurchbruchskurven im ungesättigten porösen Medium (gestrichelte Linien: gemessene Durchbrüche; durchgezogene Linien: berechnete Durchbrüche).

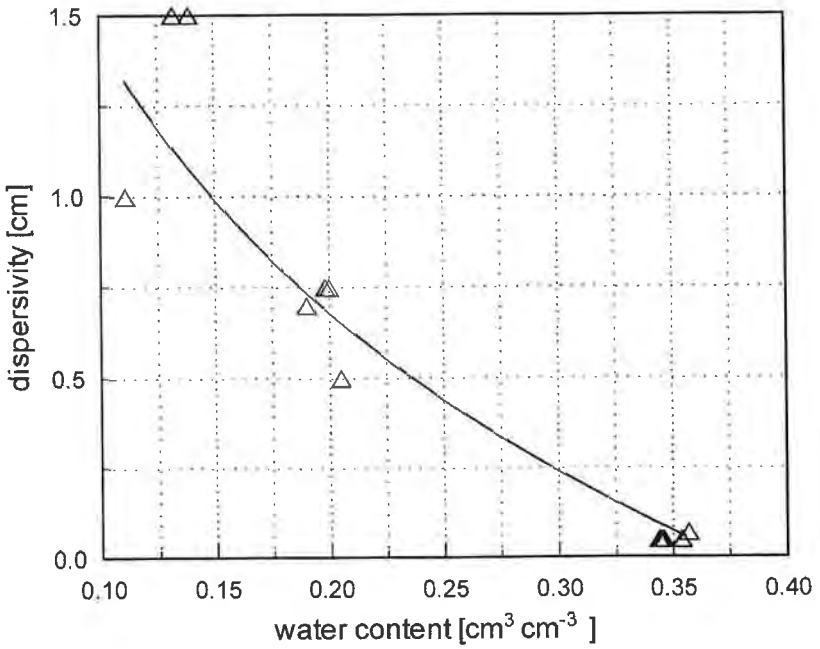

Fig. 5.3: Dependence of dispersivity on water content in an unsaturated porous medium (triangles – estimated dispersivity values from experiments, continuous line – inverse optimized function via numerical simulation with SUNTRA).
Abhängigkeit der Dispersivität vom Wassergehalt in ungesättigten porösen Medien (Dreiecke: experimentell bestimmte Dispersivität; durchgezogene Linie: durch inverse Modellierung mit SUNTRA ermittelte Funktion).

The observed and simulated breakthrough curves showed that the increase of the solute mixing proceeded with a decrease of water content was caused by growth of flow velocity fluctuations for different pathways. Thus, the dispersivity was found to increase with decreasing water content (S. MACIEJEWSKI et al., 2001).

5.2.1.2. Phosphorus Transport Model MORPHO

The assessment of the potential eutrophication of surface waters, especially in the north-eastern lowlands of Germany depends on the input from the basin. Therefore scenarios dealing with regional transport of phosphorus are helpful tools to calculate prognosis of the diffuse loading of surface waters. Therefore, the compartment model MORPHO was developed to simulate the leaching of phosphorus in the unsaturated zone in a sub-basin scale.

MORPHO consists of the three compartments: land surface, soil (unsaturated zone) and groundwater and deals with the following process:

a) Generation of time series for precipitation (P) and potential evapotranspiration (ETP) with ARMA(p,q) models (J. D. SALAS et al., 1985), where ETP is estimated by the modified MAKKINK method (DVWK, 1996).
b) Surface runoff (RO) is predicted using the SCS curve number method (USDA, 1983).
c) Infiltration rate (q in m h^{-1}) is estimated by a simple hydrological water balance q = P – ETP – RO.

d) Flow in the unsaturated zone (v in m h^{-1}) is assumed as stationary ($v = q/\theta$), where θ (vol.-%) is the volumetric water content constant for each (selected) soil layer.
e) Transport in the unsaturated zone is modelled by the one-dimensional advection-dispersion equation, solved by a finite difference approximation.
f) For flow and transport in groundwater the mixing cell approach from J. BEAR (1979) is used.
g) Reactions between P and the porous matrix of soil and groundwater are calculated with the kinetic sorption model of N. J. BARROW & T. C. SHAW (1975): $s = k \cdot c^n \cdot t^m$, where s is the amount sorbed at the matrix (g kg^{-1} of soil), c the solute concentration in the pore space (g l^{-1}) and k is a constant which gives a relative measure of the sorbing capacity of the soil for P; n and m are constants which indicate the dependence of sorption on concentration and time (t) with a high value indicating stronger dependence.

MORPHO operates on a daily time step. Spatial distribution of basin parameters (e.g., land use, soils, P-content and topography) is achieved in the horizontal through the representation of the basin by a rectangular grid network and in the vertical by a column of horizontal layers at each grid square (S. PUDENZ & G. NÜTZMANN, 1997 and S. PUDENZ, 1999).

5.2.1.3. Soil Water and Nitrogen Transport Model SIMWASER/STOTRASIM

Everyday diverse environmental pollution hit the headlines. Also the pollution of groundwater by nitrate, pesticides or other loads is discussed in connection with agricultural practices. About that the efforts for groundwater protection are often assisted by the use of simulation models.

STOTRASIM is such a tool and it calculates the soil moisture fluxes and the nitrogen dynamic of agricultural soils. The simulation of the soil moisture regime and of plant growth bases on the numerical model SIMWASER proposed by E. STENITZER (1988), which then has been enlarged to STOTRASIM (F. FEICHTINGER, 1998) by the calculation of the nitrogen cycle. This model takes into account atmospheric input and output, the influences of the vegetation, the mechanisms and reactions in the soil and directs it's main attention to the amount of leaching water and of nitrate losses to the groundwater. Calibration, verification and application of STOTRASIM are focused on these environmental aspects.

5.2.1.3.1. Concept of STOTRASIM

The model is designed to describe one-dimensional, vertical flow of water and nitrate-nitrogen in a soil profile. Interflow, preferential flow and surface runoff are neglected. Additional simplifying assumptions are:

- Nitrogen transport in the soil only takes place together with water movement.
- Nitrate-nitrogen in the soil is completely dissolved in the soil water and nitrate-nitrogen is the only nitrogen compound in the soil solution. Therefore all other nitrogen components (organic N, NH_4-N) have to be converted to NO_3-N before taking part in nitrogen transport.
- On the other hand the whole nitrogen demand in the soil (uptake by plants, immobilization) will be satisfied by the available NO_3-N.
- A limitation of potential plant growth is given by a deficiency of water and/or nitrogen. A response of plant growth to the supply other nutrients and to pests is not taken into account.

STOTRASIM consists of the two following submodels:

- water balance and plant growth,
- nitrogen cycle.

Water Balance and Plant Growth (SIMWASER)

The numeric model SIMWASER simulates the water balance and the crop yield of any number of crop rotations and years, provided that daily weather records (air temperature, humidity of air, global radiation, wind and precipitation) are available. The soil profile to be simulated is divided into a number of layers, usually 5–10 cm thick, down to a depth, where seasonal change of the water content is low and is believed to have minor impact upon the soil water regime. In case of capillary rise from groundwater the "model soil profile" is extended to the deepest groundwater level, that is measured within the simulated period, and the daily course of groundwater level has to be included into the input data.

Water balance and plant growth are linked together by the physiological interaction of assimilation and transpiration. The increase of dry matter production depends on taking carbon dioxide from the air in exchange for water vapour via the stomata. As long as the delivery of water to the stomata can satisfy potential transpiration, potential assimilation and potential plant growth occurs. The actual plant growth is calculated by the potential plant production rate and the proportion of actual transpiration to potential transpiration (Eq. 5.9).

$$P_{act} = P_{pot} \cdot \frac{T_{act}}{T_{pot}}, \tag{5.9}$$

where

P_{act}, P_{pot} = actual and potential plant production,
T_{act}, T_{pot} = actual and potential transpiration.

The potential evapotranspiration, the potential evaporation and also the potential transpiration are calculated according to the "PENMAN-MONTEITH-formula" (G. SZEICZ et al., 1969, A. S. THOM & H. R. OLIVER, 1977). The actual transpiration is equivalent to the root water uptake, which is the result of balanced forces at the root surface using eq. (5.10):

$$WUR = \frac{(\psi_p - \psi_s)}{(R_p + R_s)} \cdot RLD \cdot H, \tag{5.10}$$

where

WUR = water uptake by the roots,
ψ_p = plant water potential,
ψ_s = soil water potential,
R_p = plant resistance,
R_s = soil resistance,
RLD = root length density,
H = thickness of the soil layer.

The water balance on daily base is made at the soil surface with precipitation and irrigation as input and evaporation and transpiration as output. Interception is also taken

into account. The water movement in the soil is calculated by DARCY's law and the "continuity equation". Taking into account the soil physical parameters of each soil layer either capillary rise or seepage will be the result at the lower boundary of the soil profile.

Nitrogen Cycle

Nitrogen uptake by the plants is calculated by mass flow multiplied by a coefficient specific to each plant using eq. (5.11). Mass flow is described by water uptake of the roots and the nitrate concentration of the soil solution.

$$NUP = T \cdot CNO_3 \cdot S, \tag{5.11}$$

where

NUP = N-uptake by the plants,
T = transpiration rate = water uptake by the roots,
CNO_3 = nitrate concentration in the soil solution,
S = selection coefficient.

The selection coefficient takes into account the influence of the diffusion and of a so called "root absorbing power" (P. H. NYE & P. B. TINKER, 1977). Root length density – influencing N-uptake by plants – is already used to calculate water uptake by the roots. The capability of legumes to assimilate nitrogen from the air is described in dependence of the nitrogen supply of the soil solution. With decreasing nitrogen supply of the soil solution the contribution of biological fixation of nitrogen from the air increases to 80 % of total nitrogen uptake.

The nitrogen turnover in the soil by mineralization, nitrification, immobilization and denitrification is determined by the interaction of nitrate in the soil solution and two organic pools of nitrogen as well as the availability of carbon. Carbon has to be taken into account with regard to the consumption of energy by the microbial biomass. The processes are controlled by the soil temperature and the soil moisture. Organic matter (OM) and fresh organic matter (FOM) are two organic pools with quite different dynamics. OM equals the humus content of a soil minus a biologically inert organic fraction according to the fine-grained mineral soil particles (J. RÜHLMANN, 1999). FOM includes plant residues, manure, compost and so on. Each of them has a specific carbon content and C/N-ratio. Mineralization of OM is calculated by eq. (5.12) and eq. (5.13):

$$MNOM = MCOM \cdot CNOM, \tag{5.12}$$

where

MNOM = mineralized nitrogen from organic matter (OM),
MCOM = mineralized carbon from OM,
CNOM = C/N-ratio of OM;

$$MCOM = OM \cdot COM \cdot Mf(T) \cdot Mf(DS) \cdot MPOM \cdot DYN, \tag{5.13}$$

where

OM = mass of organic dry matter in the soil,
COM = carbon content of OM,
MPOM = mineralization potential of OM,

DYN = parameter for stimulation due to tillage,
Mf(T) = function of microbial activity depending on soil temperature (T) (Fig. 5.4a),
Mf(DS) = function of microbial activity depending on the degree of saturation (DS) (Fig. 5.4b).

The mineralization of FOM is calculated by eq. (5.14) and eq. (5.15).

$$MNFOM = MCFOM \cdot CNFOM, \tag{5.14}$$

where

MNFOM = mineralized nitrogen from fresh organic matter (FOM),
MCFOM = mineralized carbon from FOM,
CNFOM = C/N-ratio of FOM;

$$MCFOM = FOM \cdot CFOM \cdot Mf(T) \cdot Mf(DS) \cdot MPFOM, \tag{5.15}$$

where

FOM = mass of fresh organic dry matter in the soil,
CFOM = carbon content of FOM,
MPFOM = mineralization potential of FOM.

The soil moisture is represented by the degree of saturation of the pore space, which is expressed by the volumetric water content of the soil divided by the pore volume of the soil. Figure 5.4 shows the function of microbial activity for mineralization and nitrification in dependence of soil temperature according to D. E. CLAY et al. (1985) as well as in dependence of the degree of saturation in the soil. The soil temperature is calculated by a statistical approach according to G. MÜLLER & J. DÖRING (1989).

Following J. J. R. GROOT & P. DE WILLIGEN (1991) about 30 % of the mineralized carbon are necessary for the growth efficiency of the microbial biomass. Furthermore the C/N-ratio of the biomass is 10. Therefore the nitrogen demand essential for life is about 3 % of the mineralized carbon. This demand results in either net mineralization or immobilization of nitrate-nitrogen according to eq. (5.16) or eq. (5.17):

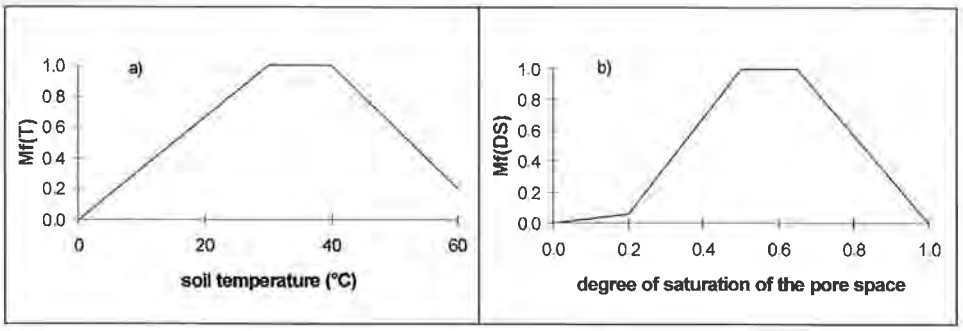

Fig. 5.4: Activity functions for mineralization and nitrification depending a) on soil temperature, b) on water saturation of the pore space.
Funktionen der mikrobiologischen Aktivität für die Mineralisation und die Nitrifikation in Abhängigkeit von a) der Bodentemperatur und b) von der Wassersättigung der Porenräume.

$$0.03 \cdot (MCOM + MCFOM) < (MNOM + MNFOM) = \text{net mineralization}, \quad (5.16)$$

$$0.03 \cdot (MCOM + MCFOM) > (MNOM + MNFOM) = \text{immobilization}. \quad (5.17)$$

The nitrification of ammonium to nitrate-nitrogen is calculated by eq. (5.18).

$$MNO_3 = MNH_4 \cdot Mf(T) \cdot Mf(DS) \cdot DYN, \quad (5.18)$$

where

MNO_3 = amount of nitrate resulting from nitrification,
MNH_4 = amount of ammonium in the soil,
DYN = parameter of stimulation due to tillage,
Mf(T) = function of microbial activity depending on soil temperature (T) (Fig. 5.4a),
Mf(DS) = function of microbial activity depending on the degree of saturation (DS) (Fig. 5.4b).

According to J. C. G. OTTOW (1992) denitrification is an aerobic process under anaerobic conditions. Therefore denitrification depends on the availability of carbon and is controlled by the oxygen content in the soil as well as by the soil temperature. The oxygen supply in the soil is described by the degree of saturation (DS) as the supplementary volume of the pore space. Assuming that nitrate of the soil solution is the source of oxygen for the aerobic process and that a good relation between dissolved carbon and the amount of carbon of OM (D. HEYDER, 1993) exists, denitrification is described by eq. (5.19).

$$DEN = CNO_3 \cdot COM \cdot Df(T) \cdot Df(DS) \cdot DEPO, \quad (5.19)$$

where

DEN = amount of nitrate losses by denitrification,
CNO_3 = nitrate cocentration in the soil solution,
COM = carbon content of organic matter (OM),
DEPO = denitrification potential,
Df(T) = function of microbial activity depending on soil temperature (T) (equal to fig. 5.4a),
Df(DS) = function of microbial activity depending on the degree of saturation (DS) (Fig. 5.5).

The function Df(T) is the same as for mineralization and nitrification (Fig. 5.4a). The function Df(DS) is additionally influenced by the soil temperature, because a lack of oxygen occurs all the more as oxygen demand is high because of a high biological activity and is shown in fig. 5.5.

In the case of organic fertilizer input (manure, slurry) a 35 % loss of the ammonium content is calculated, if an incorporation to the soil doesn't take place at the same day of fertilization (A. AMBERGER, 1989). The transport of nitrate-nitrogen within the soil is described by the differential equation for one-dimensional vertical solution transport, taking into account convection, diffusion and dispersion.

Evaporation causes a decreasing amount of the solvent and therefore an increasing nitrate concentration in the upper layer of the soil profile. The nitrate losses at the lower end of the soil profile are the result of all these above mentioned facts in conjunction with the water flux.

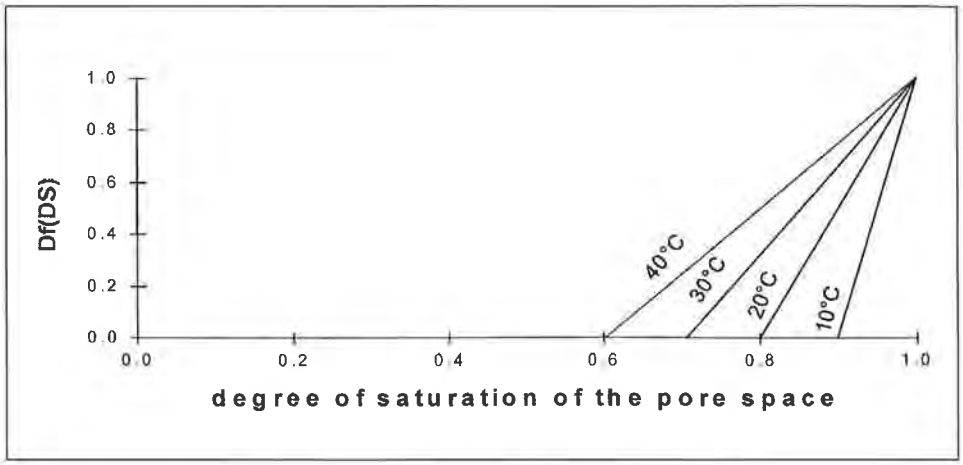

Fig. 5.5: Function of microbial activity for denitrification depending on the degree of saturation. Funktion der mikobiologischen Aktivität für die Denitrifikation in Abhängigkeit vom Sättigungsgrad.

5.2.1.3.2. Data Input/Output

Input Data

The data required for running STOTRASIM are shown in tab. 5.1.

Tab. 5.1. Required data for running STOTRASIM. (Continuation p. 86.) Datenerfordernis für STOTRASIM. (Fortsetzung S. 86.)

Information upon	Parameter
SOIL (singular input initially)	
Soil profile:	sequence of soil layers thickness of soil layers
Soil layers:	water retention characteristic hydraulic conductivity function diffusion/dispersion-coefficient soil texture bulk density humus content C/N-ratio of the humus initial values of: NO_3-N-content NH_4-N-content content of fresh organic matter (FOM) C/N-ratio of FOM
CLIMATE (daily data required)	precipitation amount air temperature (07.00, 14.00, 19.00, max., min.) relative humidity (07.00, 14.00, 19.00) averaged wind velocity sum of global radiation

AGRICULTURAL PRACTICE (adapted to the case)	
Crop rotation:	type of crop date of sowing date of harvest
Irrigation:	date of irrigation amount of irrigation NO_3-N-, NH_4-N-content of irrigation water
Inorganic fertilizer:	date of fertilization amount of NO_3-N, NH_4-N
Organic fertilizer: (manure, plant residues)	date of fertilization amount of dry matter carbon content C/N-ratio amount of NO_3-N, NH_4-N, N_{org}
Soil treatments:	date of ploughing, grubing and similar depth of ploughing, grubing and similar

Output Data

The data output is summarized in tab. 5.2.

Tab. 5.2: Available data output from STOTRASIM.
Verfügbare Ausgabedaten aus STOTRASIM.

Water cycle	Crop growth	Nitrogen cycle
• actual transpiration • actual evaporation • interception • sum of rain • sum of irrigation • water storage in the soil profile • rate of seepage or capillary rise at the lower end of the soil profile	• total dry matter production • root dry matter production	• sum of nitrogen input • nitrogen uptake by the plants • nitrogen fixation by legumes from the air • amount of organic pools (OM, FOM) • rates of nitrogen turnover • storage in the soil (NO_3-N, NH_4-N) • rate of NO_3-leaching or input by capillary rise at the lower end of the soil profile

5.2.1.3.3. Application of STOTRASIM

At the moment the following crops can be handled by STOTRASIM: wheat, barley, rye, oats, maize, sugar beet, potato, rape, sunflower, pea, bean, soybean and grassland. If STOTRASIM is applied to a single site or in case of calibration and verification of the model the input data (Tab. 5.1) have to be determined by measurements. In case of application to larger areas the input data may be derived from soil maps, from weather files of the meteorological service and from agrostatistics. Until now STOTRASIM

was applied for scientific studies as well as in practice, for example to judge the effects of different water supply for irrigation upon the nitrate pollution of the groundwater in an agricultural area of about 300 km² in the eastern part of Austria.

If there is a great uncertainty to the initial values of FOM, C/N-FOM, NO_3-N, NH_4-N and θ (Tab. 5.1), a simulation of at least two years should precede the effective case study for "preparing" these parameters.

5.2.2. Multi-Dimensional Models

5.2.2.1. Model HYDRUS2D to Simulate Water and Solute Transport

The purpose of this program (J. SIMUNEK et al., 1996) is to prepare input data for the HYDRUS2 (J. SIMUNEK et al., 1992) code, to run HYDRUS2, and to analyse the output data. A user-friendly interface written for a MS Windows 3.1 environment includes data pre-processing and graphical representation of the output results. Data pre-processing involves the specification of a flow region of arbitrary continuous shape by means of lines, arcs and splines, discretization of domain boundaries, and subsequent automatic mesh generation of an unstructured finite element mesh. An alternative structured mesh for relatively simple transport domains defined by four boundary lines can also be considered. Graphical presentation of the output results consists of simple two-dimensional x-y graphs, contour and spectral maps, velocity vectors, as well as animation of both contour and spectral maps. Graphs along any cross-sections or boundaries can be readily obtained. A small catalog of soil hydraulic properties was made part of the interface.

The code has been verified against a large number of test cases. Example applications provided with the software package visualize in an easy way very complex interrelations between hydraulic reaction and the transport of water and solutes in the unsaturated zone.

5.2.2.1.1. Concept of HYDRUS2

The HYDRUS2 computer program simulates water and solute movement in two-dimensional variably saturated media. The program numerically solves the RICHARDS' equation for saturated-unsaturated water flow and the convection-dispersion equation for solute transport. The flow equation incorporates a sink term to account for water uptake by plant roots. The solute transport equation includes provisions for linear equilibrium adsorption, zero-order production, and first-order degradation. The program may be used to analyse water and solute movement in unsaturated, partially saturated, or fully saturated porous media. HYDRUS2 can handle flow domains delineated by irregular boundaries. The flow region itself may be composed of non-uniform soils having an arbitrary degree of local anisotropy. Flow and transport can occur in the vertical plane, the horizontal plane, or in a three-dimensional region exhibiting radial symmetry about a vertical axis. The water flow part of the model considers prescribed head and flux boundaries, as well as boundaries controlled by atmospheric conditions.

The governing flow and the transport equations are solved numerically using GALERKIN-type linear finite element schemes. Depending upon the size of the problem, the matrix equations resulting from discretization of the governing equations are solved using either GAUSSian elimination for banded matrices, or the conjugate gradient method for symmetric matrices and the ORTHOMIN method for asymmetric matrices (C. A. MENDOZA et al., 1991).

Because of the non-linear nature of the RICHARDS' equation, an iterative process must be used to obtain solutions of the global matrix equation at each new time step.

For each iteration a system of linearized algebraic equations is first derived which is solved using either GAUSSian elimination or the conjugate gradient method. After inversion, the coefficients are re-evaluated using the first solution, and the new equations are again solved.

The iterative process continues until a satisfactory degree of convergence is obtained, i.e., until at all nodes in the saturated (or unsaturated) region the absolute change in pressure head (or water content) between two successive iterations becomes less than some small value determined by the imposed absolute pressure head (or water content) tolerance. The first estimate (at zero iteration) of the unknown pressure heads at each time step is obtained by extrapolation from the pressure head values at the previous two time levels.

Three different time discretizations are introduced in HYDRUS2:

(1)time discretizations associated with the numerical solution,
(2)time discretizations associated with the implementation of boundary conditions, and
(3)time discretizations which provide printed output of the simulation results (e.g., nodal values of dependent variables, water and solute mass balance components, and other information about the flow regime).

Discretizations 2 and 3 are mutually independent; they generally involve variable time steps as described in the input data file. Discretization 1 starts with a prescribed initial time increment, Δt. This time increment is automatically adjusted at each time level according to given rules. The selection of optimal time steps, Δt, is also influenced by the solution scheme for solute transport.

5.2.2.1.2. Input Data Set

The unsaturated soil hydraulic properties in the HYDRUS2 code are described by a set of closed-form equations resembling those of M. Th. VAN GENUCHTEN (1980) who used the statistical pore size distribution model of Y. MUALEM (1976) to obtain a predictive equation for the unsaturated hydraulic conductivity function.

The original VAN GENUCHTEN equations were modified to add extra flexibility in the description of the hydraulic properties near saturation (see T. VOGEL & M. CISLEROVA, 1988).

Root water uptake is implemented in form of the stress response function as used by R. A. FEDDES et al. (1988). The water uptake is assumed to be zero close to saturation and for pressure heads less than the wilting point. HYDRUS2 currently implements the same linear interpolation scheme as used in several versions of the SWATRE code (e.g. J. G. WESSELING & T. BRANDYK, 1985).

Time dependent boundary conditions for water flow and solute transport may be used without any spatial variability in the modelling domain – a strong restriction for the 2D-vertical-application on real problems.

Depending on the type of the transport problem and the substances incorporated some or all of the following solute transport parameters for each soil material have to be specified for the solution of the transport equations: bulk density, molecular diffusion coefficient in free water, longitudinal dispersivity, transverse dispersivity, FREUNDLICH isotherm coefficient, first-order rate constant for dissolved phase, first-order rate constant for solid phase, zero-order rate constant for dissolved phase, zero-order rate constant for solid phase.

Different time and space weighing schemes for the numerical solution of the solute transport equation may be selected.

5.2.2.1.3. Presentation of Modelling Results

Two-dimensional graphics is used to present results of the simulation by means of contour maps, isolines, spectral maps, velocity vectors and animation. Contour maps and spectral maps for the pressure head, water content and concentration can be drawn. Animation of the three variables is also possible, both in spectral and contour maps. One-dimensional graphs of all variables at the boundary, as well as at any selected cross-sections or any part of the boundary, may be obtained.

Observation points are used for the graphical presentation of changes in water content, pressure head and/or concentration at specified observation nodes. Observation nodes must be specified before the calculations.

The user interface enables the user to produce graphical representation of actual and cumulative boundary fluxes, solute fluxes, and average pressure heads, graphs of temporal changes in pressure head, of temporal changes in water fluxes, of temporal changes in cumulative water fluxes and of temporal changes in actual and cumulative solute fluxes across boundaries with different types of boundary conditions.

The soil hydraulic properties may be visualized graphically. Several combinations of dependent and independent variables are possible.

Graphs of the temporal changes in time steps, number of iterations necessary to solve RICHARDS' equation at a particular time level, cumulative number of iterations, and dimensionless PECLET and COURANT numbers can help to interpret the significance of model run. These variables can be drawn against either time or time level.

An ASCII file gives the information about the surface area, volume of water, inflow and outflow, mean pressure head, amount of solute, and mean concentration in the entire flow domain or at specified subregions. Absolute and relative errors in the water and solute mass balances of the entire flow domain are also given. Modelling results partly are stored in binary files. It is possible to convert these data into ASCII for a further use in other applications.

5.2.2.2. Model Coupling – Quasi 3-D Unsaturated/Saturated Flow and Transport Simulation with COMFLO

The concept to couple models for unsaturated and saturated flow and transport in one combined approach is based on the idea that transport phenomena in both compartments can be treated separately one after the other. Then, some assumptions have to be fulfilled, which are not unusual in contamination studies at the regional scale:

1) The solute transfer processes in the unsaturated zone are mainly one-dimensional (1-D).
2) Water and solute transport in aquifer take place in two-dimensional (2-D), horizontal areas.
3) The water table in the aquifer is constant in time.

In fact these assumptions are often accepted in case studies on groundwater pollution, but often not explicitly stated. A scheme of such a flow and transport situation is depicted in the fig. 5.6.

In an advanced modelling approach (E. HOLZBECHER et al., 1992) different codes with manual coupling were applied to simulate nuclide migration in the vadose and in the groundwater zones. In G. NÜTZMANN et al. (2000) it was shown that a similar good performance can be obtained when the numerical simulation codes SUNTRA (G. NÜTZMANN, 1991) and FAST (E. HOLZBECHER, 1996) for unsaturated and saturated zone are coupled. The problem to be solved is that output from the vadose zone

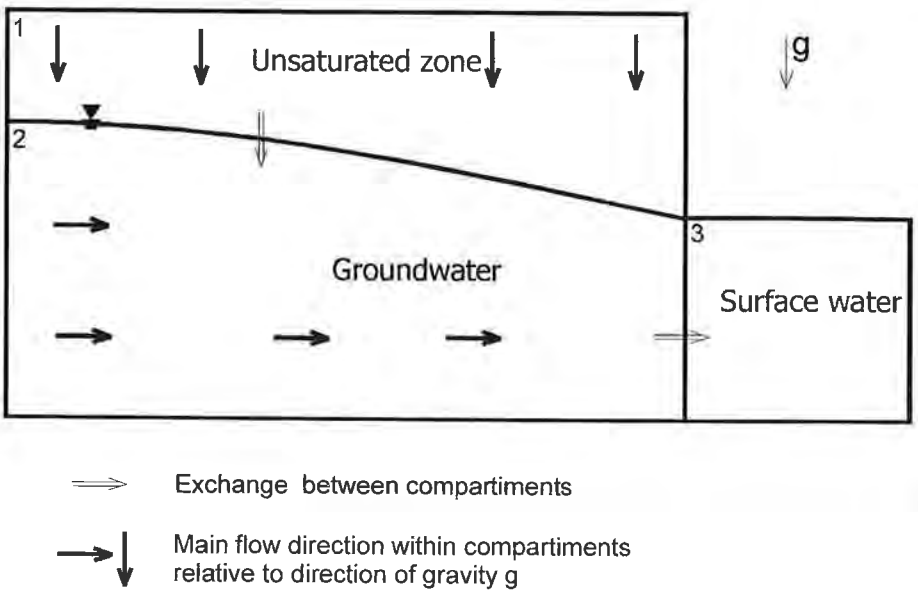

Fig. 5.6: Conceptual model: main directions of flow and transport.
Konzeptionelles Modell: Richtungen der Strömung und Schadstoffausbreitung.

model has to be transformed and transferred to the groundwater model. Here we advocate for the implementation and help of an intra-model interface. The method is especially powerful for problems of regulatory decision making and/or risk assessment dealing with diffuse contaminant sources in the unsaturated zone concerning the question if and how much groundwater is affected.

The coupling between two simulators for unsaturated and saturated zones on the computer is performed by the new implemented interface named ComFlo (Combined Flow). More precisely, ComFlo has to transform and reorganize output data obtained from multiple calculations of SUNTRA together with new input data in order to produce input data sets for FAST. The ComFlo Code is designed to perform data input, data transformation and data transfer.

Main reason for data transformation is the "decoupling" of timestepping considerations in models for unsaturated and saturated zones. This can be done separately in both simulators.

There is no need that the FAST code for modelling transport in the saturated zone identifies timesteps that were used before in SUNTRA code for transport in the unsaturated zone. Within SUNTRA no additional requirements have to be considered when the code is connected with FAST to form a combined model with variable saturation. This advantage can hardly be underestimated because restrictions for time steps, like NEUMANN or COURANT criteria, are often very different in the saturated and in the vadose part of the subsurface.

Within the time intervals breakthrough curves are transformed into 5^{th} order polynomials. A first approximation is done automatically but can be controlled and extended by the modeller. If the correspondence between the simulated breakthrough curve and polynomial approximation is not good enough, there are several options to improve the accuracy and the calculation of polynomial coefficients.

In order to obtain a polynomial of 5th order six coefficients have to be determined. The first two parameters a_1 and a_0 are chosen to get the values in the first and last time point exactly. The other parameters are determined from all data by a method of least squares.

The start approximation consists of one or two fitted polynomials, i.e. a polynomial approximation is proposed in one or two intervals. The number of intervals may be too small to obtain a sufficient accuracy. The approximation can be improved by the user choosing a different number of polynomials and interval divisions of the whole time period. In ComFlo this can be done in by adding or removing of interval limits for the polynomial approximation.

Model formulations and solution schemes are applied to simulate long-term behaviour of heavy metals (Cd, Zn) in the subsurface of a former sewage farm. These contaminants were measured in the solid phase of the upper soil horizons at high concentration levels, and intensive mineralization processes and acid precipitation led to strong changes of physical and chemical soil properties in the unsaturated zone followed by a mobilization of heavy metals.

To prevent a remarkable breakthrough into the groundwater, a soil improvement by increasing the sorption capacity with the help of boulder clay was approached. Referring that heavy metal desorption and leaching is to be considered as a very slow process, possible effects on the groundwater and surface water quality were predicted with the help of the coupled transport models.

The test area is situated in the northeastern part of Berlin where the unsaturated zone has a mean thickness of 3.25 m and an uncovered near-surface aquifer thickness of 3–10 m. The hydrogeological cross section is depicted in fig. 5.7.

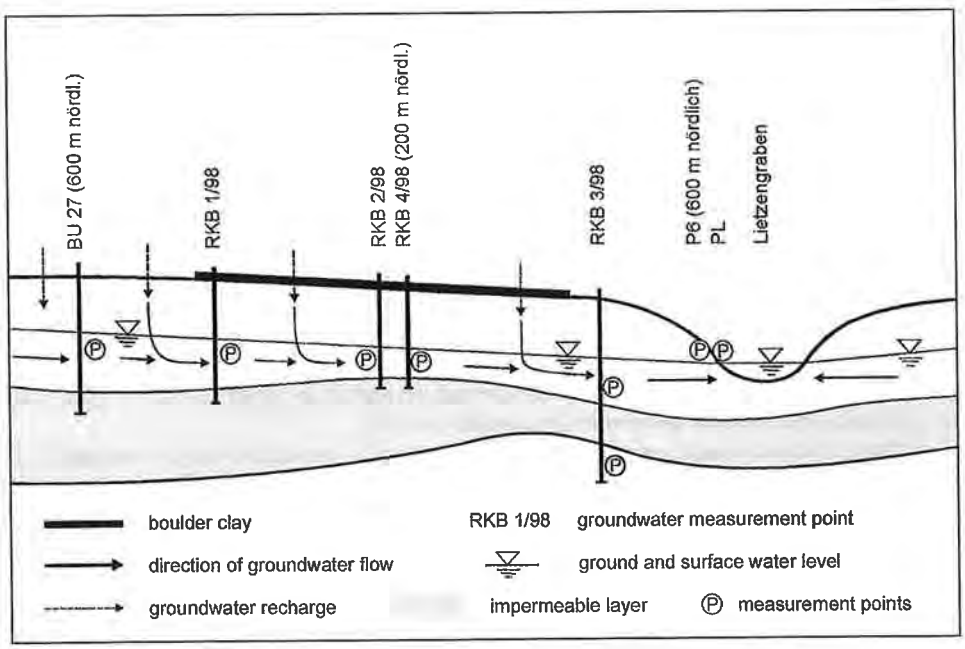

Fig. 5.7: Hydrogeological cross-section of the test area.
Vertikal-ebenes hydrogeologisches Schema der Testfläche.

The mean annual rainfall is between 400 mm/a and 680 mm/a, which leads to a mean groundwater recharge rate of 150 mm/a. In 1998 during a field experiment, boulder clay was mixed into the upper soil layer of selected areas of a former sewage farm in the NE of Berlin, and an investigation program was started to measure the retention effect of these areas compared with the remaining ones (G. NÜTZMANN et al., 2000). In accordance with the natural hydrologic processes, the coupled water flow and heavy metal transport in the vadose zone must be modelled at first, followed by the flow and transport in the near-surface groundwater layer. This was done using the ComFlo-code as described above.

Assuming that water flow in the unsaturated zone is accepted to be one-dimensional, there are several arguments that transport can be treated as 1-D as well. Because of the long-term character of these modelled processes, the water flow both in the unsaturated and in the saturated zone must be assumed as steady-state. It is supposed that the unsaturated part can be divided into zones with equal soil profiles. Based on data from several measurement campaigns, nine different soil profiles were classified. The classification concerns all characteristics that determine flow and transport through the soil column, i.e. recharge, soil layers, dispersion and sorption coefficients and more. For example, a typical recharge/discharge rate can be associated to every zone. Using this classification of profiles, the concentration in groundwater recharge is given by one representative breakthrough curve for each zone with no feedback between flow and transport of neighbouring profiles. The boundary material flux from unsaturated zone to groundwater can be computed at every time-step as $m_L = c_L\, q_L\, \Delta t$, where c_L and q_L are the computed concentration and water flux at $x = L$, and L is the bottom of the column. In fig. 5.8 simulated breakthrough curves for Cd from the unsaturated zone into the near-surface groundwater are depicted. The soil profile II is located near the groundwater sampling point RKB 2/98, see fig. 5.7. The graph shows the retardation effect of the new soil profile with boulder clay because of the increased sorption capacity.

Due to the small thickness of the near-surface aquifer and the underlaying aquitard, the assumption of horizontal flow was made for modelling the heavy metal transport in groundwater. At first, similar to the unsaturated zone a steady-state groundwater flow has to be computed, and than, based on the flow field, transient transport was simulated. Initial conditions for transport simulation in the unsaturated zone and in groundwater are given by several measurements during the experimental programme. It can be assumed that heavy metal concentrations in precipitation are negligibly small, so that only a leaching of Zn and Cd from soil to groundwater takes place. Initial heavy metal concentrations in groundwater are taken from measurements. Regarding that groundwater modelling was started with homogeneous aquifer parameters it becomes obvious that spatial variable distributions of heavy metals in the unsaturated zone lead to a heterogeneous distribution in the aquifer as well.

Further, main concentrations of Cd (and Zn too) in groundwater are located under regions where soil improvement with boulder clay does'nt occur. From these areas, a fast breakthrough into the surface water can be predicted. Contamination from areas with boulder clay covering takes place much slower (more than twice as much time) and with lower concentration.

The method is described for a case study for non-point source heavy metal pollution at a former sewage irrigation field. The procedure is demonstrated for a steady state flow and a transient transport regime, but can be generalized for transient flow regimes as well.

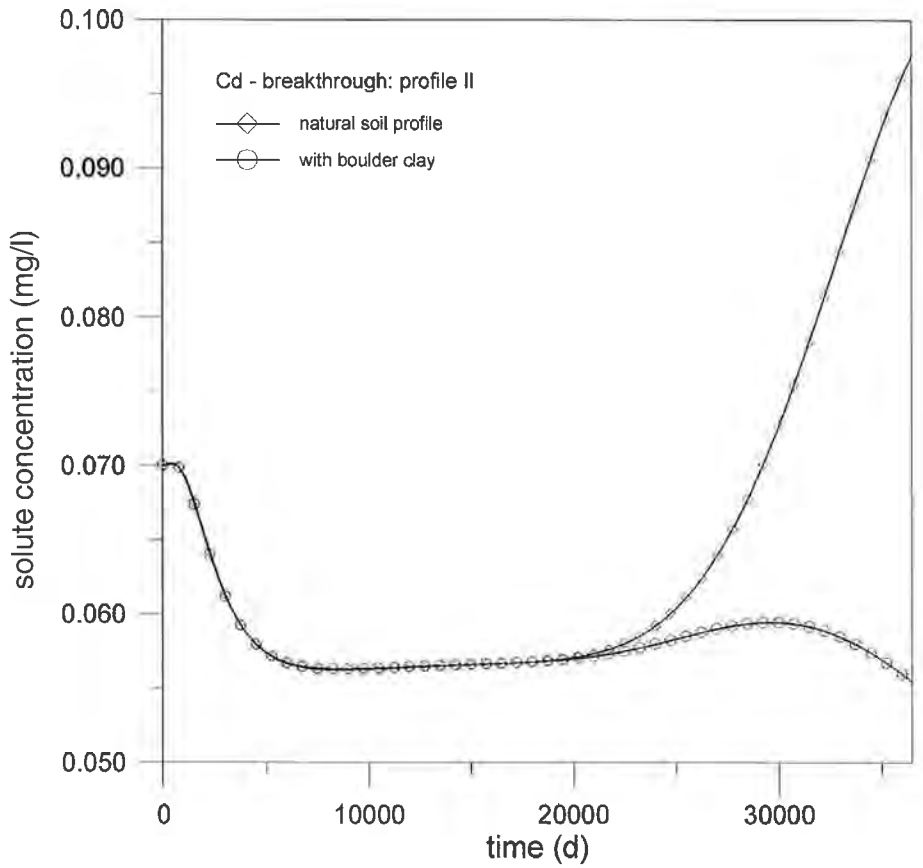

Fig. 5.8: Comparison of Cd-breakthrough curves for the natural soil profile II and the same profile with mixed boulder clay.
Vergleich von Cd-Durchbruchskurven für das Bodenprofil II, naturbelassen und mit eingearbeitetem Geschiebemergel.

The interface software ComFlo forms a handy framework for customization to other codes used by the modeller. The procedure could be used to couple codes with higher dimensionality as well. For example: a 1-D simulator for the vadose zone can be coupled with a 3-D groundwater code.

Summary and Conclusions (H. ZOJER)

Some part of the precipitation which reaches the ground surface may flow along the surface as overland flow, while some may move downwards through the soil, subsoil and rock layers towards the groundwater table. In general terms of the aspects of soil moisture concern the entry of water through the surface layers of the soil and its ability to serve as a temporary storage reservoir for infiltrating precipitation and its vertical movement.

With respect to unconsolidated rocks the main factors governing infiltration capacities are depending on the transmissibility of the soil mass determined by infiltrometers, lysimeters and similar devices as well as on flow models based on DARCY's law. The properties of the unsaturated zone are summarized in R. A. FREEZE & J. A. CHERRY (1979). Since dispersion processes occur usually in microscopic dimensions, in case of tracer experiments they are often neglected, unless they can be detected also at macroscopic scale. Many tracer experiments have been carried out in the unsaturated zone of porous media in order to consider also the preferential flow, because most of the present models are based on an idealized homogeneous system.

In karst regions the unsaturated zone, also known as vadose zone, can reach regionally a tremendous thickness and the water passage is closely linked with the preferential flow along conduits and the fissured flow along small joints respectively. Thus the application of mathematical models either related to hydraulic criteria or to environmental and artificial tracers are limited on the boundary conditions of inhomogeneous systems.

Artificial tracers are subjected on different physical, chemical and biological processes along their subsurface pathway. Their properties are generally known but the individual and combined human impacts from the land surface to the hydrogeological system can effect influences on the tracer properties which provokes special research demands in the field of tracer hydrology.

Four of the five experimental sites are located in granular aquifers: Berlin, Leibnitz, Scheyern and Kecskemet, only Sinji Vrh in Slovenia represents the karst water flow in the uppermost sequences of the aquifer. In the Berlin test site bromide and deuterium (as a spike) have been injected as irrigated water. The calculated residence time indicated a mean vertical flow velocity of 75 m/y. At Leibnitz test site sodium bromide has been dissolved and injected by a sprinkler irrigation system, the flow velocity in the unsaturated zone was calculated with some 1.4 m/y. These results are confirmed by more than one sampling site in the investigated field. In order to visualize preferential flow a dye tracer was directly sprinkled on the upper soil prepared as special excavations.

Coloured pictures of the dye migration through the soil were transformed and finally the images were imported into GIS. The comparison of the profiles shows a great heterogeneity from profile to profile. In Scheyern/Southern Germany deuterium as a non-reactive tracer has been injected, samples were collected through suction cups. From the breakthrough curves of deuterium it becomes evident that matrix flow ranges between 0.7 and 1.2 m/y in Loess and Tertiary sands and gravels. On the other hand bypass-flow can reach velocities up to two magnitudes higher. At the lysimeter station near Kecskemet in the Great Hungarian Plain tracer experiments with environmental isotopes have been performed. With the help of isotopically (oxygen-18) deriched water and tritium-free water a quantitative approach of water dynamics within the lysimeter configuration could be obtained. Best conditions for quantitative evaluation is offered by tritium whenever the results in the individual lysimeter blocks look rather different.

The experimental site Sinji Vrh is located at the Trnovski Gozd plateau in Western Slovenia consisting of carbonate rocks of upper Triassic to upper Cretaceous age. The experimental site in the vadose zone of fractured and karstified rocks presents a 340 m long observation tunnel, located 5–25 m below surface. Tracer experiments have been carried out at a rock overburden of 10–15 m applying inorganic salts and uranine. With regard to water transport it could be clearly distinguished between conduit and matrix flow.

Flow and transport models for subsurface water are developed to relate as much as possible to field scale processes. With reference to porous media and based on the theory of multiphase flow the governing equations of fluid flow have been applied to a set of non-linear partial differential equations describing the main physical and chemical conditions. The one-dimensional models STOTRASIM and SIMWATER represent the soil moisture fluxes/nitrogen dynamics of agricultural soils and the water balance/plant growth respectively, the multi-dimensional model HYDRUS2D was developed to simulate water and solute transport. Finally the concept of coupled models for both, the unsaturated and the saturated flow and transport, is a combined approach based on the transport phenomena in both compartments.

As a result of the comparative investigations in the porous media model approaches will be optimized regarding the water transport especially to the links between the unsaturated and saturated zone. Investigations with artificial tracers, environmental isotopes and hydrochemical compounds should result to reasonable models with a variable degree of process resolution.

In fractured rocks the basis of modelling is much more difficult to define. First approaches should include the simulation of areal, linear and punctual infiltration fluxes considering molecular components and soluble matter.

References

AMBERGER, A. (1989): NH_3-Verluste aus der Anwendung organischer und anorganischer Dünger.– Kongreßband, VDLUFA-Schriftenreihe, **30**, 103–108.

ARAGUAS-ARAGUAS, L., K. ROZANSKI, R. GONFIANTINI & D. LUVAT (1995): Isotope effects accompanying vacuum extraction of soil water for stable isotope analysis.– J. Hydrol., **168**, 159–171.

AUBERTIN, G. M. (1971): Nature and Extent of Macropores in Forest Soils and Their Influence on Subsurface Water Movement.– U.S.D.A. Forest Service Research Paper NE-192.

BAKER, D. & K.-P. SEILER (1982): Zur Wasserbewegung im gesättigten Lockergestein.– In: KLOTZ, D., W. RAUERT & K.-P. SEILER (Eds., 1982): Beiträge über hydrologische Tracermethoden und ihre Anwendungen.– GSF-Bericht R 290, 166–174, Neuherberg.

BAKER, R. S. & D. HILLEL (1991): Observations of fingering behaviour during infiltration into layered soils.– In: GISH, T. J. & A. SHIRMOHAMMADI (Eds., 1991): Preferential flow.– Am. Soc. Agricult. Engineers, 87–99.

BARROW, N. J. & T. C. SHAW (1975): The Slow Reactions between Soil and Anions: 2. Effect of Time and Temperature on the Decrease in Phosphate Concentration in the Soil Solution.– Soil Sci., **119**, 176–177, Baltimore.

BEAR, J. (1979): Hydraulics of groundwater.– 567 p., New York (McGraw-Hill).

BEHRENDT, H. & A. BOEKHOLD (1993): Phosphorus saturation in soils and groundwaters.– Land degradation and rehabilitation, **4**, 233–243, Amsterdam.

BEHRENS, H., K.-P. SEILER & F. NEUMAIER (1980): Geländeversuche mit Fluoreszens-Tracern zur Wasserbewegung im wasserungesättigten Lockergestein in den Tälern der Bayerischen Alpen.– Z. dt. geol. Ges., **131**, 129–138, Hannover.

BERG, W., J. FANK & A. LEIS (1999): Digitale Bildverarbeitung als Hilfsmittel zur Quantifikation von bevorzugten Fließwegen in der ungesättigten Zone.– Bericht über die 8. Lysimetertagung, BAL Gumpenstein, Irdning.

BEVEN, K. (1982): On subsurface storm flow: an analysis of response times.– Hydrological Sciences Journal, **4/12**, 505–521, Oxfordshire (IAHS Press).

BEVEN, K. & P. F. GERMANN (1982): Macropores and Water Flow in Soils.– Water Resources Research, **18/5**, 1311–1325, Washington D.C. (U.S.A.).

BLASCHKE, A. P., J. DEAK, D. JAYAWARDENA, P. LIEBE, W. PAPESCH, V. RAJNER, D. RANK, J. REITINGER, K.-H. STEINER & Z. VARGAY (2000): Markierungsversuche und Modellrech-

nungen in der Lysimeterstation Kecskemét 1996–1999.– Forschungsbericht, Techn. Universität Wien, Inst. f. Hydraulik, Gewässerkunde und Wasserwirtschaft, **17**, 89 p., Wien.
BUSER, S., (1968): Basic geological map of Slovenia, Gorica sheet, 1:1,000.000.– Ljubljana.
ČAR, J. (1997): Geological description, in Karst Hydrogeological Investigations in South-Western Slovenia.– Acta carsologica, **26/1**, 68–73, Ljubljana.
ČENČUR CURK, B. (1997): Terenski eksperimentalni poligoni kot osnova pri študiju prenosa snovi v nezasičeni kraško-razpoklinski kamnini (Experimental field sites as a basis for the study of solute transport in the vadose zone of karstified rock).– Acta Hydrotechnica, **15/20**, 111 p., Ljubljana.
ČENČUR CURK, B. (2001): Flow and solute transport in fractured and karstified rocks.– Doctor Thesis, University of Ljubljana, Ljubljana (in print).
ČENČUR CURK, B. & M. VESELIČ (1999): Laboratory and Experimental Study of Contaminant Transport in Fractured and Karstified Rock.– RMZ – Materials and geoenvironment, **46/3**, 425–442, Ljubljana.
ČENČUR CURK, B., M. PINTAR, M. KARAHODŽIČ & M. VESELIČ (2000): Nitrate transport through karstic soil and unsaturated karstic rock.– KARST 2000, 16. 9.–21. 9. 2000, Turkey (in print).
CHAPMAN, D. (1992): Water quality assessments.– 585 p., London (Chapman & Hall).
CLAY, D. E., J. A. E. MOLINA, D. E. CLAPP & D. R. LINDEN (1985): Nitrogen – Tillage – Residue Management: II. Calibration of potential rate of nitrification by model simulation.– Soil Sci. Soc. Am. J., **49**, 322–325.
DEMUTH, N. & A. HILTPOLD (1993): Fast-Flow. Eine Übersicht über den heutigen Wissensstand.– Z. Pflanzenern. Bodenk., **156**, 479–484.
DIERSCH, H.-J. (1980): Mehrphasiger Stoff-, Impuls- und Wärmetransport im ungesättigten und gesättigten porösen Medium.– Acta Hydrophysica, **25/4**, 351–407, Berlin.
DIERSCH, H.-J. & G. NÜTZMANN (1986): Modellierung und numerische Simulation geohydrodynamischer Transportprozesse: 2. Finite-Element-Methoden.– Technische Mechanik, **7**, 5–20, Karl-Marx-Stadt.
DIMENT, G. A. & K. K. WATSON (1985): Stability Analysis of Water Movement in Unsaturated Porous Materials. 3. Experimental Studies.– Water Resources Research, **21/7**, 979–984, Washington D.C. (U.S.A.).
DVWK (1996): Estimation of Evaporation from Land and Water Surface (in German).– DVWK-Merkblätter zur Wasserwirtschaft, No. **238**, Deutscher Verband für Wasserwirtschaft und Kulturbau e.V., Bonn.
EINSELE, G., D. C. BOZORGZAD-ARBAB, H. HEITELE, M. KLOCK & K.-P. SEILER (1968): Geohydrologische Untersuchungen in der Buntsandsteinzone des südlichen Saarlands.– Geol. Mitt., **9**, 1–72.
EISENHUT, M., J. FANK & P. RAMSPACHER (1992): Einfluß der Bodenbewirtschaftung auf die Temperaturverhältnissse in der ungesättigten Zone am Beispiel der Lysimeteranlage Wagna (Steiermark, Österreich).– Mitt. d. Österr. Bodenkundlichen Gesellschaft, H. **45**, 25–44, Wien.
EULENSTEIN, F. & H. DRECHSLERM (1992): Ursachen, Differenzierung und Steuerung der Nitratkonzentration im Grundwasser überwiegend agrarisch genutzter Wassereinzugsgebiete.– Ph. D. Thesis, Univ. Göttingen, 269 p., Göttingen.
FANK, J. (1999): Die Bedeutung der ungesättigten Zone für Grundwasserneubildung und Nitratbefrachtung des Grundwassers in quartären Lockesediment-Auiferen am Beispiel des Leibnitzer Feldes (Steiermark, Österreich).– Beiträge zur Hydrogeologie, **49/50**, Graz.
FANK, J. & T. HARUM (1994): Solute transport and water movement in the unsaturated zone of a gravel filled valley: tracer investigations under different cultivation types.– In: SOVERI, J. & T. SUOKKO (Eds., 1994): Future Groundwater Resources at Risk (Proceedings of the Helsinki Converence, June 1994).– IAHS Publ., **222**, 341–354, Great Yarmouth (Galliard Ltd.).
FEDDES, R. A., KADAT, P., P. J. T. VAN BAKEL, J. J. B. BRONSWYK & J. HALBERTZSMA (1988): Modeling Soil Water Dynamics in the Unsaturated Zone. State of the Art.– J. Hydrol., **100**, 69–111.
FEICHTINGER, F., (1998): STOTRASIM – Ein Modell zur Simulation der Stickstoffdynamik in der ungesättigten Zone eines Ackerstandortes.– Schriftenreihe des BA f. Wasserwirtschaft, **7**, 14–41, Petzenkirchen.
FLÜHLER, H., M. FLURY, W. A. JURY, J. LEUENBERGER, K. ROTH & B. STUDER (1994): Pesticide Transport through Unsaturated Field Soils: Preferential Flow.– A research report submitted to Ciba Ltd. Schlieren.

FORRER, I. (1997): Solute Transport in an Unsaturated Field Soil: Visualisation and Quantification of Flow Patterns Using Image Analysis.– A Dissertation submitted to the Swiss Federal Institute of Technology Zürich, Diss. ETH No. 12476.
FREEZE, R. A. & J. A. CHERRY (1979): Groundwater.– 604 p., New York (Prentice Hall).
FRITZ, S. & D. KLOTZ (1998): Das Wägesystem der GSF-Lysimeteranlage Neuherberg.– In: KLOTZ, D. & K.-P. SEILER (Eds., 1998): Die GSF-Lysimeteranlage Neuherberg.– GSF-Bericht, **23/98**, 41–47.
GELBRECHT, J., E. DRIESCHER, H. LADEMANN, J. SCHÖNFELDER & H.-J. EXNER (1996): Diffuse nutrient impact on surface water bodies and its abatement by restoration measures in a small catchment area in north-east Germany.– Water Sci. Technol., **33 (4–5)**, 167–174, Oxford.
GERMANN, P. F. (1990): Preferential flow and the generation of runoff. 1. Boundary layer flow theory.– Water Resources Research, **26/12**, 3055–3063, Washington D.C. (U.S.A.).
GLASS, R. J., T. S. STEENHUIS & J.-Y. PARLANGE (1989): Mechanism for finger persistence in homogeneous, unsaturated porous media: Theory and verification.– Soil. Sci., **148**, 60–70.
GROOT, J. J. R. & P. DE WILLIGEN (1991): Simulation of the nitrogen balance in the soil and a winter wheat crop.– Fertilizer Research, **27**, 261–272.
HASSANIZADEH, S. M. & W. G. GRAY (1979a): General conservation aquations for multiphase systems: 1. Averaging procedure.– Adv. Water Resour., **2**, 131–144, Oxford.
HASSANIZADEH, S. M. & W. G. GRAY (1979b): General conservation equations for multiphase systems: 2. Mass, Momenta, Energy and Entropy Equations.– Adv. Water Resour., **2**, 191–203, Oxford.
HASSANIZADEH, S. M. & W. G. GRAY (1993): Toward an improved description of the physics of two-phase flow.– Adv. Water Resour., **16**, 53–67, Amsterdam.
HEYDER, D., (1993): Nitratverlagerung, Wasserhaushalt und Denitrifikationspotential in mächtigen Lößdecken und einem Tonboden bei unterschiedlicher Bewirtschaftung.– Bonner Bodenkundliche Abhandlungen, **10**, 171 p., Bonn.
HILL, D. E. & J.-Y. PARLANGE (1972): Wetting front instability in layered soils.– Am. Soil. Sci. Proceed., **36**, 697–702.
HILLEL, D. (1971): Soil and Water.– New York/London (Acad. Press).
HOLZBECHER, E. (1996): Modellierung dynamischer Prozesse in der Hydrologie: Grundwasser und ungesättigte Zone.– Heidelberg/New York (Springer).
HOLZBECHER, E. (1998): Modeling density-driven flow in porous media.– Heidelberg/New York (Springer).
HOLZBECHER, E., G. NÜTZMANN & S. HOSSAIN (1992): Numerical simulation of the near-surface radioactive waste disposal facilities (NSARS test case 1).– In: HÖTZL H. & A. WERNER (Eds.,1992): 6th Symposium on Water Tracing, Karlsruhe, Proceedings.– 445–451, Rotterdam (Balkema).
HUYAKORN, P. S. & G. F. PINDER (1983): Computational methods in subsurface flow.– 473 p., Orlando (Academic Press).
INGRAHAM, N. L. & C. SHACHEL (1992): A comparison of the toluen distillation and vacuum/heat methods for extraction soil water for stable isotope analysis.– J. Hydrol., **140**, 371–387.
JANEŽ, J. (1997): Hydrogeology, in Karst Hydrogeological Investigations in South-Western Slovenia.– Acta carsologica, **26/1**, 73–86, Ljubljana.
JARDIN, P. M., G. U. WILSON, J. F. MCCARTHY, R. J. LUXMOORE, D. L. TAYLOR & L. W. ZELANY (1990): Hydrogeochemical processes controlling the transport of dissolved organic carbon through a forested hillslope.– J. Cont. Hydrol., **6**, 3–19.
JAYAWARDENA, D., A. P. BLASCHKE, D. RANK, J. REITINGER, K.-H. STEINER & Z. VARGAY (1997): Transport of solutes in the unsaturated zone under transient flow.– Proceedings of the workshop on "Groundwater depletion in basin regions: problems arising in the area between the Rivers Danube and Tisza", 17–22, Budapest.
KARAHODŽIČ, M. (2000): Nitrate Pollution in Karst Groundwater.– Diploma Thesis, University of Ljubljana, 70 p., Ljubljana.
KÄSS, W. (1998): Tracing Technique in Geohydrology.– 581 p., Rotterdam/Brookfield (A.A. Balkema).
KENDAL, C. & J. J. MCDONNEL (1998): Isotope tracers in catchment hydrology.– 839 p., Amsterdam/Lausanne/New York/Oxford/Singapore/Tokyo (Elsevier).
KIRBY, M. & J. WILEY (1980): Hill Slope Hydrology.– Chichester.
KLOTZ, D. & G. HINREINER (1999): Applikationsvorrichtung für Markierungs- und Schadstoffe auf Gefäß-Lysimeter von kreisförmigem Querschnitt.– In: KLOTZ, D. & K.-P. SEILER (Eds., 1999):

Bestimmung der Sickerwassergeschwindigkeit in Lysimetern.– GSF-Bericht, **01/99**, 109–112, Neuherberg.

KLOTZ, D. & K.-P. SEILER (1999): Einführung in die Lysimeteranlage Neuherberg. – In: KLOTZ, D. & K.-P. SEILER (Eds., 1999): Bestimmung der Sickerwassergeschwindigkeit in Lysimetern.– GSF-Bericht, **01/99**, 73–77, Neuherberg.

KÖRNER, J. (1996): Abflussbildung, Interflow und Stoffbilanz im Schönbuch Waldgebiet.– Tübinger Geowissenschaftliche Arbeiten, C **27**, 206 p.

KRAUSE, S. (2000): Untersuchung unterirdischer Abflussprozesse in der Sicker- und Grundwasserzone des nordostdeutschen Flachlandes mit Hilfe von Simulationsmodellen.– Diploma Thesis, Univ. Potsdam, 100 p., Potsdam.

KUNG, K.-J. S. (1990): Influence of plant uptake on the performance of bromide tracer.– Soil Sci. Am. J., **54**, 975–979.

KUNG, K.-J. S. (1990a): Preferential flow in sandy vadose zone. 1. Field observations.– Geoderma, **46**, 51–58.

KUNG, K.-J. S. (1990b): Preferential flow in sandy vadose zone. 2. Mechanisms and Implications.– Geoderma, **46**, 59–71.

LADEMANN, H. & R. PÖTHIG (1994): Untersuchungen zur Phosphorbelastung, Phosphorverlagerung und Phosphorsorptionsfähigkeit dränierter Ackerflächen als Beitrag zum Gewässerschutz.– Vom Wasser, **82**, 323–334, Weinheim.

LENDA, A. & A. ZUBER (1970): Tracer dispersion in groundwater experiments. – Isotope Hydrology **1970**, 619–641, Wien (IAEA).

MACIEJEWSKI, S., G. NÜTZMANN & K. JOSWIG (2001): Experimental analysis and modelling studies of tracer transport in unsaturated porous media for estimating the dependence of dispersion coefficient on water saturation.– Adv. Water Resour., Oxford (in prep.).

MALOSZEWSKI, P. & A. ZUBER (1990): Mathematical modeling of tracer behaviour in short-term experiments in fissured rocks.– Water Resources Research, **26/7**, 1517–1528, Washington D.C. (U.S.A.).

MALOSZEWSKI, P., A. HERRMANN & A. ZUBER (1999): Interpretation of tracer tests performed in fractured rock of the Lange Bramke basin, Germany.– Hydrogeology J., **7/2**, 209–218, Berlin/Heidelberg (Springer).

MENDOZA, C. A., R. THERRIEN & E. A. SUDICKY (1991): ORTHOFEM User's guide, Version 1.02.– Waterloo Centre for Groundwater Research, Univ. of Waterloo, Waterloo, Ontario, Canada.

MOSER, H. & W. RAUERT (1980): Isotopenmethoden in der Hydrologie.– Lehrbuch der Hydrogeologie, **8**, 400 p., Berlin/Stuttgart (Borntraeger).

MUALEM, Y. (1976): A new model for predicting the hydraulic conductivity of unsaturated porous media.– Water Resources Research, **12/3**, 513–522, Washington D.C. (U.S.A.).

MÜLLER, G. & J. DÖRING (1989): Zur Berechnung der Bodentemperatur in unbewachsenem Boden und unter Kulturpflanzenbeständen – Bedeutung und Methodik.– Arch. Acker-Pfl. Bodenkd., **7**, 379–383, Berlin.

NACHTNEBEL, H. P. (Project manager, 1994): Hydrologie Österreichs – Schutz des Grundwassers in Tal- und Beckenlagen.– Unveröff. zusammenfassender Endbericht in 4 Bänden, BOKU Wien.

NATERMANN, E. (1951): Die Linie des langjährigen Grundwassers und die Trockenwetterabflüsse (TWL).– Die Wasserwirtschaft, **41**,12–14, Stuttgart.

NIELSEN, D. R., M. Th. VAN GENUCHTEN & J. W. BIGGAR (1986): Water flow and solute transport processes in the unsaturated zone.– Water Resources Research, **22**, 89–108, Washington D.C. (U.S.A.).

NÜTZMANN, G. (1991): A simple finite element method for modelling one-dimensional water flow and solute transport in variably saturated soils.– Acta Hydrophysica, **35**, 33–59, Berlin.

NÜTZMANN, G. (1998): Modellierung ungesättigter Transportprozesse in porösen Medien.– Habil. Schrift im Fachbereich Bauingenieurwesen und Angewandte Geowissenschaften, TU Berlin, 206 p., Berlin.

NÜTZMANN, G., M. THIELE, S. MACIEJEWSKI & K. JOSWIG (1998): Inverse modeling techniques for determining hydraulic properties of coarse-textured porous media by transient outflow methods.– Adv. Water Resour., **22/3**, 273–284, Oxford.

NÜTZMANN, G., S. MACIEJEWSKI & K. JOSWIG (1999): Experimental investigations and modelling studies about tracer transport in unsaturated porous media: the dependence of dispersion coef-

ficient on water saturation.– Proc. Int. Conf. on "Calibration and reliability in groundwater modelling" ModelCARE99, Zürich, 20–23 Sept. 1999, 131–137, Zürich.

NÜTZMANN, G., G. GINZEL, E. HOLZBECHER, H. SCHOLZ & C. HOFFMANN (2000): Grundwasserschutz durch Bodenverbesserung auf ehemaligen Rieselfeldern: Folgenabschätzung mit Hilfe gekoppelter Modelle.– Wasser und Boden, **52/9**, 9–14, Berlin (Blackwell Verlag).

NÜTZMANN, G., S. MACIEJEWSKI, W. STICHLER & E. ZWIRNMANN (2001): Dual tracer test and modelling studies for determining the unsaturated flow components in a sandy catchment area.– XXXI IAH Congress "New approaches to characterizing groundwater flow" (in preparation), Munich.

NYE, P. H. & P. B. TINKER (1977): Solute movement in the soil-root system.– Studies in Ecology, **4.**, 342 p., Oxford/London/Edinburgh/Melbourne (Blackwell Scientific Publications).

OTTOW, J. C. G. (1992): Denitrifikation, eine kalkulierbare Größe in der Stickstoffbilanz von Böden?– Wasser und Boden, **44**, 578–581, Berlin.

PETRIČ, M. (1997): Trnovsko-Banjška Planota Plateau and Surroundings.– Acta Carsologica, **26/1** – Supplementum, 36–55 (7th Int. Symp. on Water Tracing, Field Guide of Karst in Slovenia), Ljubljana.

PUDENZ, S. (1999): Modellierung der regionalen Phosphorverlagerung im Boden und Grundwasser.– Wiss. Schriftenreihe Umwelttechnik, **8**, 146 p., Berlin (Verlag Dr. Köster).

PUDENZ, S. & G. NÜTZMANN (1997): Estimation of the phosphate transport in soil and groundwater with the compartment model MORPHO (in German).– DGM, **41/2**, 72–74, Koblenz.

RANK, D., D. JAYAWARDENA, W. PAPESCH, J. REITINGER & Z. VARGAY (1997): Lysimeterstudie zur Versickerung im Sandboden der Großen Ungarischen Tiefebene.– 7. Gumpensteiner Lysimetertagung, BAL Gumpenstein, 85–88, Gumpenstein.

RENGER, M., G. WESSOLEK, R. KÖNIG, F. FAHRENHORST, B. SWARTJES & B. KASCHANIAN (1989): Modelle zur Ermittlung und Bewertung von Wasserhaushalt, Stoffdynamik und Schadstoffbelastbarkeit in Abhängigkeit vom Klima, Bodeneigenschaften und Nutzung.– Abschlussbericht für das Forschungszentrum Jülich, Techn. Univ. Berlin, Berlin.

RICHARDS, L. A. (1931): Capillary Conduction of liquids through porous mediums.– Physics, **1**, 318–333.

RITSEMA, C. J., L. W. DEKKER, J. M. H. HENDRICKX & W. HAMMINGA (1993): Preferential Flow Mechanism in a Water Repellent Sandy Soil.– Water Resources Research, **29**, 2183–2193, Washington D.C. (U.S.A.).

ROTH K., H. FLÜHLER, W. A. JURY & J. C. PARKER (Eds., 1990): Field-scale water and solute flux in soils.– 294 p., Basel (Birkhäuser Verlag).

RÜHLMANN, J. (1999): A new approach to estimating the pool of stable organic matter in soil using data from long-term field experiments.– Plant and Soil, **213**, 149–160, Netherland.

RUSSO, D. & G. DAGAN (Eds., 1993): Water flow and solute transport in soils.– Advanced Series in Agricultural Sciences, **20**, 306 p., Berlin (Springer).

RUSSOW, R., S. KNAPPE, H. FÖRSTEL & R. MEISSNER (1995): Vergleich der Wasser- und Anionenbewegung in agrarisch genutztem Sandlöß und Löß-Schwarzerde-Böden anhand von Multitracer-Untersuchungen.– Arch. Acker-Pfl. Bodenkd., **40**, 453–471, Berlin.

SALAS, J. D., J. W. DELLEUR, V. YEVJEVICH & W. L. LANE (1985): Applied modelling of hydrologic time series.– Water Resources Publication, Littleton, Colorado.

SAUTY, J.-P. (1977): Contribution à l'identification des paramètres de dispersion dans les aquifères par interprétation des expériences de traçage.– Bur. de Recherches Géol. et Minières, Dépt. Hydrogéol. 77SGN515HYD, 157 p., Orléans.

SCHEFFER, F., P. SCHACHTSCHABEL, H.-P. BLUME, G. BRÜMMER, K. H. HARTGE & U. SCHWERTMANN (1998): Lehrbuch der Bodenkunde.– 14. Aufl., Stuttgart (Enke).

SCOTTER, D. R. (1978): Preferential solute movement through larger soil voids I. Some computations using simple theory.– Austr. J. Soil. Res., **16**, 257–267.

SEILER, K.-P. & D. BAKER (1985): Der Einfluß der Schichtung auf die Sickerwasserbewegung bei punkt- und linienförmiger Infiltration.– Z. dt. geol. Ges., **136**, 659–672, Hannover.

SEILER, K.-P., Th. PFAFF & H. BEHRENS (1987): Ergebnisse von Karstgrundwasseruntersuchungen im Malm der Südlichen Frankenalb.– Z. dt. geol. Ges., **138**, 377–386, Hannover.

SEILER, K.-P., H. BEHRENS & M. WOLF (1996): Use of artificial and environmental tracers to study storage and drainage of groundwater in the Franconian Alb, Germany, and the consequences for groundwater protection.– Proceedings on Isotopes in Water Resources Management, IAEA, **2**, 135–145.

SEILER, K.-P. & C. HELLMAIER (2000): Humic substances and agrochemicals in discharge components in Scheyern.– Freiburger Geographische Hefte (in print).
SIMUNEK, J., T. VOGEL & M. Th. VAN GENUCHTEN (1992): The SWMS_2D code for simulating water flow and solute transport in two-dimensional variably saturated media, Version 1.1.– Research Report, **126**, 169 p., U.S. Salinity Laboratory, USDA, ARS, Riverside, California.
SIMUNEK, J., M. SEJNA & M. Th. VAN GENUCHTEN (1996): HYDRUS2D-Application, Version 1.1.– U.S. Salinity Laboratory, USDA, ARS, Riverside, California.
SKLASH, M. G., R. N. FARVOLDEN & P. FRITZ (1976): A conceptual model of watershed response to rainfall, developed through the use of oxygen-18 as a natural tracer.– Can. J. Earth Sc., **13**, 271–283.
SKLASH, M. G. & R. N. FARVOLDEN (1979): The role of groundwater in storm runoff.– J. Hydrol., **43**, 45–65.
STEENHUIS, T. S. & J.-Y. PARLANGE (1991): Preferential flow in structured and sandy soils.– In: GISH, T. J. & A. SHIRMOHAMMADI (1991): Preferential flow.– Am. Soc. Agricult. Engineers.
STENITZER, E., (1988): SIMWASER – Ein numerisches Modell zur Simulation des Bodenwasserhaushaltes und des Pflanzenertrages eines Standortes.– Mitteilung Nr. **31**, 203 p., BA f. Kulturtechnik und Bodenwasserhaushalt, Petzenkirchen.
SZEICZ, G., G. ENDRÖDI & S. TAJCHMAN (1969): Aerodynamic and surface factors in evaporation.– Water Resources Research., **5**, 380–394, Washington D.C. (U.S.A.).
THEURETZBACHER, H. (1997): Makroporosität und präferentielle Fließbewegung in der wasserungesättigten Zone der Kleineinzugsgebietes Höhenhansl/Pöllau.– Diplomarbeit an der Karl-Franzens-Universität Graz.
THOM, A. S. & H. R. OLIVER (1977): On Penman's equation for estimating regional evaporation.– Q.J.R. Meteorol. Soc., **103**, 345–357.
TISCHNER, T. (2000): Untersuchungen zur Phosphatverlagerung und Phosphatbindung im Boden und Grundwasser einer landwirtschaftlich genutzten Fläche.– Bodenökologie und Bodengenese, **33**, 187 p., Berlin.
TRČEK, B. (2001): Mass transport monitoring in the unsaturated zone of the karst aquifer by natural tracers.– Doctor Thesis, University of Ljubljana, Ljubljana (in print).
TRČEK, B., M. VESELIČ & J. URBANC (2000a): The suitability of carbon isotope composition as natural tracer in karst aquifer investigations.– Acta Carsologica, **29/1**, 153–161, Ljubljana.
TRČEK, B., M. ČAR & M. VESELIČ (2001): The use of isotopic, hydrogeochemical and ground-penetrating radar investigations in the study of the unsaturated zone of the karstic aquifer – Uporaba izotopskih, hidrogeokemijskih in georadarskih raziskav pri študiju nezasičene cone kraškega vodonosnika.– RMZ – Materials and geoenvironment, **47/3–4**, 335–344, Ljubljana.
USDA SOIL CONSERVATION SERVICE (1983): National Engineering Handbook. Hydrology Section 4, Chapters 19–21.– Washington D.C. (U.S. Government Printing Office).
VAN GENUCHTEN, M. Th. (1980): A closed-form equation for predicting the hydraulic conductivity of unsaturated soils.– Soil Sci. Soc. Am. J., **44**, 892–898.
VAN GENUCHTEN, M. Th. (1994): New Issues and Challenges in Soil Physics Research.– In: 15th World Congress of Soil Science, Acapulco, Mexico, Vol. 1: Inaugural and State of the Art Conferences, 5–27.
VAN GENUCHTEN, M. Th. & D. R. NIELSEN (1985): On describing and predicting the hydraulic properties of unsaturated soils.– Annales Geophysicae, **3**, 615–628, Baltimore.
VESELIČ, M. (1995): Study of Mass Transport in Fractured and Karstified Rocks.– Project Proposal for 1995–1997 Research Grant of the Ministry of Science and Technology of the Republic of Slovenia, 12 p., Ljubljana.
VESELIČ, M., B. ČENČUR CURK & S. ŠEBELA (1998): An evaluation of structural analysis of discontinuities in carbonate rock.– Geological journal, **33/4**, 205–221, Chichester, England.
VOGEL, T. & M. CISLEROVA (1988): On the reliability of unsaturated hydraulic conductivity calculated from the moisture retention curve.– Transport in Porous Media, **3**, 1–15.
WANG, J. S. Y. (1991): Flow and transport in fractured rocks.– Rev. Geophys., **29**, 254–262.
WERNER, A. (1998a): Hydraulische Charakterisierung von Karstsystemen mit künstlichen Tracern.– Shriftenreihe Angewandte Geologie Karlsruhe, **51**, 169 p., Karlsruhe.
WERNER, A. (1998b): TRACI – An example for mathematical tracing interpretation model.– In: KÄSS, W. (1998): Tracing Technique in Geohydrology.– 376–381, Rotterdam/Brookfield (A.A. Balkema).

WESSELING, J. G. & T. BRANDYK (1985): Introduction of the occurrence of high groundwater levels and surface water storage in computer program SWATRE.– Nota **1636**, Institute for Land and Water Management Research (ICW) Wageningen, The Netherlands.
WITTHÜSER, K. & B. ČENČUR CURK (2000): Groundwater pollution by contaminant transport from soil to fractured rock.– Acta Carsologica, **29/1**, 173–181, Ljubljana.
ZOJER, H. (1993): The effect of short term events on transport phenomena in the unsaturated zone with special regard to environmental isotopes.– IAEA-TECDOC on "Isotope Techniques on Groundwater Pollution Studies", Vienna.
ZUIDEMA, P. K. (1985): Hydraulik der Abflußbildung während Starkniederschlägen.– Mitt. Inst. Wasserbau, Hydrologie u. Glaziologie, **79**, ETH Zürich.

Zusammenfassung (H. ZOJER)

Ein Teil des Niederschlages, der die Erdoberfläche erreicht, fließt oberflächlich ab, der Rest infiltriert in den Untergrund und erreicht nach Überbrückung der ungesättigten Zone das Grundwasser. Dabei ist die Speicherfunktion des Bodens in allen quantitativen und qualitativen Überlegungen zu berücksichtigen.

In Porenaquiferen wird die Infiltration über die Transmissivität des Bodens gesteuert. Infiltrometer, Lysimeter und andere technische Einrichtungen sind geeignet, den Wasser- und Stofftransport zu messen und zu berechnen. Die daraus abgeleiteten mathematischen Modelle basieren auf dem DARCY'schen Gesetz. Nachdem die Dispersion in der vertikalen Bewegung des Wassers in der ungesättigten Zone nur geringe Dimensionen erreicht, wird sie bei Tracerversuchen großteils vernachlässigt. In Karstgebieten kann die ungesättigte Zone gemäß der lithologisch-tektonischen Entwicklung große Mächtigkeiten erreichen. Die Wasserbewegung in diesen hydrogeologischen Systemen ist im Vergleich zu Porenaquiferen noch wesentlich mehr von der Inhomogenität der Gesteinsstruktur geprägt. Der schnelle Abfluss entlang von Schächten und Höhlen steht im Gegensatz zum Matrixfluss in den Mikroklüften. Die Entwicklung von mathematischen Modellen ist daher besonders stark an die Randbedingungen des hydrogeologischen Systems gebunden.

Künstliche Tracer unterliegen auf ihrem unterirdischen Weg physikalischen, chemischen und biologischen Prozessen. Ihre Eigenschaften sind heute durchaus bekannt, doch die unterschiedlichen Formen der Grundwasserbelastung durch die intensive Landnutzung kann ihren Habitus oft erheblich beeinflussen, was naturgegeben einen weiteren Forschungsbedarf mit sich bringt.

Vier der fünf Testgebiete beziehen sich auf Porenaquifere: Berlin, Leibnitz, Scheyern und Kecskemet, nur Sinij Vrh in Slowenien repräsentiert einen Karstaquifer. Im Testgebiet Berlin wurden Bromid und Deuterium über künstlichen Regen an der Oberfläche aufgebracht, die mittlere Sickergeschwindigkeit mit 0,75 m/a berechnet. Im Leibnitzer Testgebiet gelangte Natriumbromid als Tracer zur Anwendung, die Sickergeschwindigkeit liegt dort bei 1,4 m/a unter Berücksichtigung mehrerer Probenahmestellen in unterschiedlicher Tiefe. Für die Visualisierung des Wassertransportes in der Bodenzone wurde ein Farbtracer direkt in Bodenprofile eingebracht, die Farbmigration photographisch festgehalten und über Darstellungen, die aus der Fernerkundung bekannt sind, in ein GIS eingebracht. Der Profilvergleich zeigt eine große Heterogenität des Bodenaufbaues. In Scheyern wurde Deuterium als nicht-reaktiver Tracer eingesetzt. Der Matrixfluss erreicht eine Geschwindigkeit zwischen 0,7 und 1,2 m/a, bevorzugte Wasserwege können eine Geschwindigkeit bewirken, die bis zu zwei Grö-

ßenordnungen höher liegt. Tracerversuche mit abgereichertem Sauerstoff-18 und tritiumfreiem Wasser im Testgebiet Kecskemet führten zu quantitativen Aussagen über den Wassertransport im Lysimeter.

Sinij Vrh liegt in West-Slowenien, der geologische Aufbau besteht aus Karbonatgesteinen aus der Trias, der Jura und der Kreide. Ein 340 m langer Tunnel, der nur bis zu 25 m überlagert wird, stellt einen hervorragenden Ansatz für Tracerversuche in der Karst-Infiltrationszone dar. Für Tracerversuche wurden anorganische Salze und Uranin verwendet, sie zeigen deutliche Unterschiede im Fließverhalten gemäß der Gesteinsstruktur.

Fließ- und Stofftransportmodelle werden heute vorwiegend in Porenaquiferen angewandt. Die Modelle STOTRASIM und SIMWATER beschreiben den Wasser- und Stofftransport in der ungesättigten Zone. Sie sind eindimensional orientiert, während das Modell HYDRUS2D auf zwei Dimsionen ausgerichtet ist. Sinnvoll ist eine Koppelung von Modellen im Übergang zwischen der ungesättigten und gesättigten Zone.

Die Ergebnisse der vergleichenden Untersuchungen in den verschiedenen Testgebieten von Porengrundwasserkörpern werden die Anstrengungen zu Modellkoppelungen noch verstärken. Traceruntersuchungen sollen zu nachvollziehbaren Modellen führen, um einen Vergleich mit den hydraulisch orientierten Ansätzen zu ermöglichen. In Karstgebieten werden die Modellüberlegungen von den unterschiedlichen Infiltrationsbedingungen auszugehen haben und dies unter Berücksichtigung des Wasser- und des Stofftransportes.